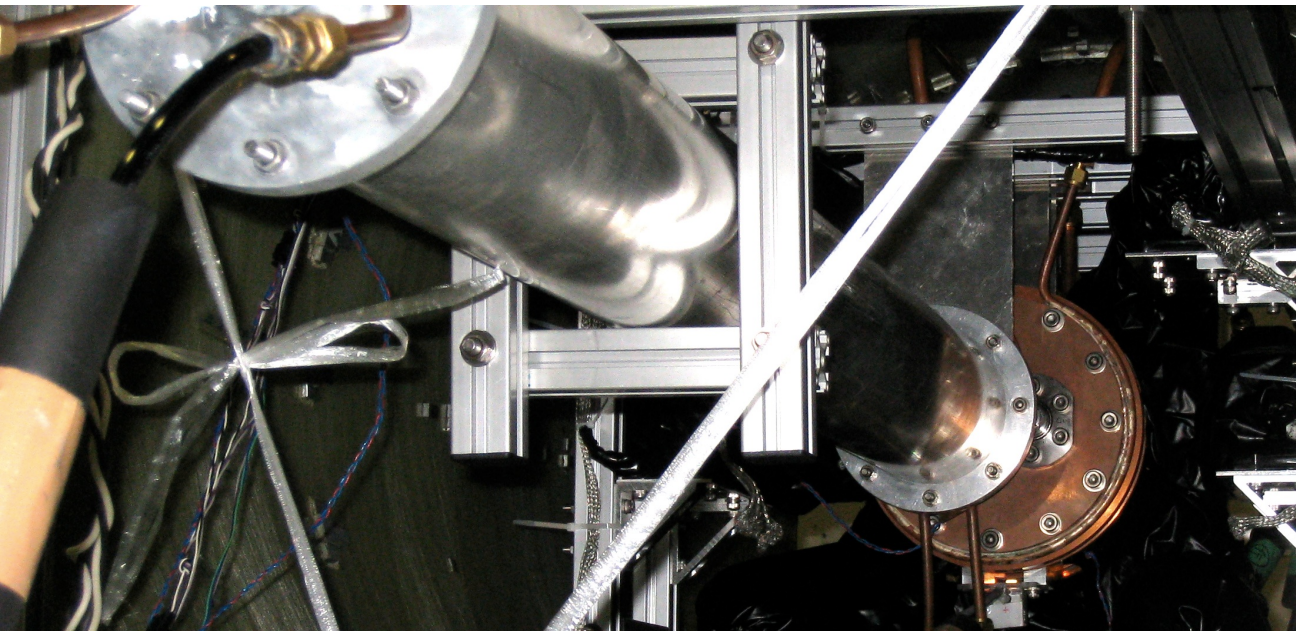


New Precision Measurement of the Hyperfine Splitting of Positronium



Akira Ishida

The University of Tokyo (stationed at CERN)

DESY Physics Seminar

21/04/2015 Hamburg, Germany

Members

A. Ishida, T. Namba, S. Asai, T. Kobayashi

Department of Physics and ICEPP, The University of Tokyo

H. Saito

Department of General Systems Studies, The University of Tokyo

M. Yoshida, K. Tanaka, A. Yamamoto

High Energy Accelerator Research Organization (KEK)



Warm thanks to facilities and the entire members
of the Cryogenics Science Center at KEK



Outline

- Positronium Hyperfine Splitting (Ps-HFS)
- Material effect and Ps thermalization
- Our New Experiment
- Analysis and Results
- Prospects & conclusion

Physics Letters B 734 (2014) 338–344



Contents lists available at [ScienceDirect](#)

Physics Letters B

www.elsevier.com/locate/physletb



New precision measurement of hyperfine splitting of positronium

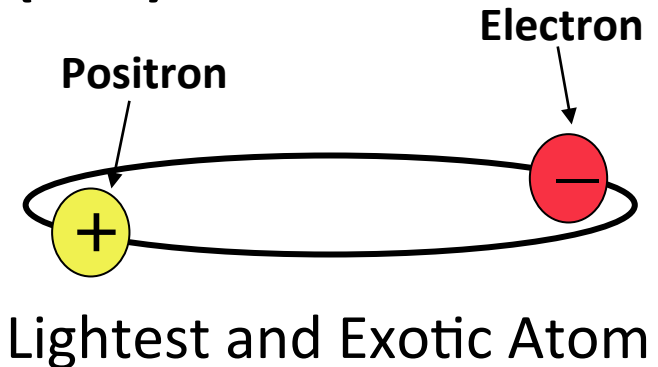
A. Ishida ^{a,*}, T. Namba ^a, S. Asai ^a, T. Kobayashi ^a, H. Saito ^b, M. Yoshida ^c, K. Tanaka ^c,
A. Yamamoto ^c



- Positronium Hyperfine Splitting (Ps-HFS)
- Material effect and Ps thermalization
- Our New Experiment
- Analysis and Results
- Prospects & conclusion

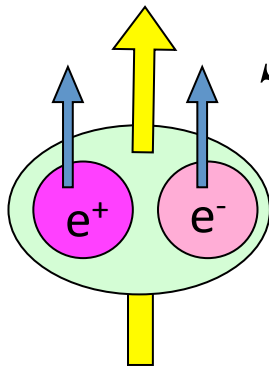
Positronium (Ps)

Bound state of an electron (e^-)
and a positron (e^+)



- Lightest hydrogen-like atom (mass = 1.022 MeV)
- Pure leptonic system. Free from uncertainties of hadronic interactions.
 - > Ideal system for precision test of bound-state Quantum ElectroDynamics (QED).
- Particle-antiparticle system
 - > Sensitive to physics beyond standard model.
- The lowest energy $e^+ e^-$ “collider”

Positronium (Ps)

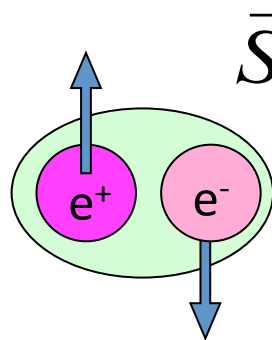
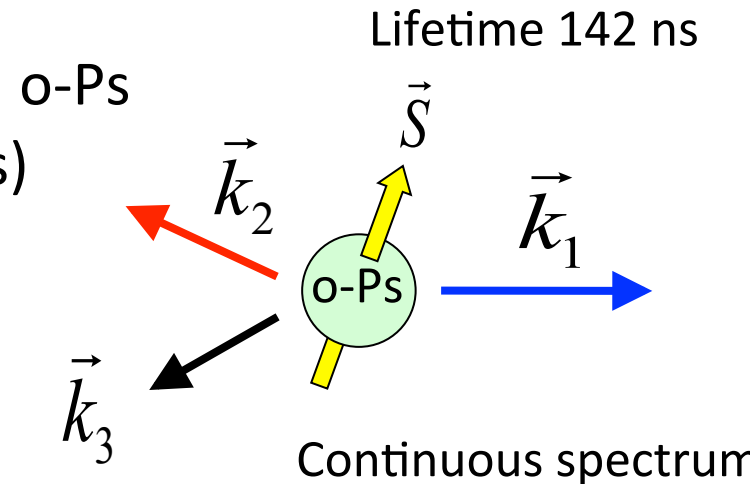


$$\vec{S} = 1 \text{ (Triplet)}$$

Ortho-positronium (o-Ps)

Spin=1 The same quantum number as photon

$$o\text{-Ps} \rightarrow 3\gamma (, 5\gamma, \dots)$$

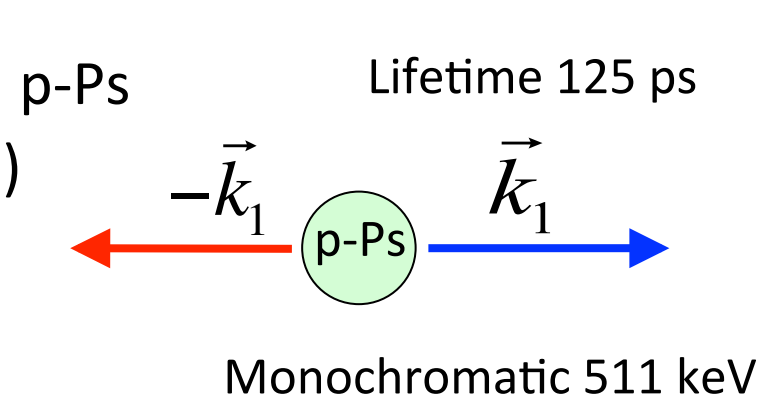


$$\vec{S} = 0 \text{ (Singlet)}$$

Para-positronium (p-Ps)

Spin=0 pseudo-scalar

$$p\text{-Ps} \rightarrow 2\gamma (, 4\gamma, \dots)$$



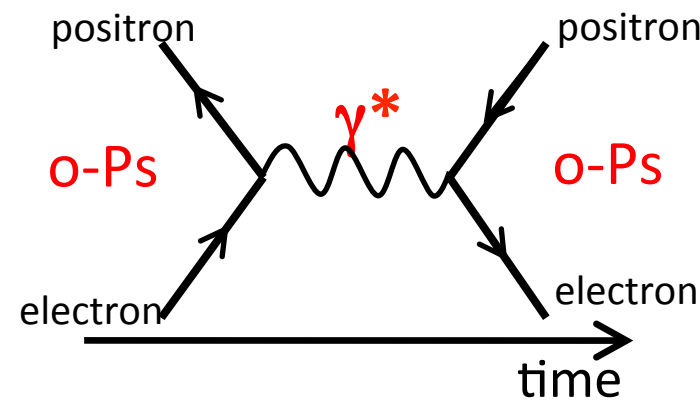
Positronium Hyperfine Splitting (Ps-HFS)

Energy difference between two spin eigenstates of the ground state Ps

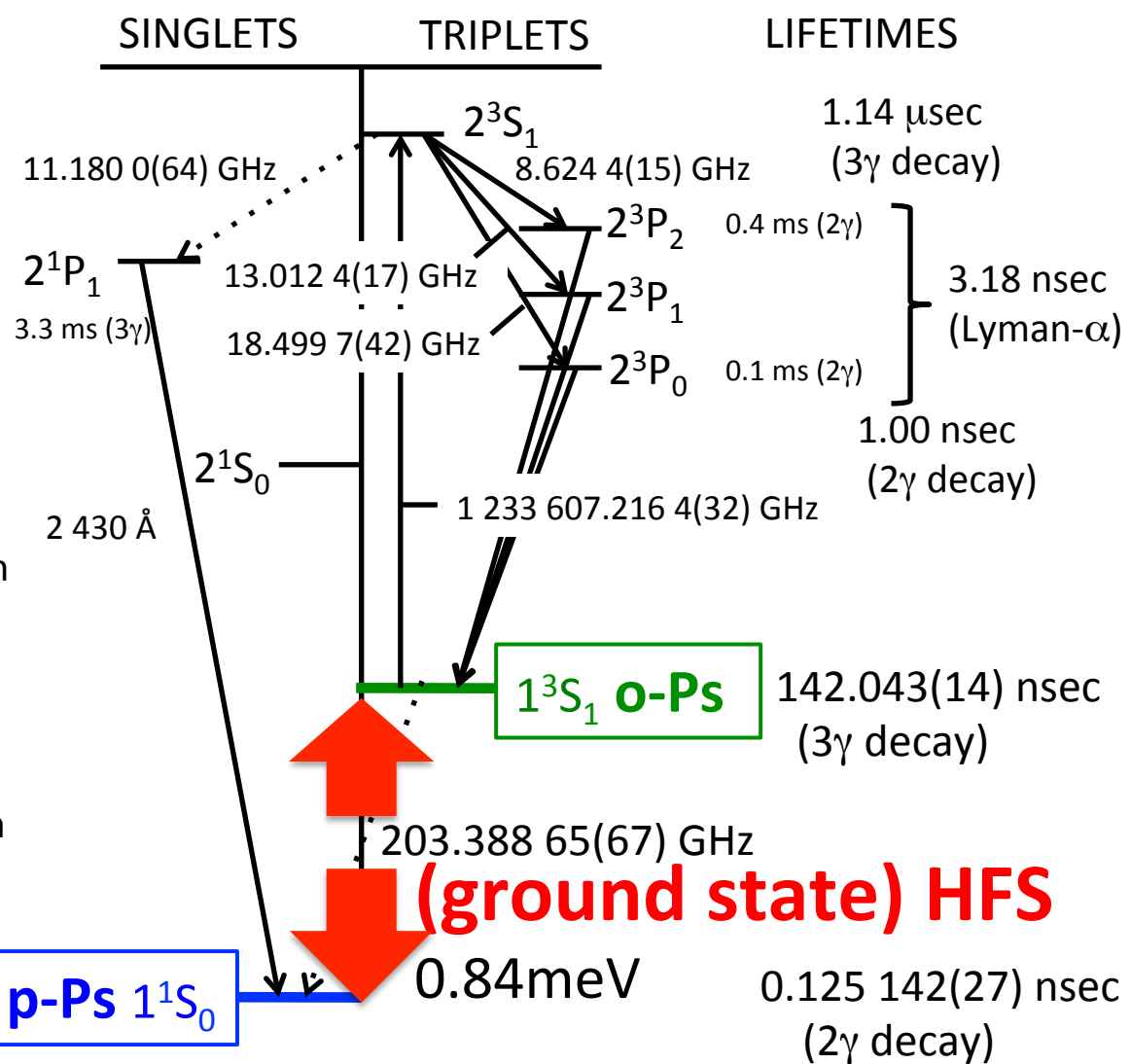
\rightarrow Ps-HFS (203 GHz)

$$\mu = e/2m \sigma$$

spin-spin interaction

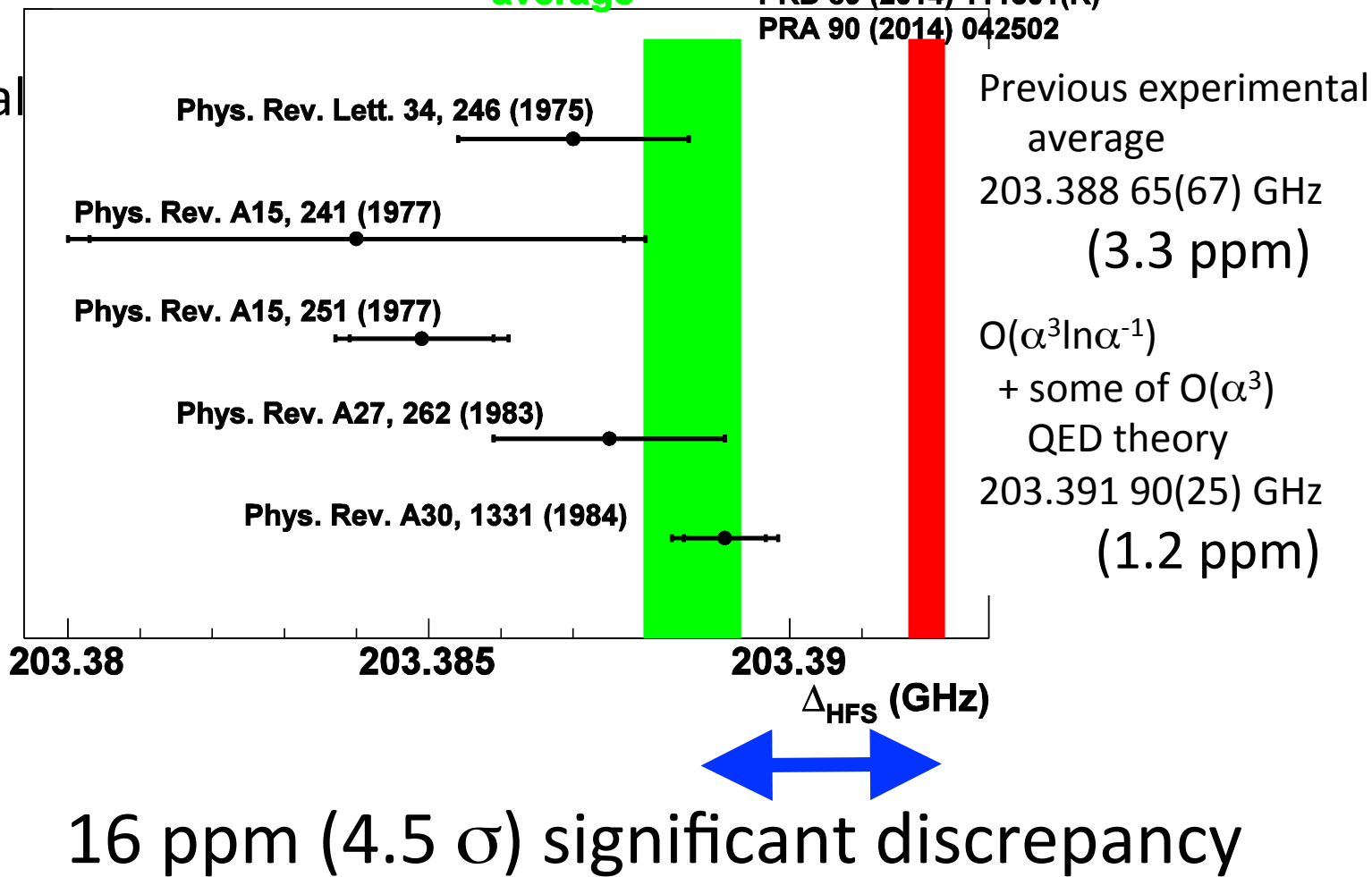


Quantum oscillation effect is also large (40%)



Discrepancy Between Previous Experiments and Theory

Previous experimental results are consistently lower than theory.



Possible reasons for the discrepancy

- Common systematic uncertainties in the previous experiments
 1. Non-uniformity of the magnetic field.
 2. Underestimation of material effects. Unthermalized o-Ps can have a significant effect especially at low material density. *cf. o-Ps lifetime puzzle (1990's)*

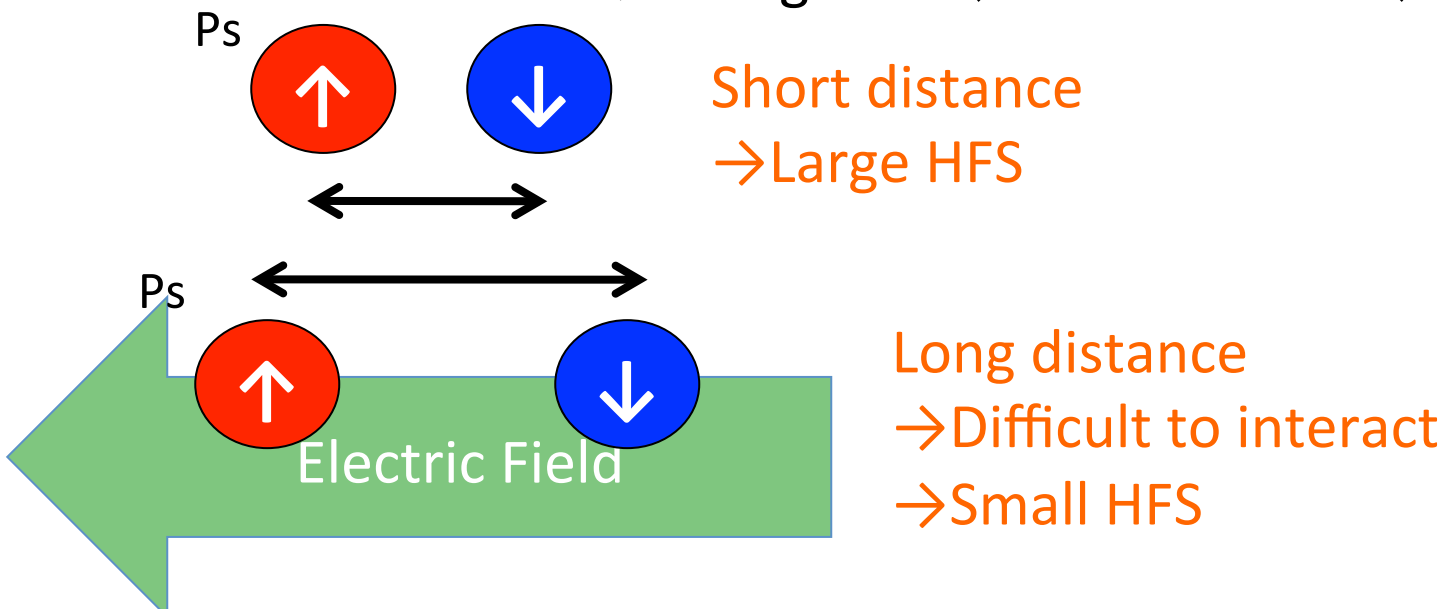
We introduced new methods to reduce these systematic errors.

- Need new development on calculation of bound-state QED or New physics beyond the Standard Model.

- Positronium Hyperfine Splitting (Ps-HFS)
- Material effect and Ps thermalization
- Our New Experiment
- Analysis and Results
- Prospects & conclusion

Material Effect on Ps-HFS

- Need material (in this case gas molecules) so that positron can get electron and form Ps.
- Ps-HFS
 - = Spin-spin interaction + quantum oscillation
 - Depends the distance between e^- and e^+ .
- Materials make electric field around Ps
 - Change the distance of the electron and the positron
 - Change HFS (The Stark Effect)



Estimation of Material Effect in previous experiments

- Need material (in this case gas molecules) so that positron can get electron and form Ps \rightarrow Ps feels electric field of material

Strength of the Stark Effect

$\propto \sim$ Collision rate with surrounding molecules

\propto (Density of surrounding molecules) \times (Ps velocity v) $^{3/5}$

→ If the Ps velocity is constant (under assumption that Ps is well thermalized), the material effect is proportional to gas density.

→ The Previous experiments

Phys. Rev. A
1984 **30** 1331
Ritter, Egan, Hughes et al.

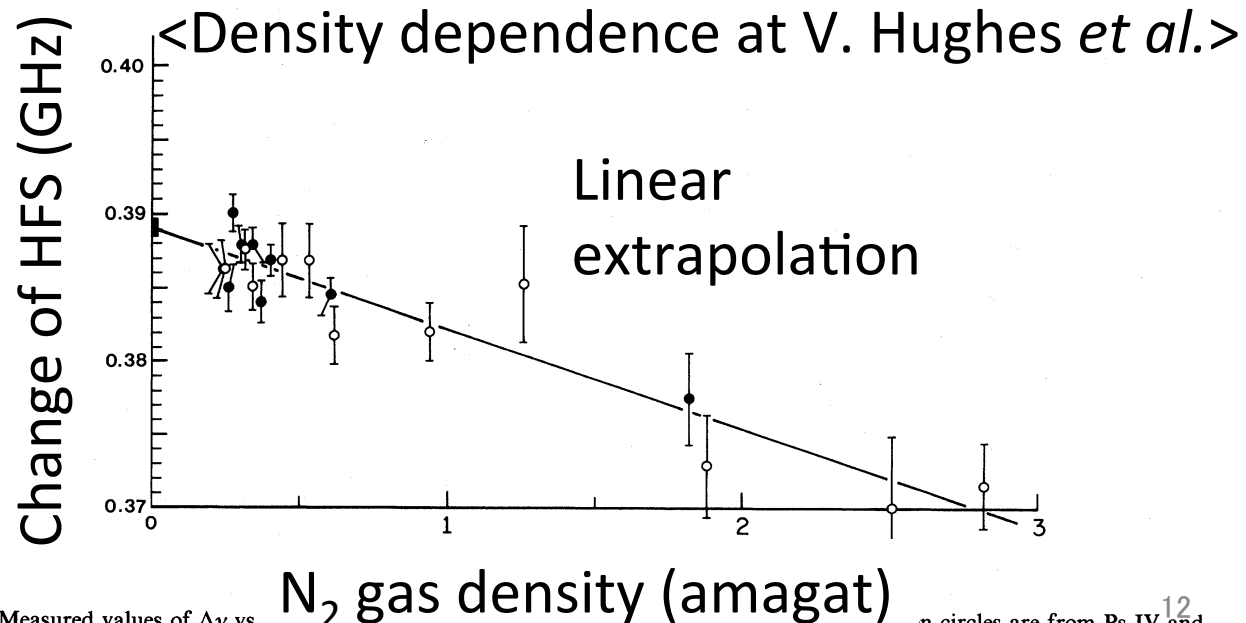


FIG. 7. Measured values of $\Delta\nu$ vs the closed circles are from the present work. The straight line is the best fit described in Eq. (14). ¹² n circles are from Ps IV and

Evolution of Ps velocity

Strength of the Stark Effect

$\propto \sim$ Collision rate with surrounding molecules

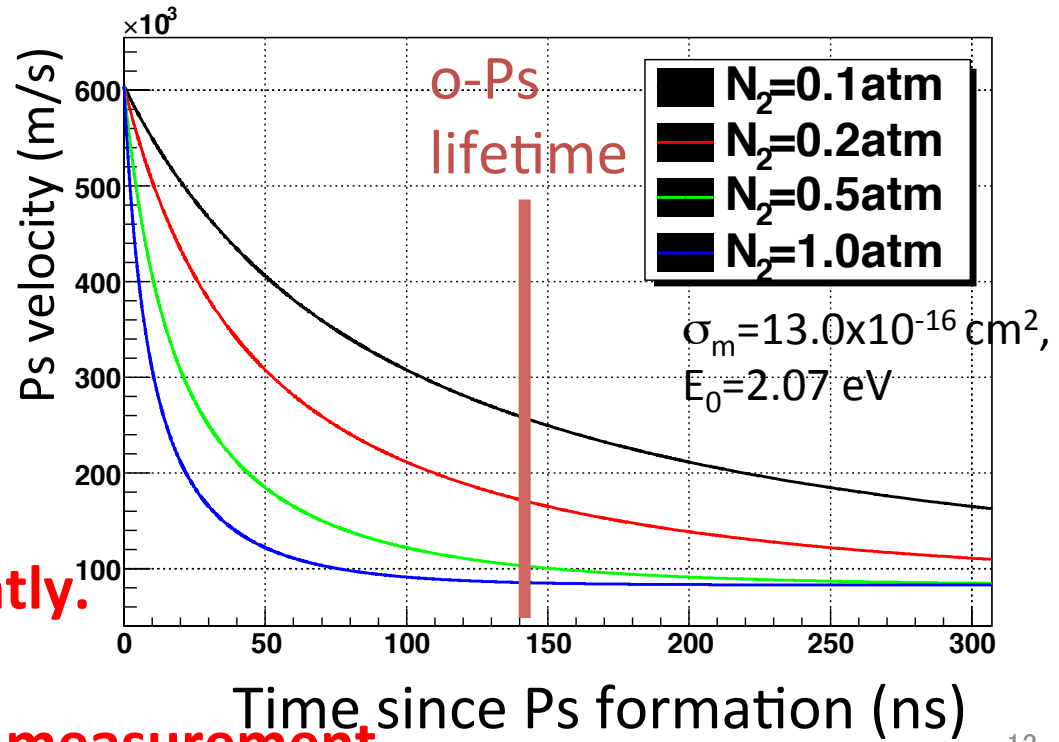
\propto (Density of molecules) \times (Ps velocity $v(t)$)^{3/5}

Ps loses its kinetic energy
and gets room temperature
= Thermalization

It takes longer time to
thermalize in lower density
 \rightarrow Linear extrapolation
could be a large O(10ppm)
systematic uncertainty

**→We also measured Ps
thermalization independently.
Used obtained result for
analysis of our new Ps-HFS measurement.**

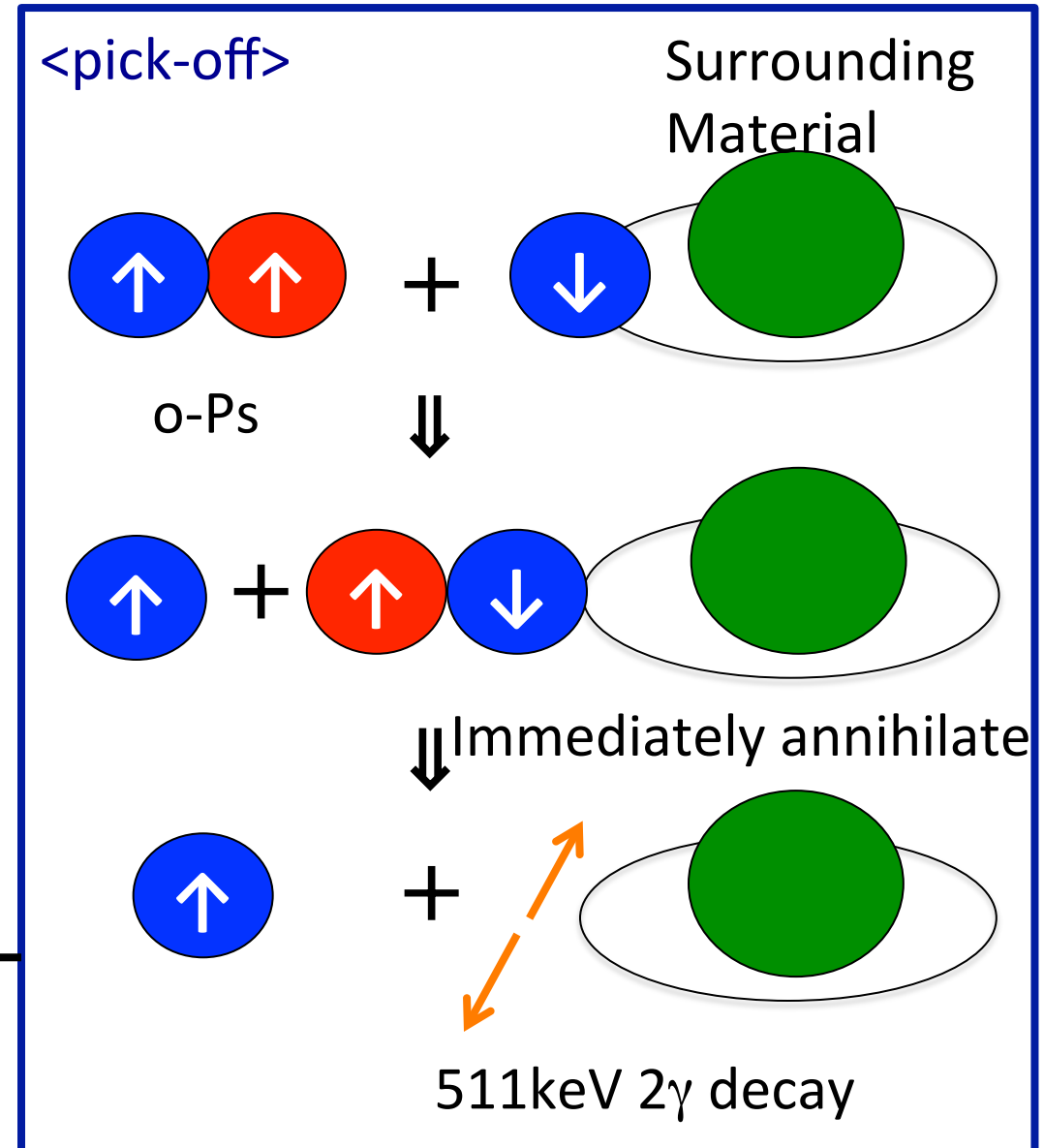
< Simulation of time evolution of Ps
velocity in N₂ gas >



How to measure the Ps velocity $v(t)$?

- Use pick-off of o-Ps
- $\text{pick-off}(t)$
= pick-off cross section
 \times density of material
 \times o-Ps amount (t)
 \times $v(t)^{0.6}$

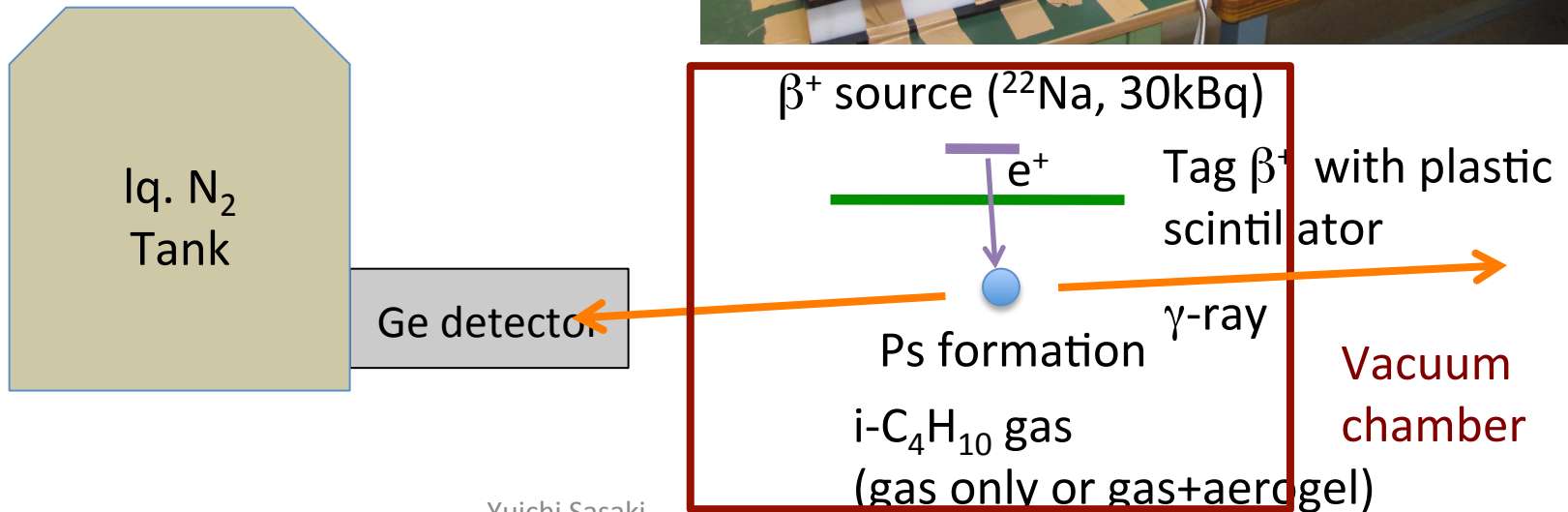
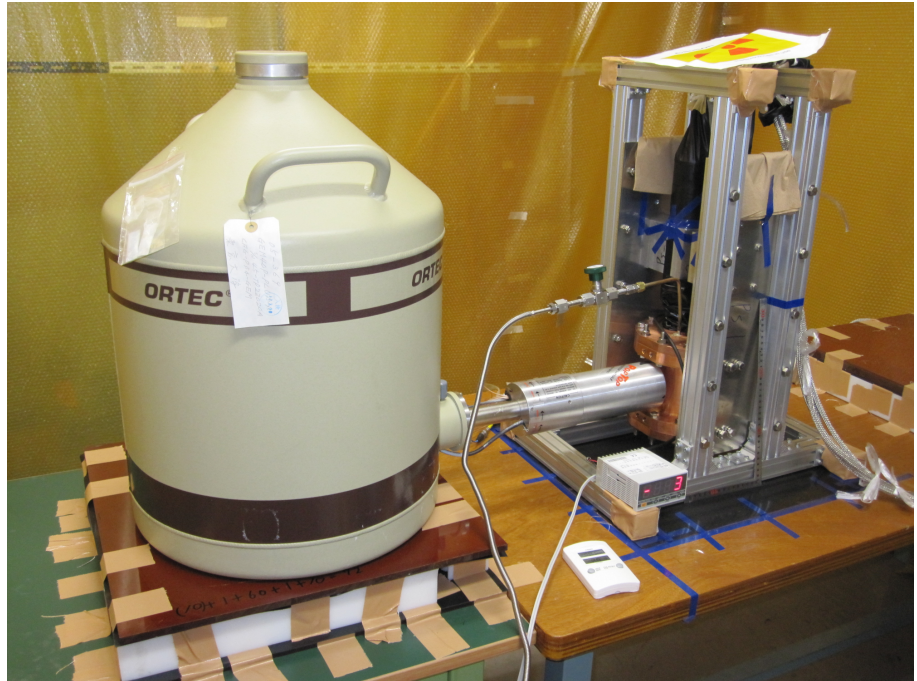
$$\frac{v(t)^{0.6}}{\infty} \frac{\text{pick-off } (2\gamma \text{ decay})}{\text{o-Ps } (3\gamma \text{ decay})}$$



Measurement of Ps Thermalization

Experimental Setup (Overall)

- Timing; START by Plastic Scintillator & STOP by Ge detector
- Stop e^+ in the gas and form Ps
- Source is inside the vacuum chamber.
- Change thermalization condition by changing the gas pressures.



Estimate amounts of o-Ps and pick-off

1, Make energy spectrum at each timing window

2, o-Ps is normalized at continuous region (480—500 keV).

3, 511 ± 3 keV is taken as pick-off

4, Efficiencies of o-Ps, pickoff, and pileup are estimated by MC simulation.

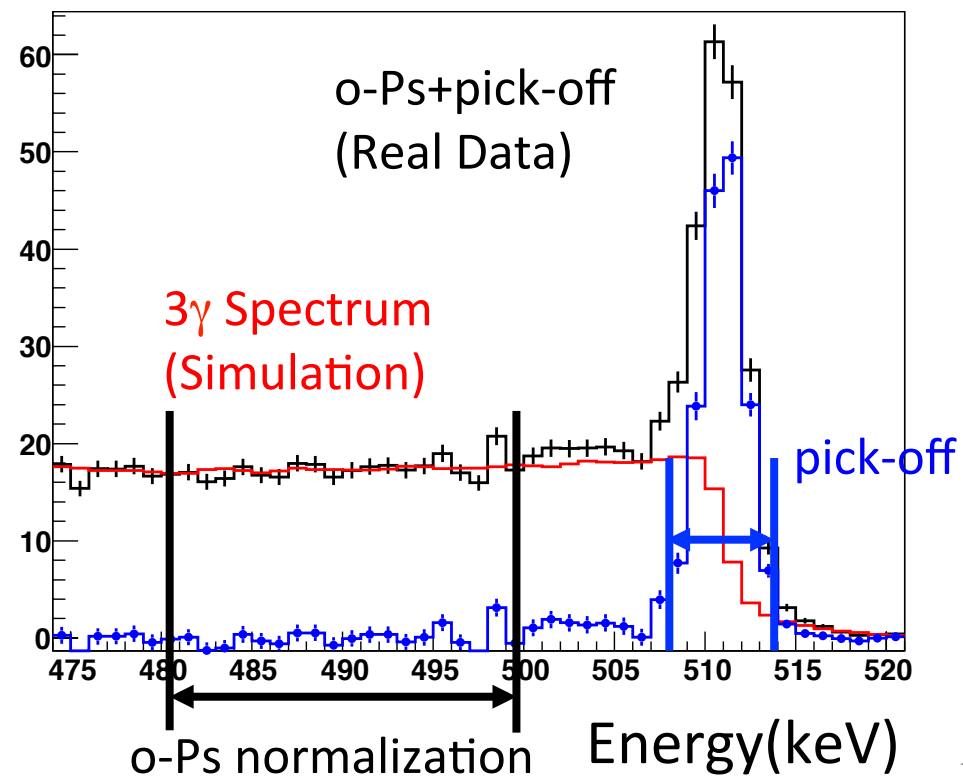
Isobutane only / Isobutane + aerogel measurement.

Change gas pressure, measure 2g/3g at various gas pressures

$$v(t)^{0.6}$$

pick-off (2γ decay)

$$\propto \frac{1}{\text{o-Ps} (3\gamma \text{ decay})}$$



Analysis of thermalization measurement

- Use timing window of 40–800 ns in order to avoid prompt peak. Use the following equation for fitting.

Parameter to fit : σ_m : Momentum-transfer cross section

$$\frac{d}{dt} E_{av}(t) = -\sqrt{2m_{Ps}E_{av}(t)} \left(E_{av}(t) - \frac{3}{2}k_B T \right) \left(\frac{8}{3}\sqrt{\frac{2}{3\pi}} \frac{2\sigma_m n}{M} + \alpha \left(\frac{E_{av}(t)}{k_B T} \right)^\beta \right)$$

from J. Phys. B **31** (1998) 329 Y. Nagashima, et al. M : mass of molecule

Aerogel term

m_{Ps} : Ps mass
 n : gas density

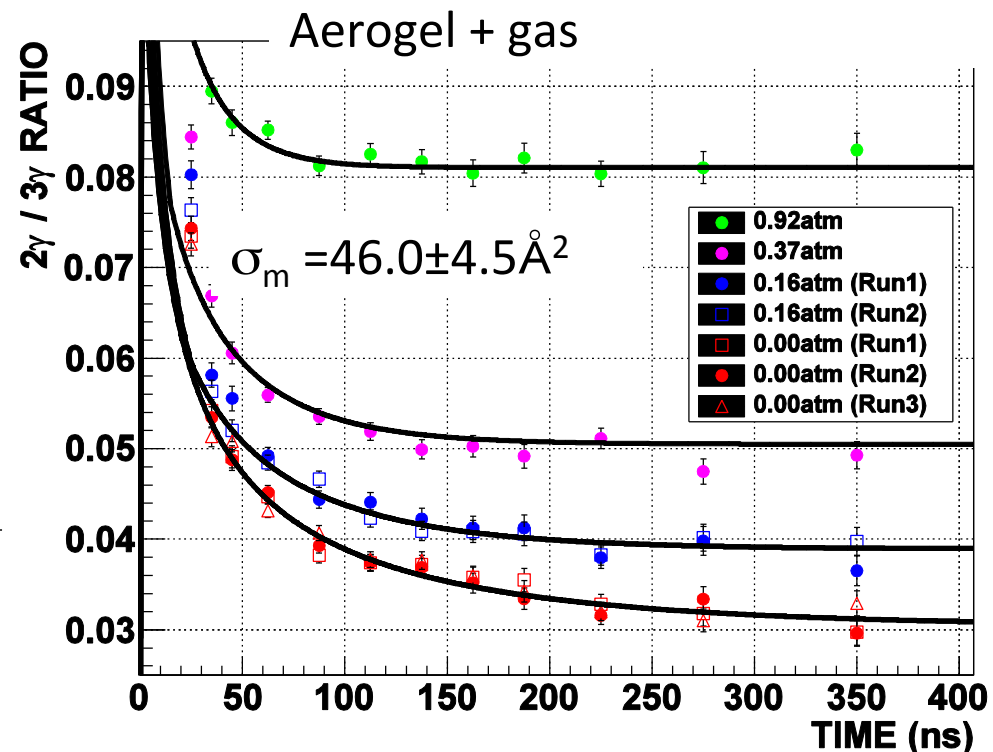
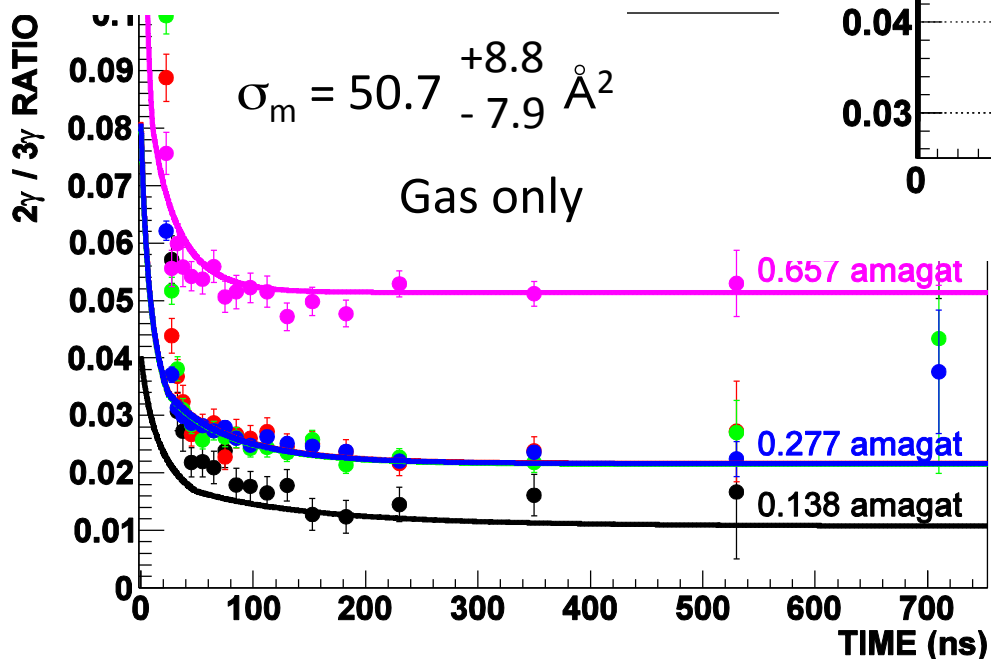
- Thermalization of Ps before 40 ns, where kinetic energy is high (>0.15 eV), has been already measured by Doppler Broadening Spectroscopy (DBS) method to be $\sigma_m = 146 \pm 11 \text{ \AA}^2$, $E_0 = 3.1^{+1.0}_{-0.7}$ eV (initial kinetic energy)
DBS: Phys. Rev. A **67**, 022504 (2003)
- Isobutane has a rovibrational level at 0.17 eV. Value of σ_m can be different above (DBS) and below (pick-off) this level. → Fit with fixed initial condition of DBS result, but change σ_m at 0.17 eV.

$2\gamma/3\gamma$ fitting

Velocity dependence of pickoff rate in isobutane gas

$$\propto v^{0.6} (= E^{0.3})$$

Simultaneous fit of all gas densities



Consistent results from gas-only measurement and with aerogel measurement.

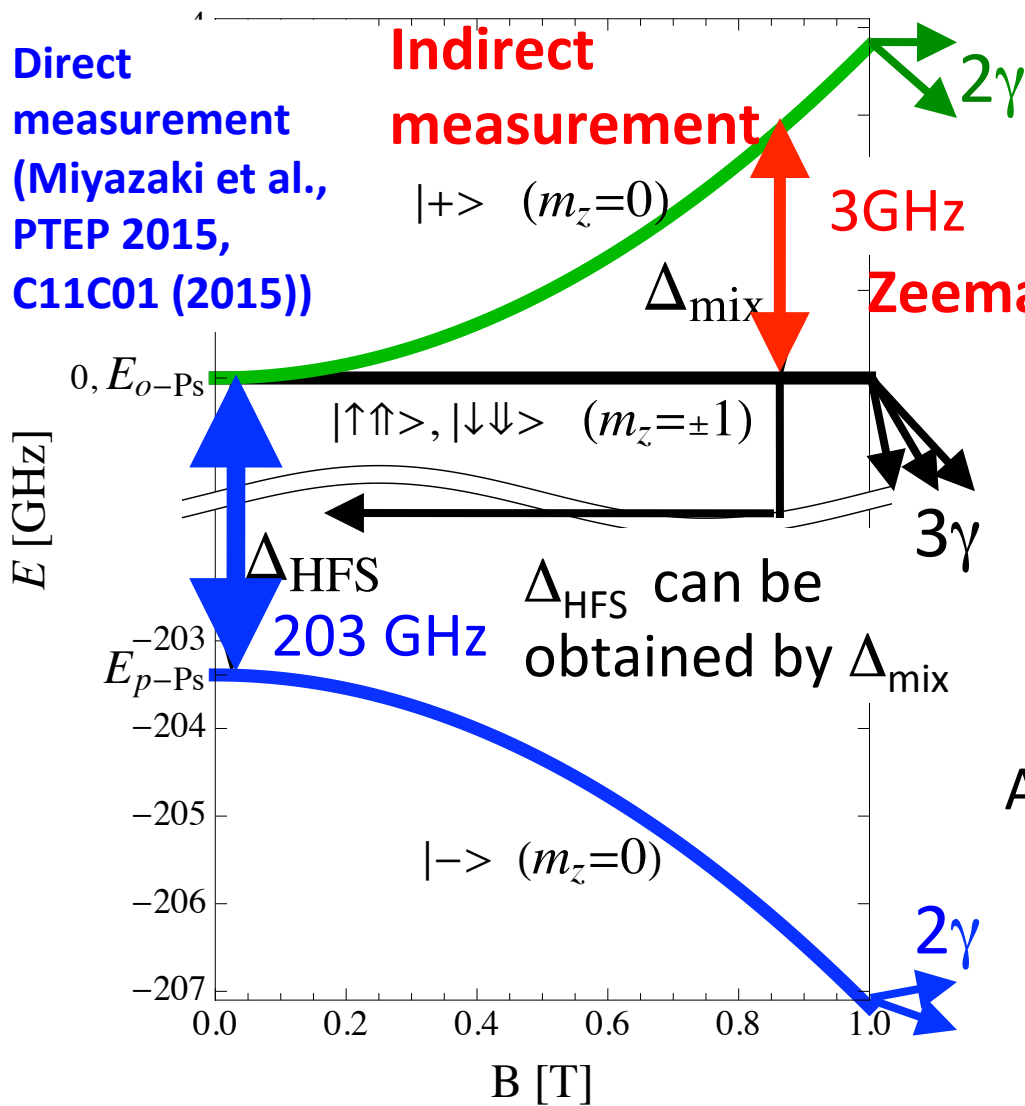
mean $\sigma_m = 47.2 \pm 3.9 \text{ \AA}^2$
systematic error 5.4 \AA

- Positronium Hyperfine Splitting (Ps-HFS)
- Material effect and Ps thermalization
- **Our New Experiment**
- Analysis and Results
- Prospects & conclusion

Experimental Technique

Indirect Measurement using Zeeman Effect

Direct measurement
(Miyazaki et al.,
PTEP 2015,
C11C01 (2015))



In a static magnetic field, the **p-Ps** state mixes with the **$m_z=0$** state of **o-Ps** (Zeeman effect).

Zeeman transition

→ **2 γ -ray annihilation (511 keV monochromatic signal)** rate increases.

This increase is our experimental signal.

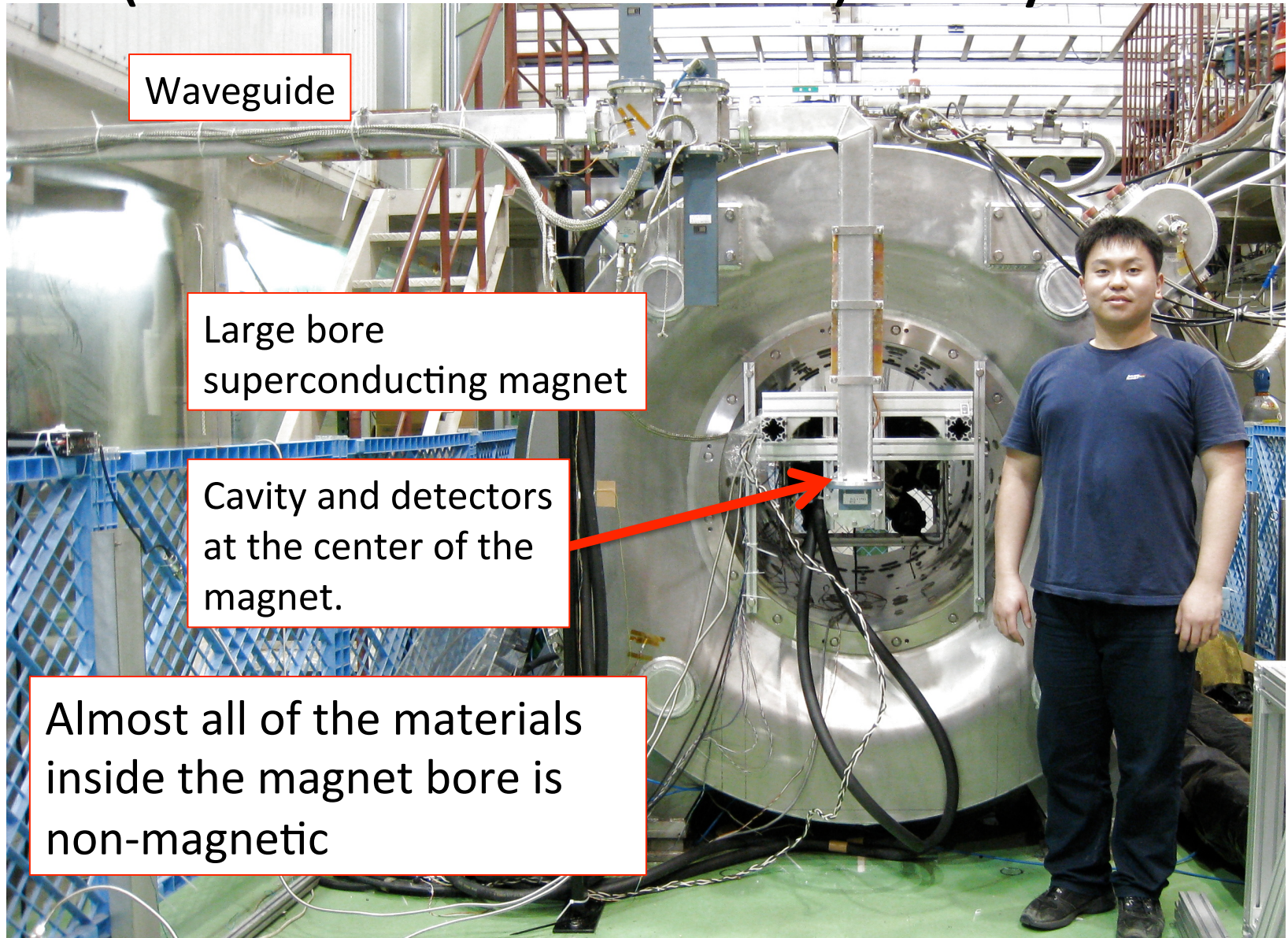
Approximately,

$$\Delta_{mix} \approx \frac{1}{2} \Delta_{HFS} \left(\sqrt{1 + 4x^2} - 1 \right)$$

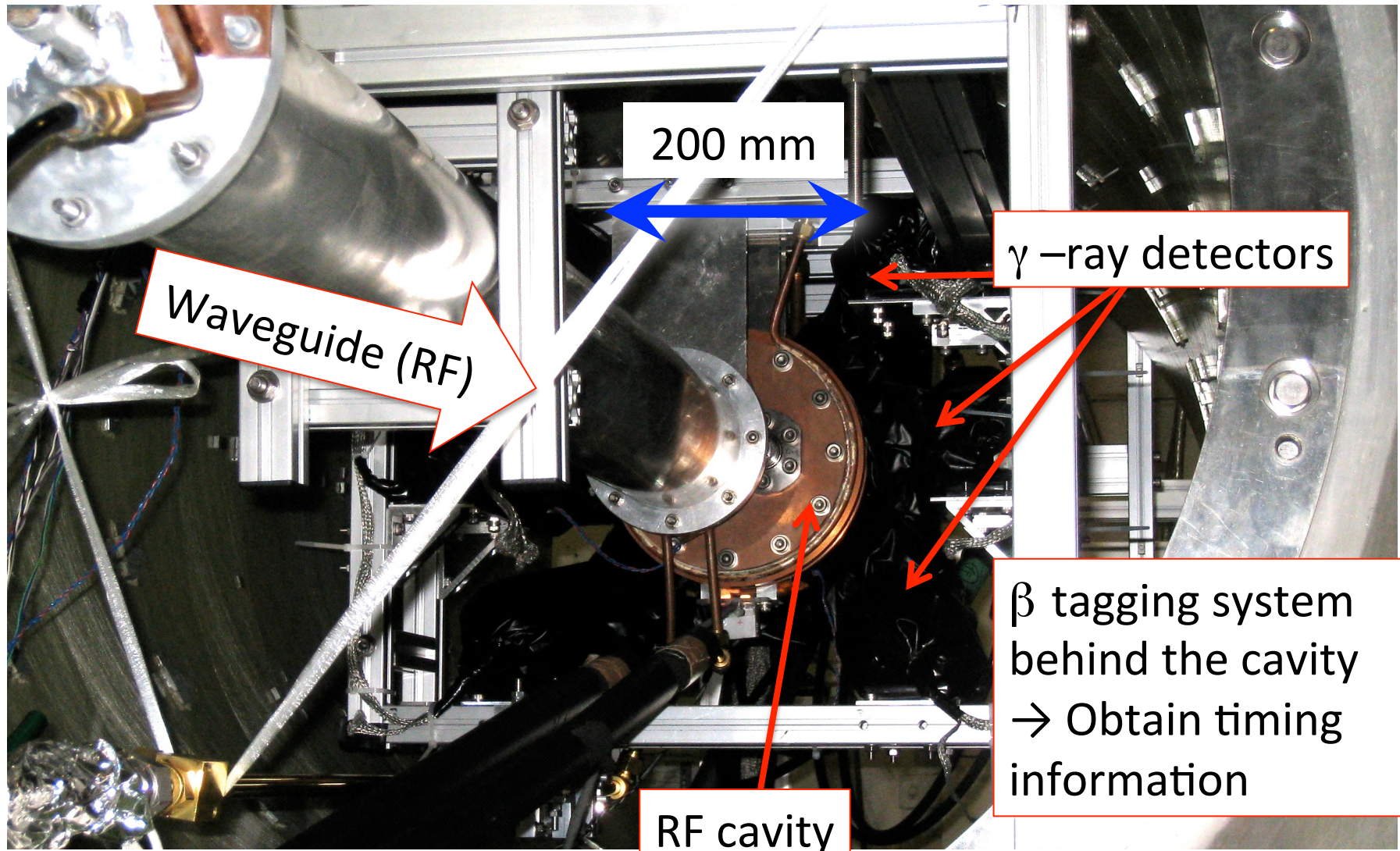
$x = \frac{g'\mu_B B}{h\Delta_{HFS}}$. This is not precise enough, so we solve time evolution of density matrix.

Measurement @ KEK CSC

(Jul 2010 – Mar 2013) ~3 years



Center of the magnet



Our new Experiment

High power RF
(500W CW)

β -tagging system
→Solve systematic error
from *non-thermalized Ps.*

Large bore
superconducting
magnet +
compensation coils
→Solve systematic
error from
non-uniformity of
magnetic field.

High performance
 γ -ray detectors
→Solve systematic
error from *non-thermalized Ps.*

waveguide

B (0.866 T)

1.5 ppm uniformity
and 1 ppm stability

^{22}Na
(1 MBq)

PMT

RF cavity
(Filled with
pure i-C₄H₁₀)

10 cm

Our new Experiment

High power RF
(500W CW)

β -tagging system
→Solve systematic error
from *non-thermalized Ps.*

Large bore
superconducting
magnet +
compensation coils
→Solve systematic
error from
non-uniformity of
magnetic field.

High performance
 γ -ray detectors
→Solve systematic
error from *non-thermalized Ps.*

waveguide

B (0.866 T)

1.5 ppm uniformity
and 1 ppm stability

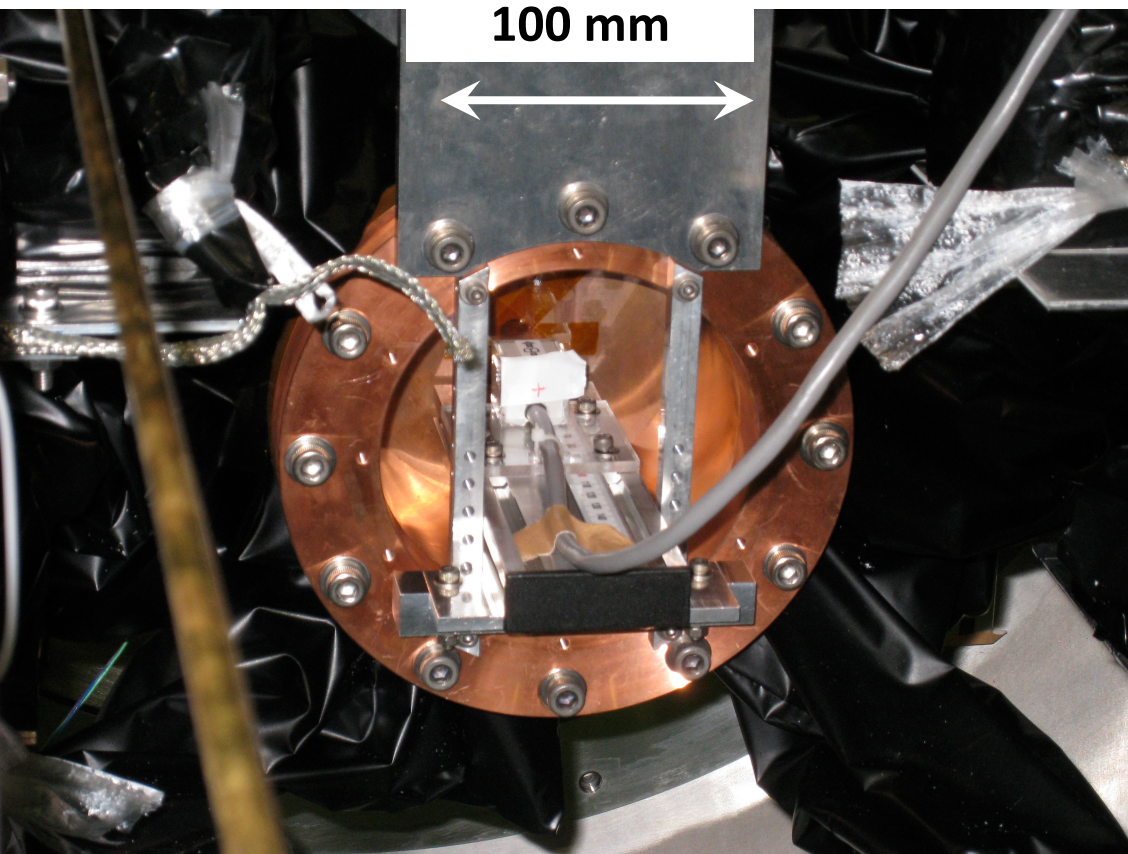
PMT
PMT

^{22}Na
(1 MBq)

PMT

RF cavity
(Filled with
pure i-C₄H₁₀)

Magnetic Field



Made the map of
the magnetic field.

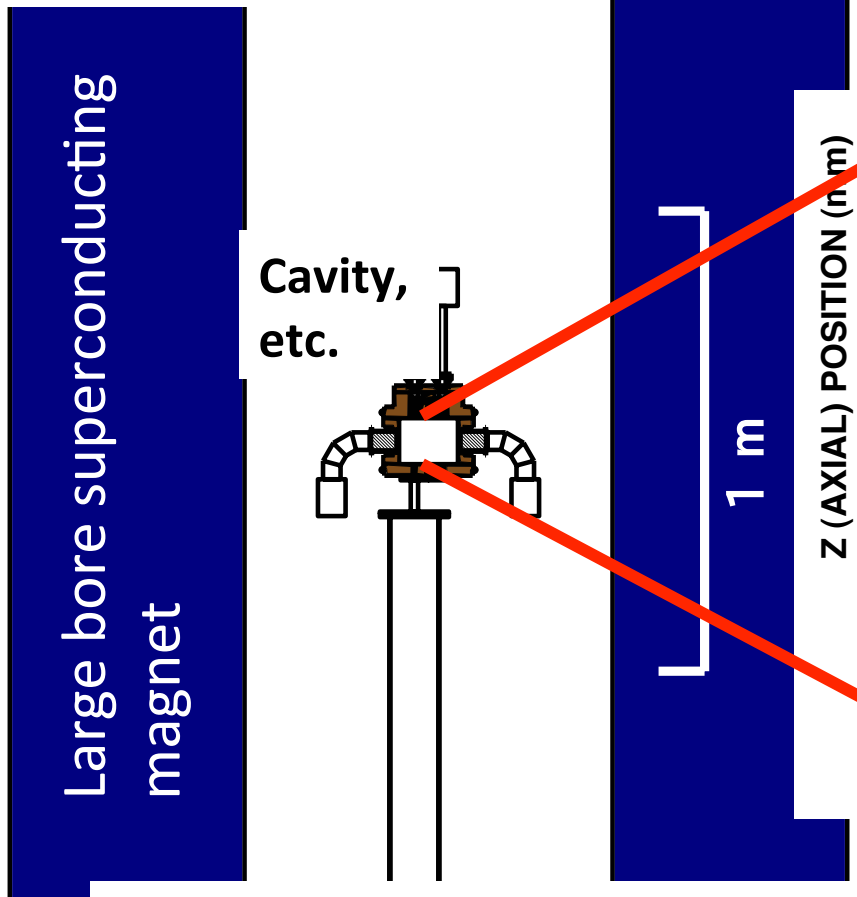
Measured the magnetic
field at 310 points in the RF
cavity using NMR probe.



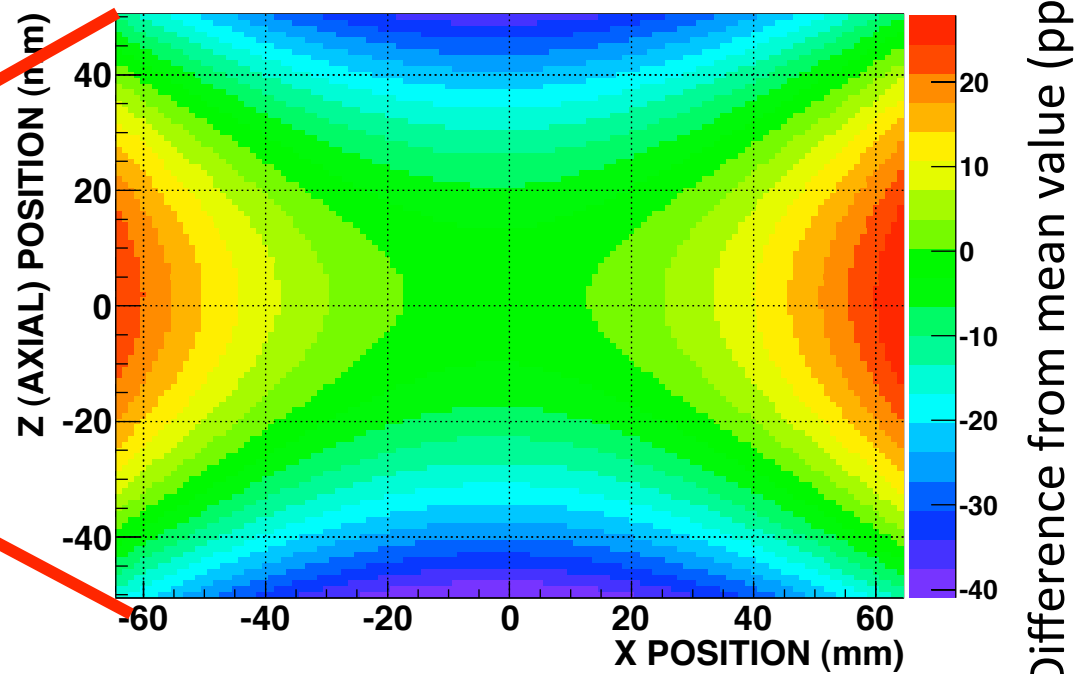
200 mm

Uniformity of the Magnetic Field

Top view



Magnetic field distribution on $Y=0$ plane. (O is the center of the cavity)

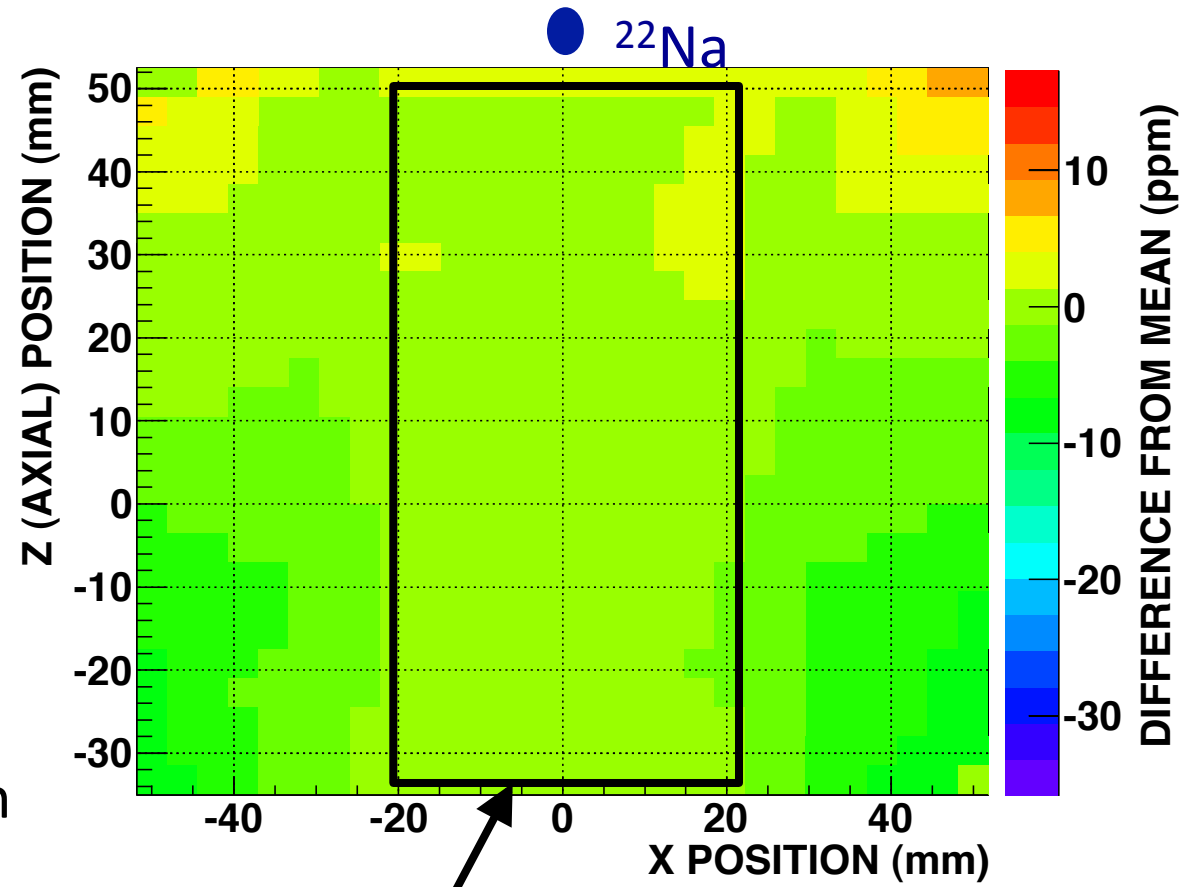
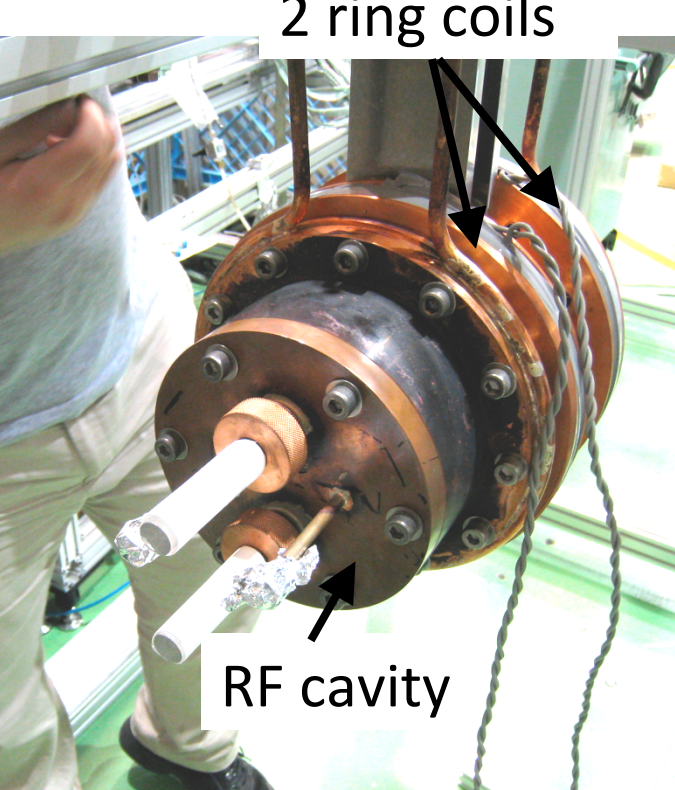


- Non-uniformity in the Ps formation volume is 10 ppm (RMS) without any compensation coil.
- Effects of PMT (strongly magnetic) and jigs are also big. Compensation coil was made to get O(ppm) homogeneity including these materials.

Compensation Magnet

Magnetic Field distribution (Horizontal)

(O is the center of the cavity)



- 2 ring-coils are rolled on the cavity flange.
- They make the opposite field and reduce the gradient.

1.5 ppm (RMS) uniformity in the Ps formation volume (10.4 ppm w/o coils)
→ 3.0 ppm systematic errors ($\mathcal{P}_{\text{HFS}} \mu B^2$).
27

Our new Experiment

High power RF
(500W CW)

β -tagging system
→Solve systematic error
from *non-thermalized Ps.*

*Large bore
superconducting
magnet +
compensation coils*
→Solve systematic
error from
*non-uniformity of
magnetic field.*

*High performance
 γ -ray detectors*
→Solve systematic
error from *non-thermalized Ps.*

waveguide

B (0.866 T)

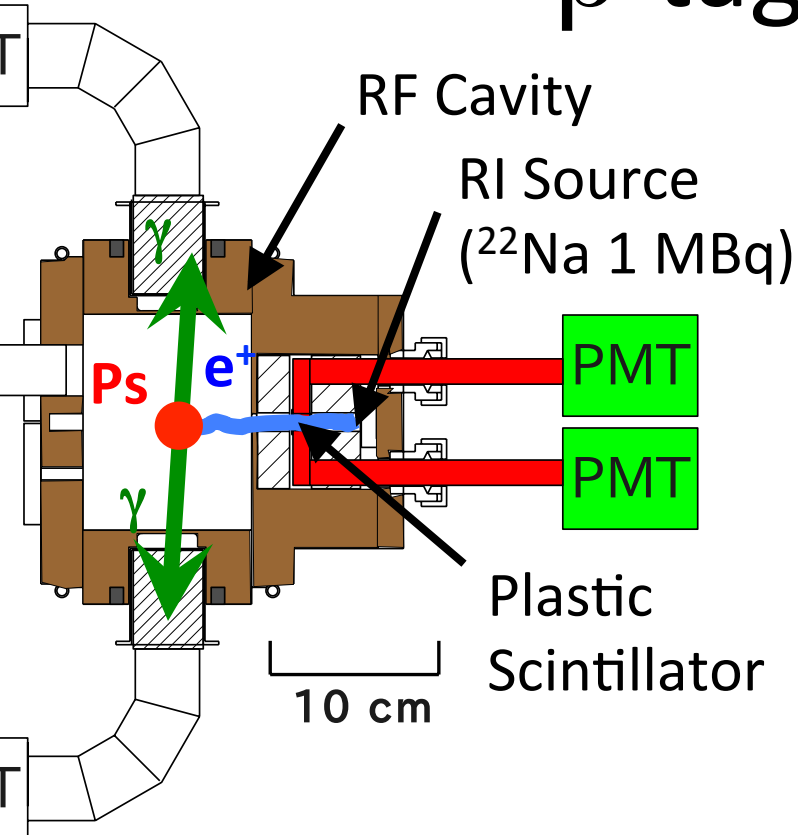
PMT
PMT

1.5 ppm uniformity
and 1 ppm stability

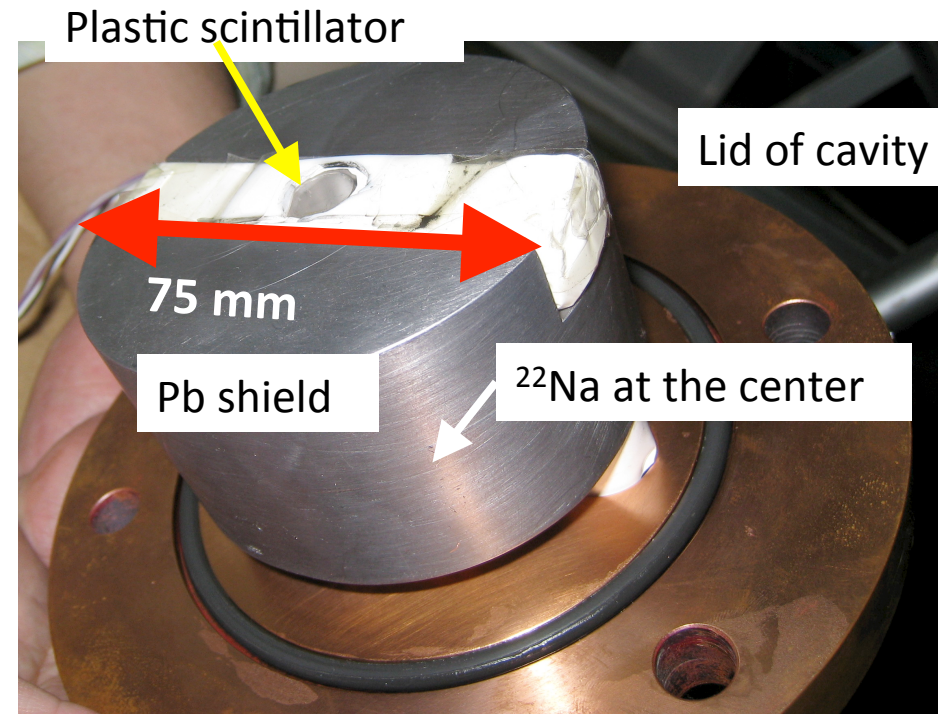
^{22}Na
(1 MBq)

RF cavity
(Filled with
pure i-C₄H₁₀)

β -tagging system

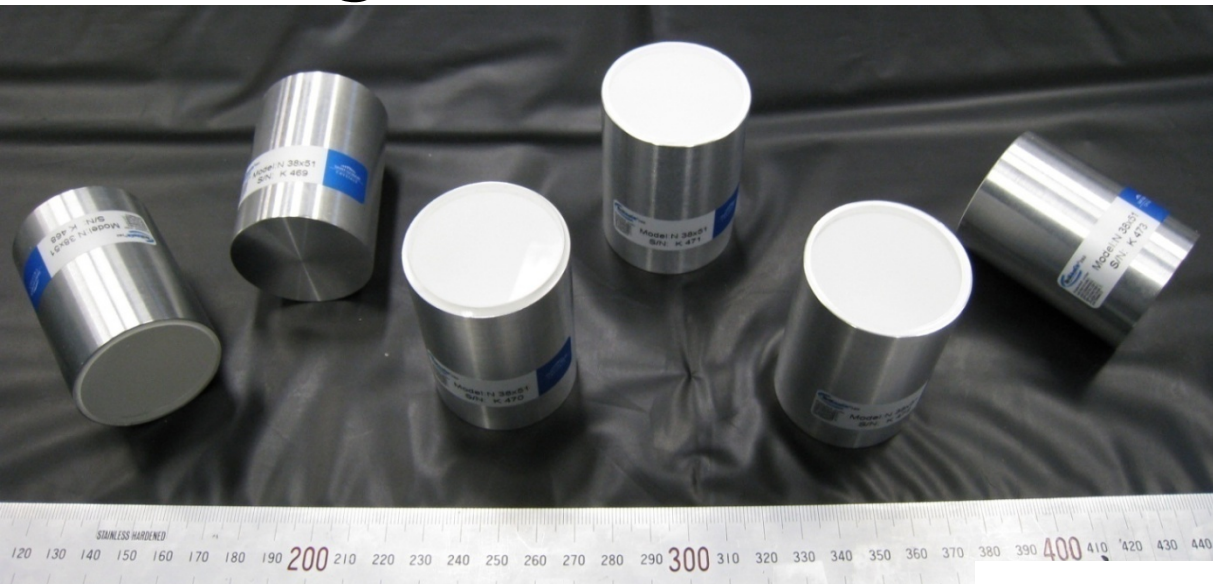


- Tag e^+ from the ^{22}Na by thin (0.1 mm) plastic scintillator.
 $\rightarrow t=0$



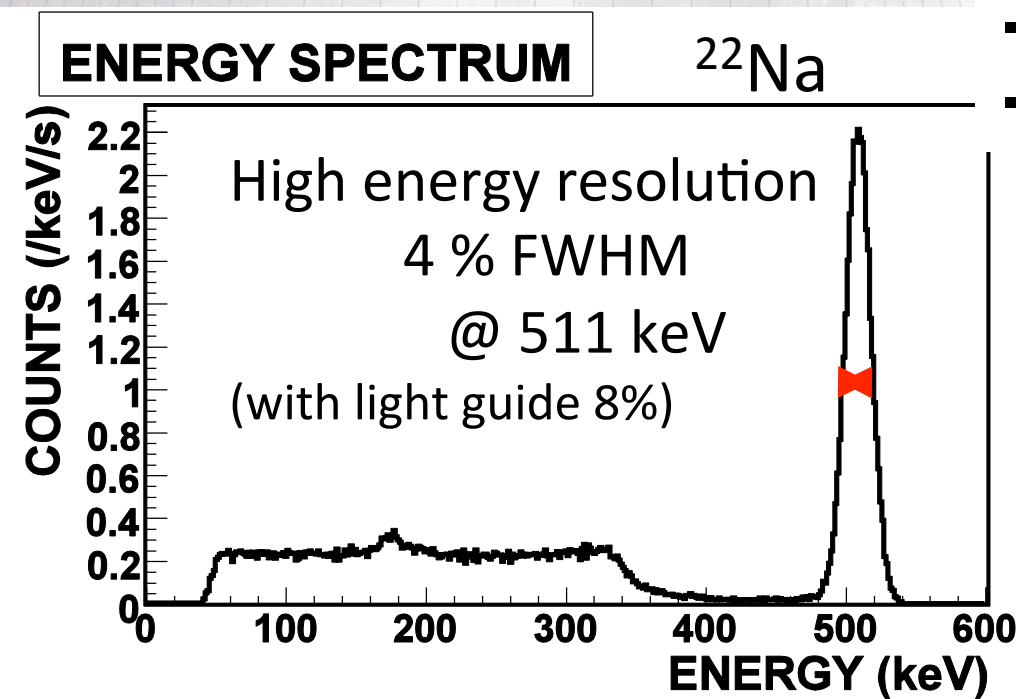
- DAQ Trigger is made by coincidence of e^+ tag signal and γ -ray detection.
- Time difference of these signals is Ps life time of each event.

γ -ray detectors $\sim \text{LaBr}_3 \sim$

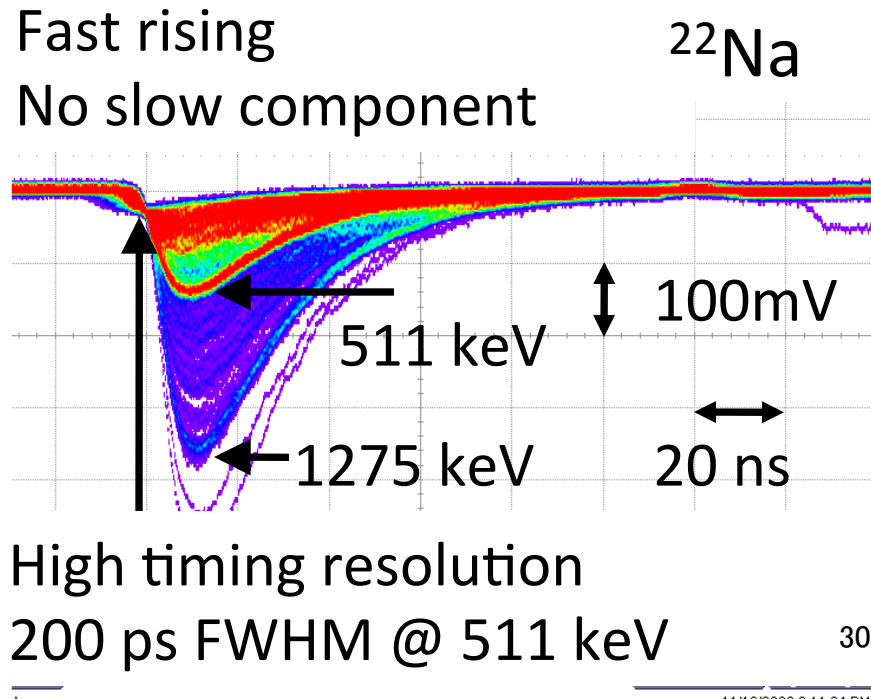


$\text{LaBr}_3(\text{Ce})$ scintillator x 6
(38.1 mm in diam., 50.8 mm long)

Guide scintillation light by UVT
(Ultra-Violet Transmitting)
light guides.
Detect photons by Fine-mesh
PMTs in the magnetic field.



- Fast rising
- No slow component



Treat Ps thermalization correctly by introducing a completely new concept (Timing Information)

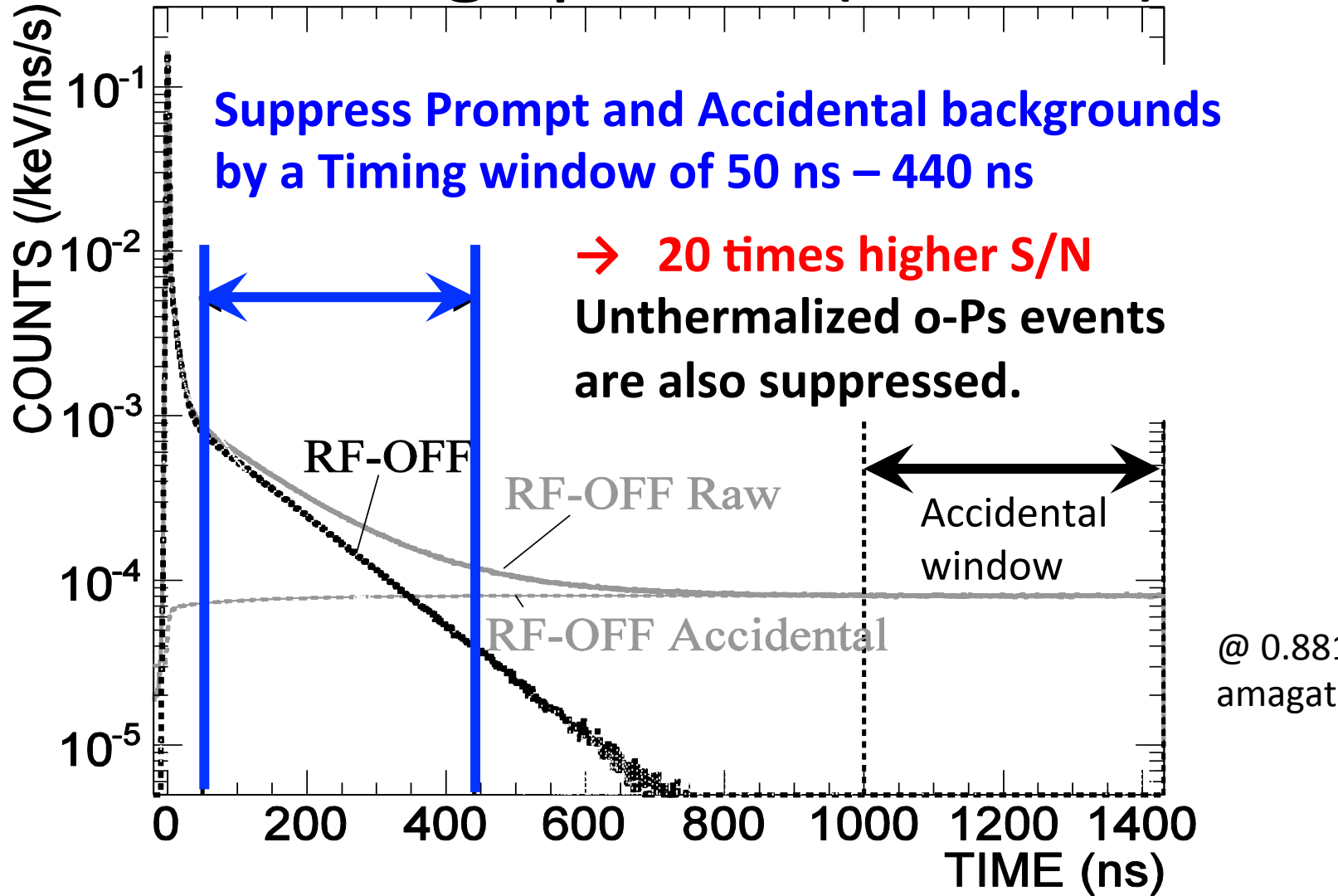
- Underestimation of Ps thermalization effect could be a large systematic error of $O(10\text{ppm})$.
- Obtain timing information, which was not considered in the previous experiments.
 - Reduce the effect from non-thermalized o-Ps.

Analysis can treat Ps thermalization correctly by measuring the time evolution precisely.

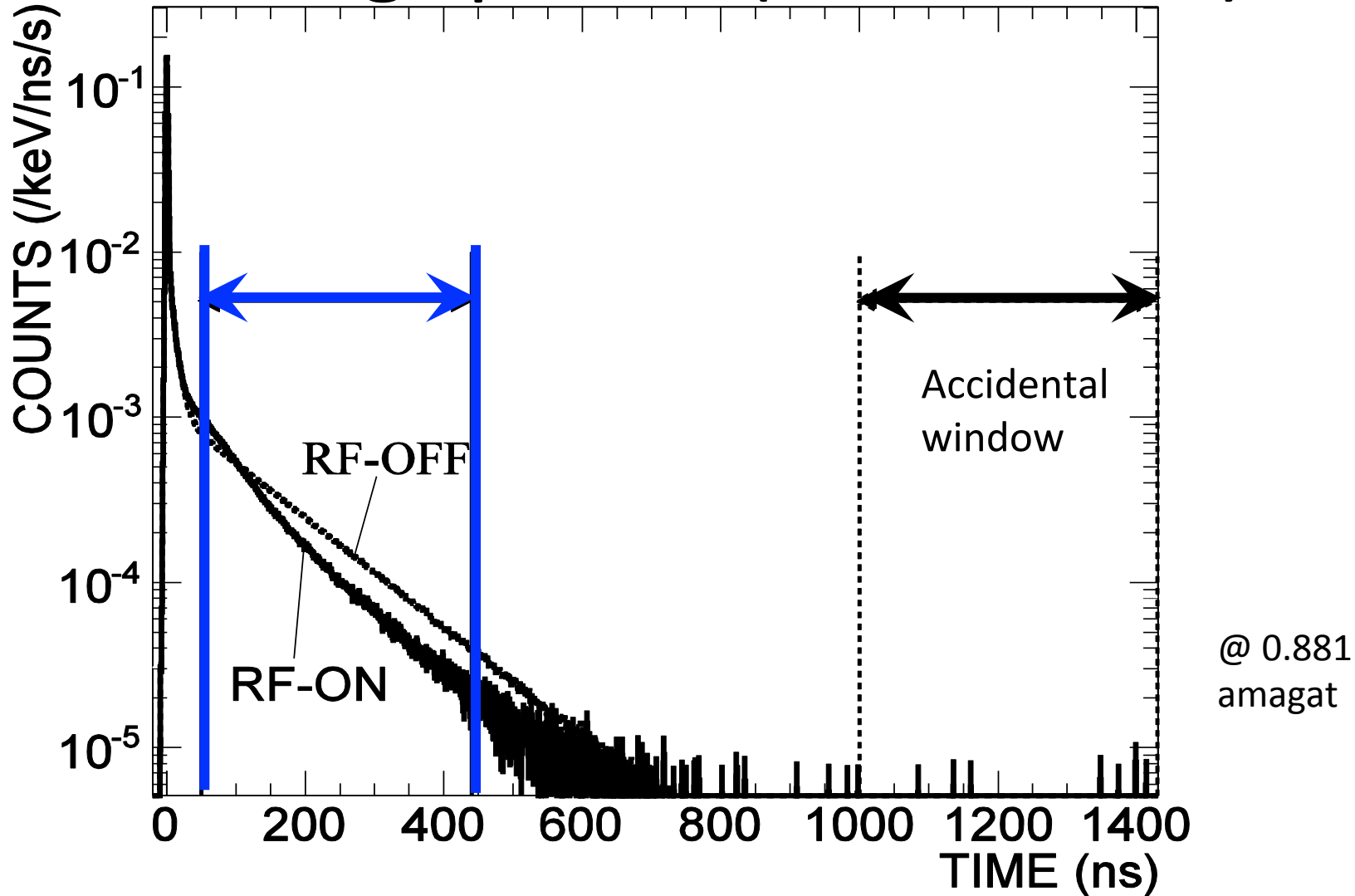
The first precision measurement of Ps-HFS using timing information

- Positronium Hyperfine Splitting (Ps-HFS)
- Material effect and Ps thermalization
- Our New Experiment
- **Analysis and Results**
- Prospects & conclusion

Timing spectra (RF-OFF)

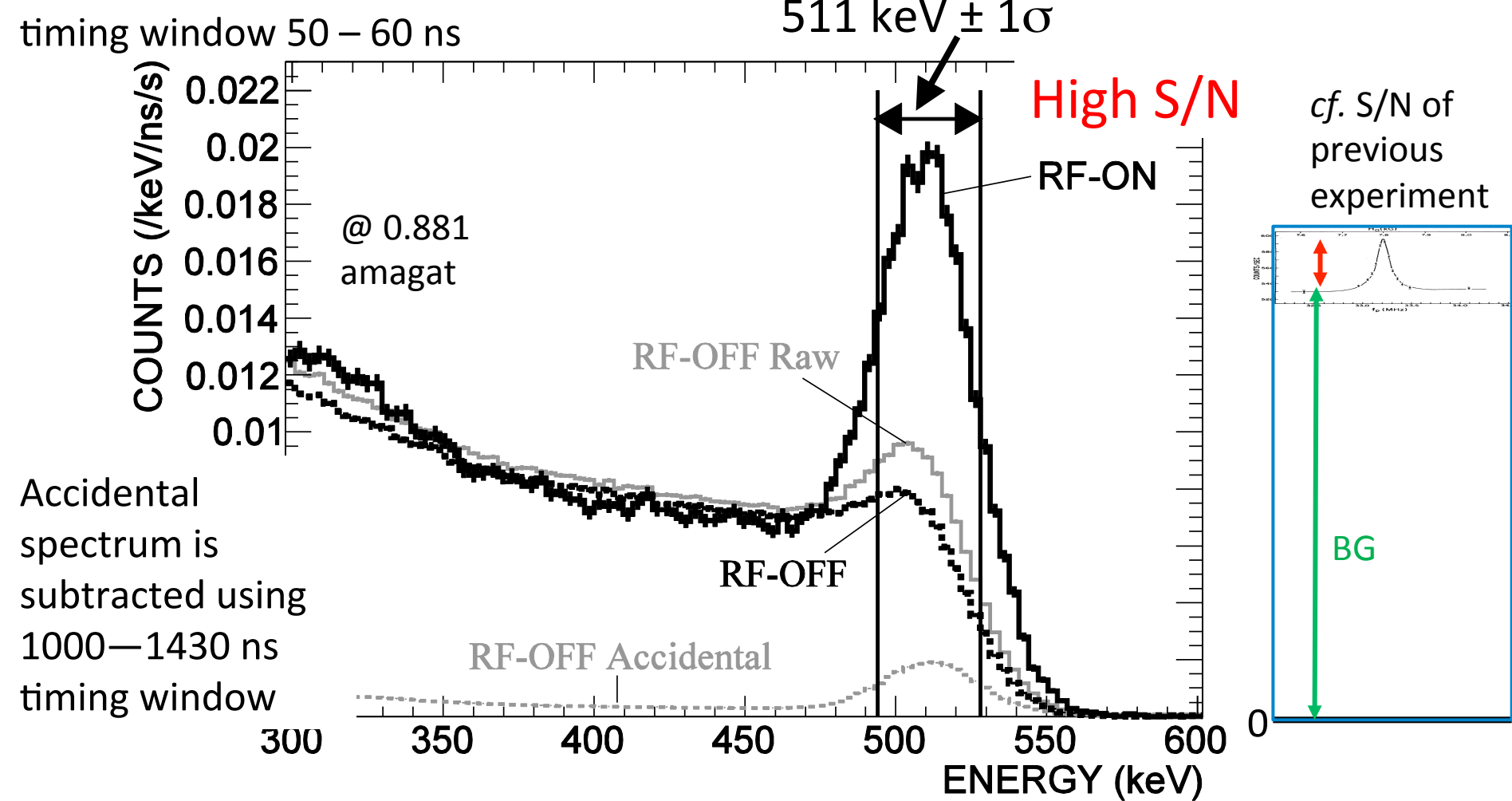


Timing spectra (RF-ON/OFF)



Lifetime is clearly shortened by RF due to the Zeeman transition.

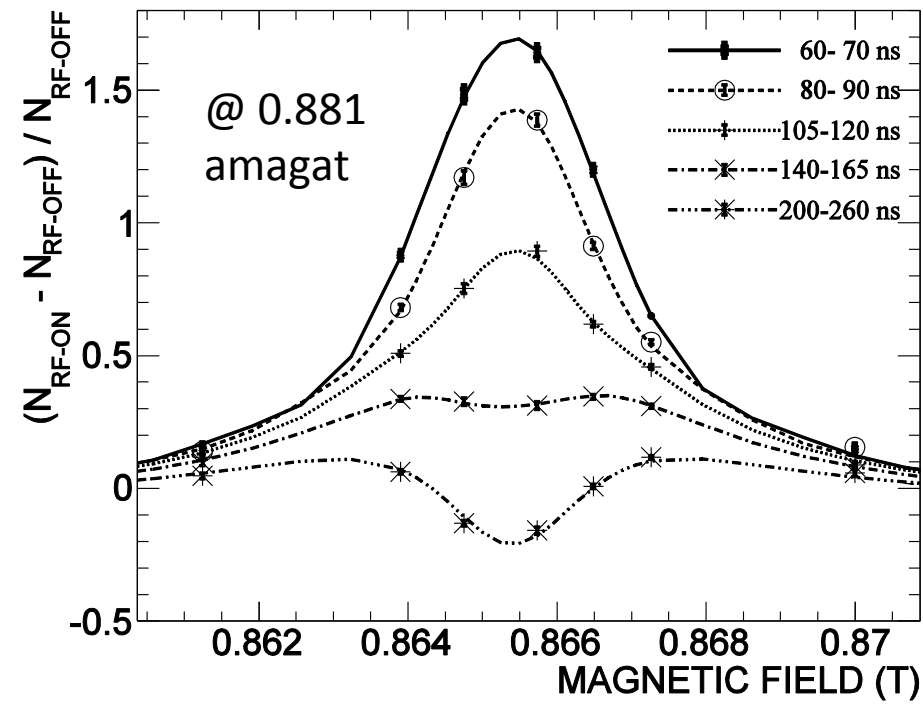
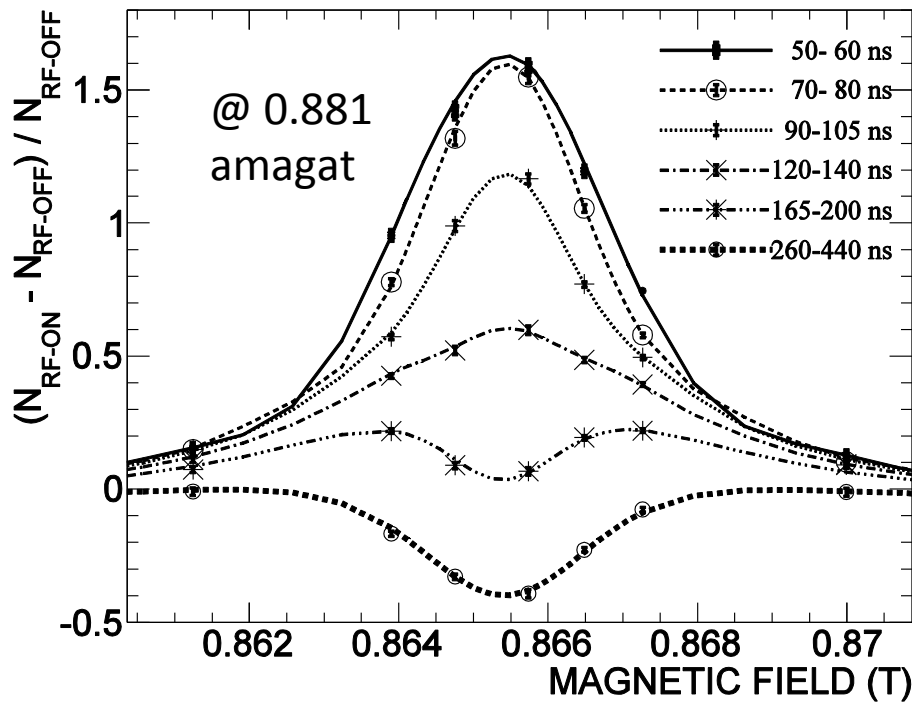
Energy spectra



2γ decay rate increases because of the Zeeman transition. Calculate $(\text{RF-ON} - \text{RF-OFF}) / \text{RF-OFF}$ of count rates in the $511 \text{ keV} \pm 1\sigma$ energy window.

Resonance line

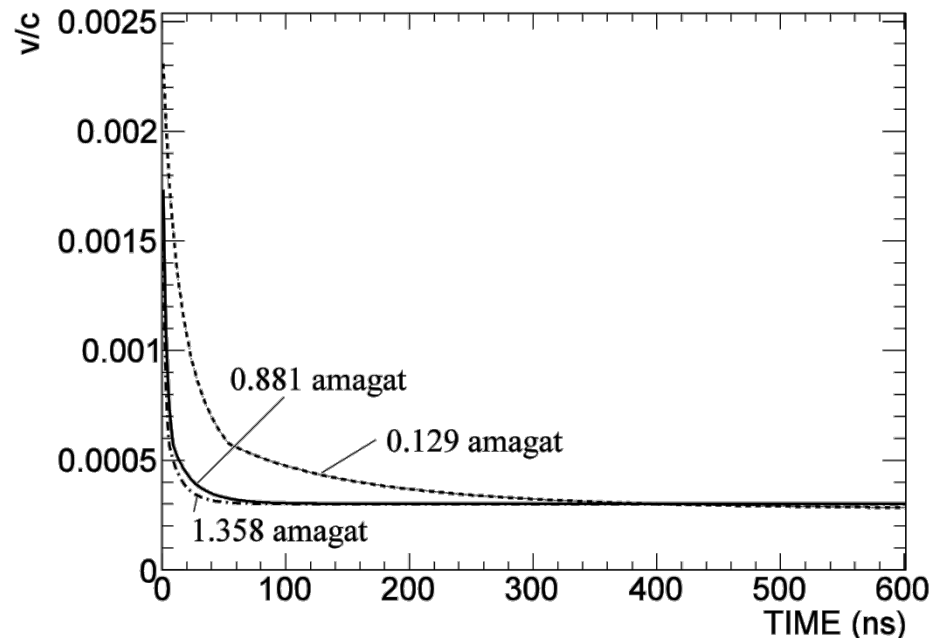
- Scanned by Magnetic Field with the fixed RF frequency and power.
- 50–440 ns is divided to 11 sub timing windows.
- Simultaneous fit of all of the gas density, magnetic field strength, and (sub) timing windows.
- Time evolution of Δ_{HFS} and pick-off rate ($\propto nv^{3/5}$) is taken into account.



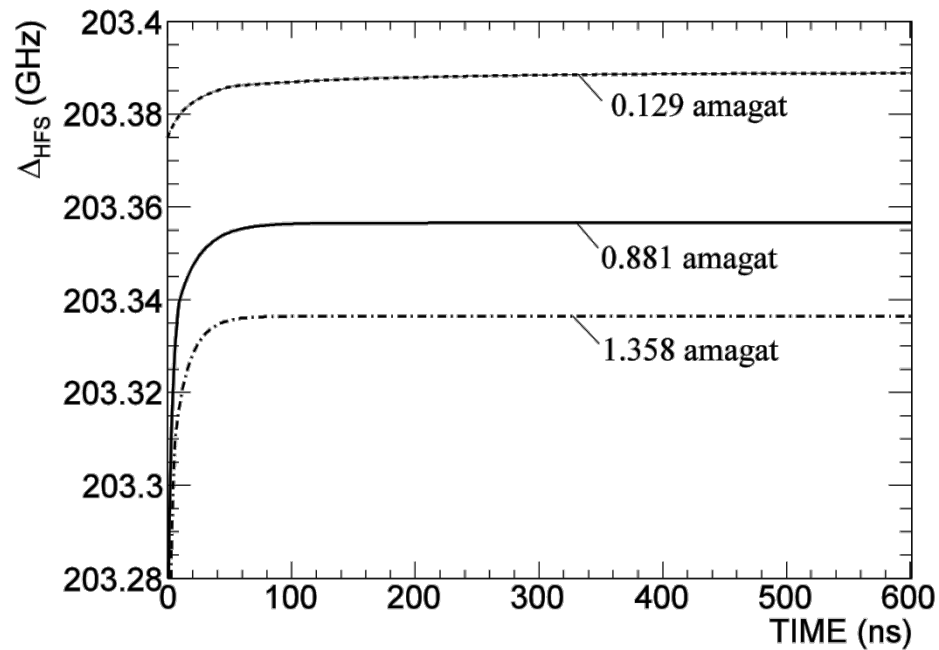
$$\Delta_{\text{HFS}} = 203.394 \text{ 2(16) GHz (8.0 ppm)} \chi^2/\text{ndf} = 633.3 / 592 (\text{p} = 0.12)$$

Time evolution of some parameters (fitting results)

Ps velocity / c



Ps-HFS

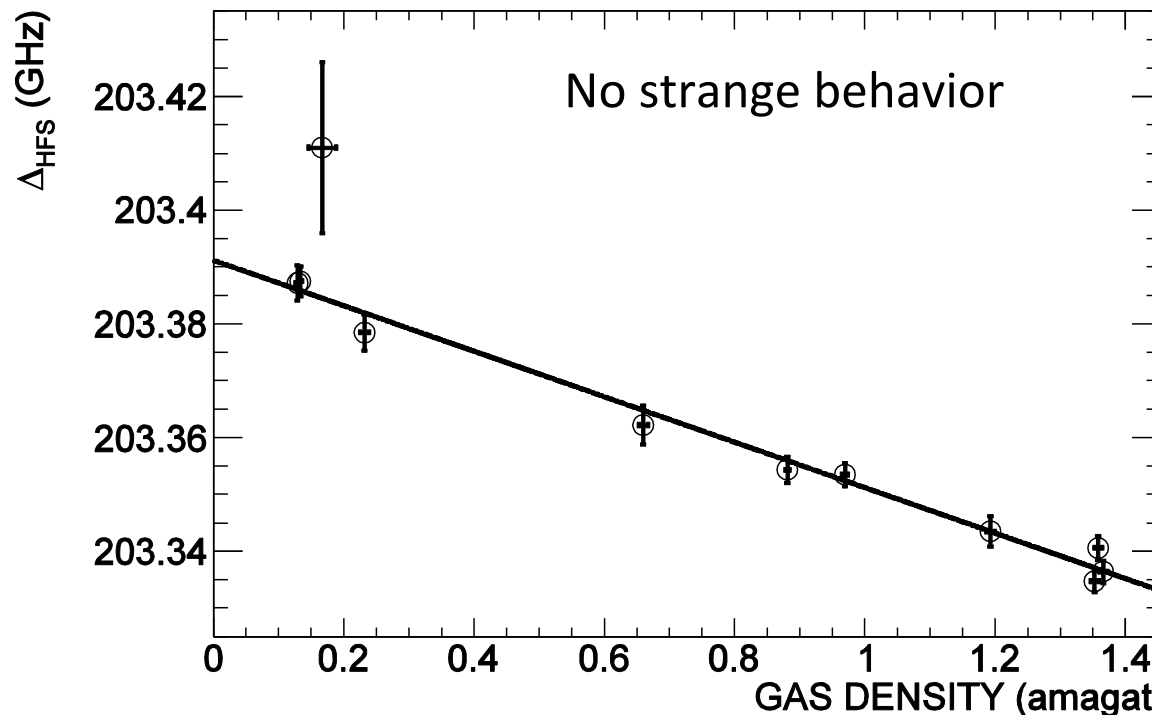


- Slow change at low gas density.
- Kinks are due to change of s_m from DBS value to our pick-off value.

- O(100 ppm) change in 0–50 ns TW.
- O(10 ppm) slow change at low gas density.

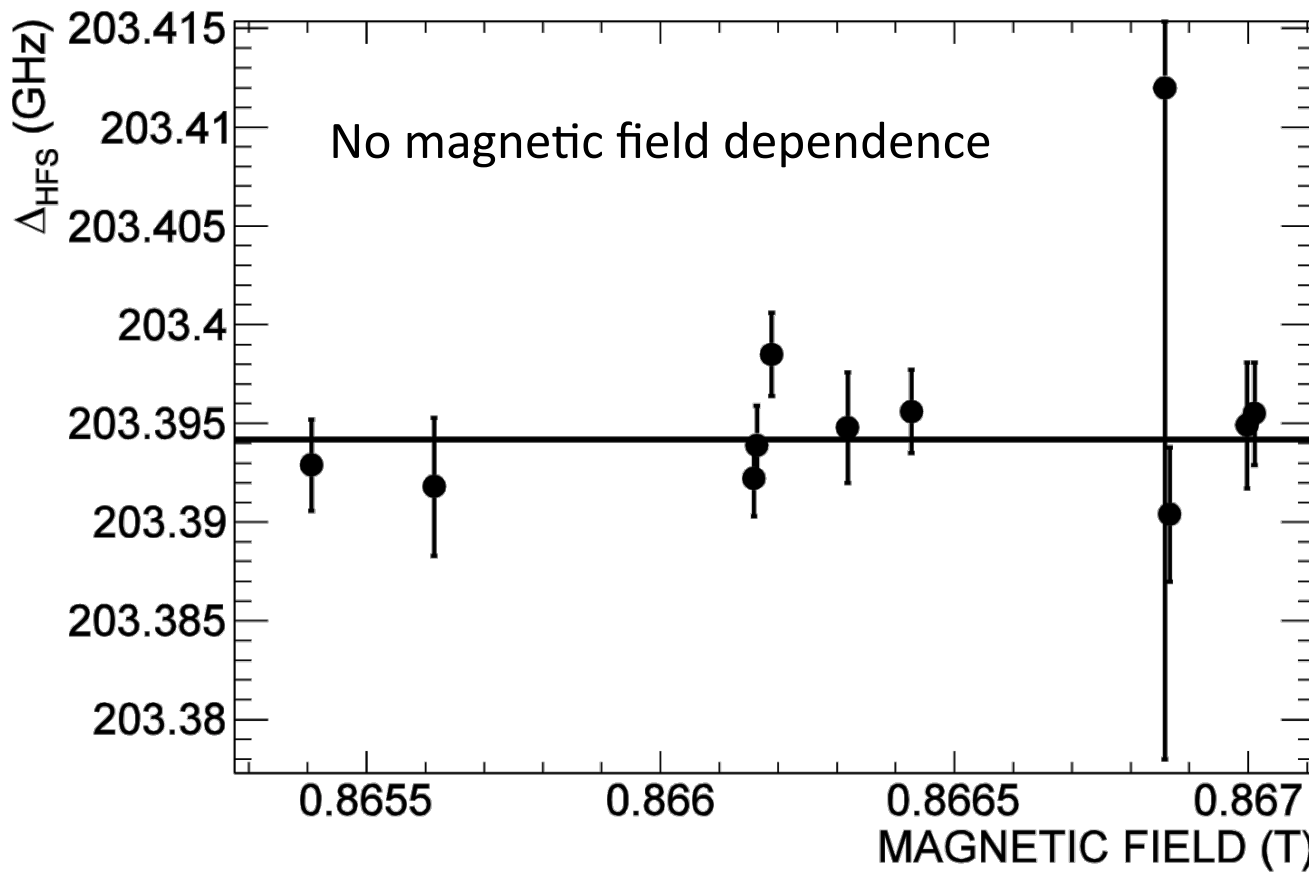
Quality check: gas-density dependence of Ps-HFS

Completely separate analysis which determine Δ_{HFS} value at each gas density has been performed to provide additional insight into the complete experimental data set and confirm their quality, although **this method cannot take into account the time evolution of Ps-HFS.**



Magnetic field dependence

Checked magnetic field (center value of the resonance) dependence. The material-effect parameter C (“slope” in density dependence plot) was fixed in this check.



Systematic errors (Main ones)

	Source	ppm in D_{HFS}
Material Effect	o-Ps pick-off rate	3.5
	Gas density measurement	1.0
	Spatial distribution of density and temperature of gas in the RF cavity	2.5
	Thermalization of Ps	1.9
Magnetic Field	Non-uniformity	3.0
	Offset and reproducibility	1.0
	NMR measurement	1.0
RF	RF power	1.2
	Q_L value of RF cavity	1.2
	RF frequency	1.0
Analysis	Choice of timing window	1.8
	Quadrature sum	6.4

Combined with 8.0 ppm stat. err., $\Delta_{HFS} = 203.394\ 2(21)\ \text{GHz}$ (10 ppm).

Systematic errors (Main ones)

*Material
Effect*

*Magnetic
Field*

RF

Analysis

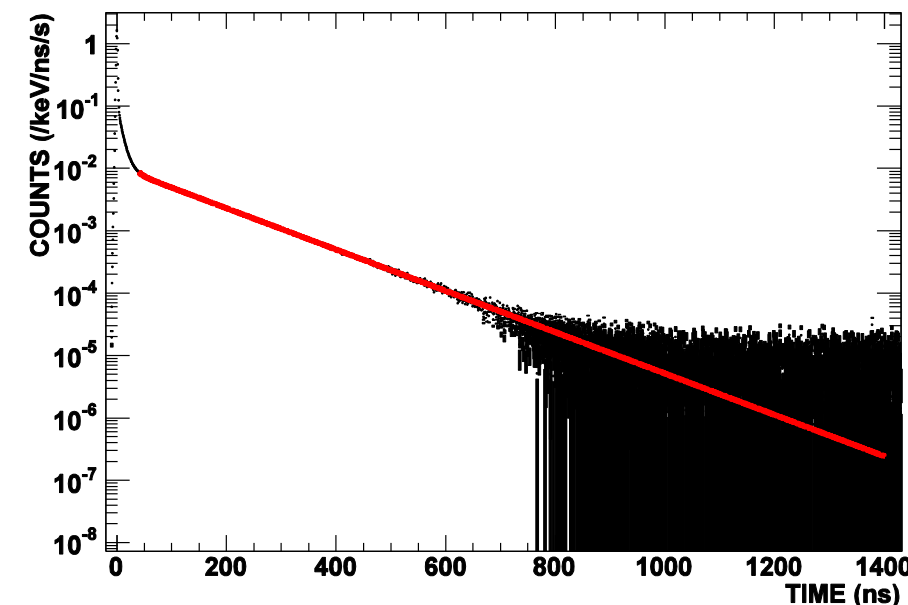
Source	ppm in D_{HFS}
o-Ps pick-off rate	3.5
	Gas density measurement
	Spatial distribution of density and temperature of gas in the RF cavity
	Thermalization of Ps
Non-uniformity ($\Delta_{HFS} \propto B^2$)	3.0
	Offset and reproducibility
	NMR measurement
RF power	1.2
	Q_L value of RF cavity
	RF frequency
Choice of timing window	1.8
	Quadrature sum

Combined with 8.0 ppm stat. err., $\Delta_{HFS} = 203.394\ 2(21)\ \text{GHz}$ (10 ppm).

Systematic error (o-Ps pick-off rate)

We obtain HFS by fitting the data with theoretical transition line shape. This calculation needs o-Ps pick-off rate ($\Gamma_{\text{pick}}(t)$) as an input parameter. Obtain this rate by fitting the RF-OFF time spectra by the following function which **includes Ps thermalization**.

$$N(t) = N_0 \exp \left[-\Gamma_{\text{o-Ps}} \int_0^t \left(1 + \frac{\Gamma_{\text{pick}}(t')}{\Gamma_{\text{o-Ps}}} \right) dt' \right] + N_1 \exp \left[-\Gamma_{|+\rangle} \int_0^t \left(1 + \frac{\Gamma_{\text{pick}}(t')}{\Gamma_{|+\rangle}} \right) dt' \right]$$



$$\Gamma_{\text{pick}}(n, t) = \underline{\Gamma_{\text{pick}}(n, \infty)} \times \left[\frac{v(t)}{v(\infty)} \right]^{0.6}$$

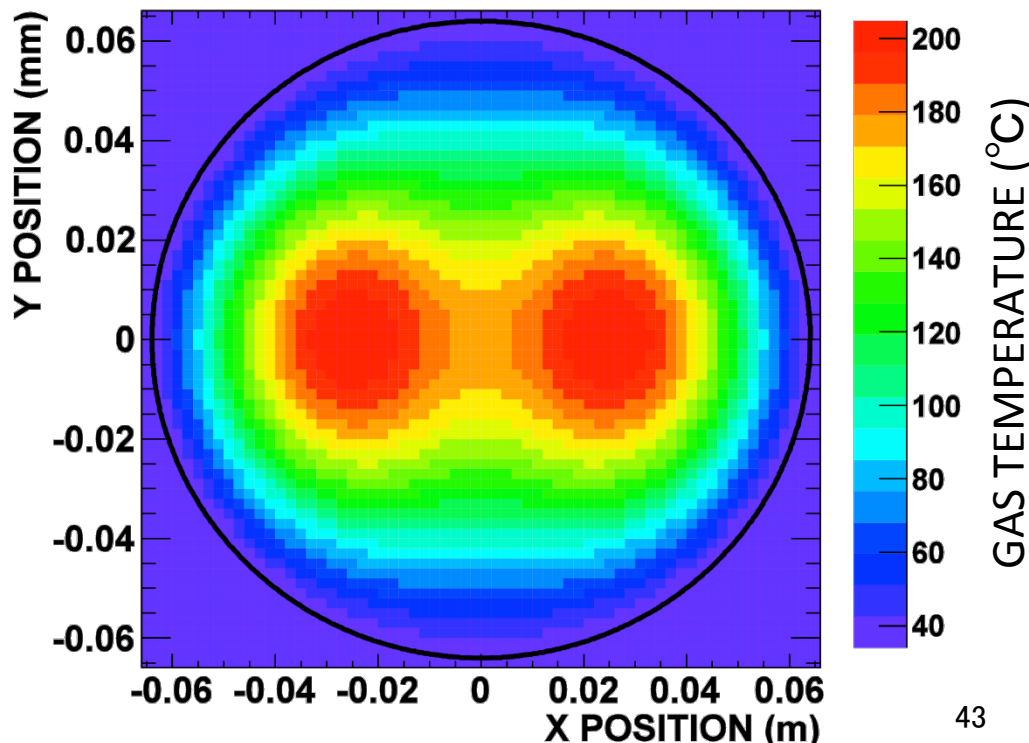
Obtain this value

Error of $\Gamma_{\text{pick}}(n, \infty)$ in this fit corresponds to 3.5 ppm of Ps-HFS error.

Systematic error

(Spatial distribution of density and temperature of gas in the RF cavity)

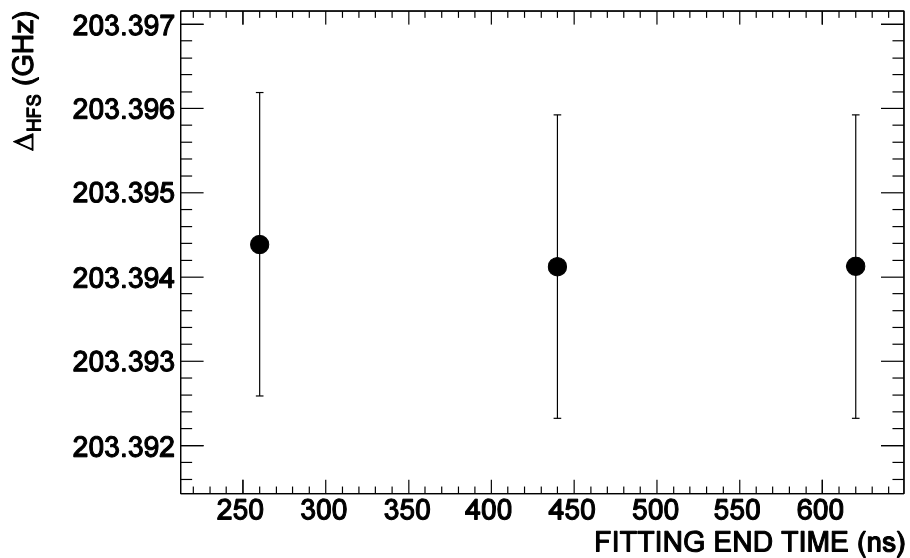
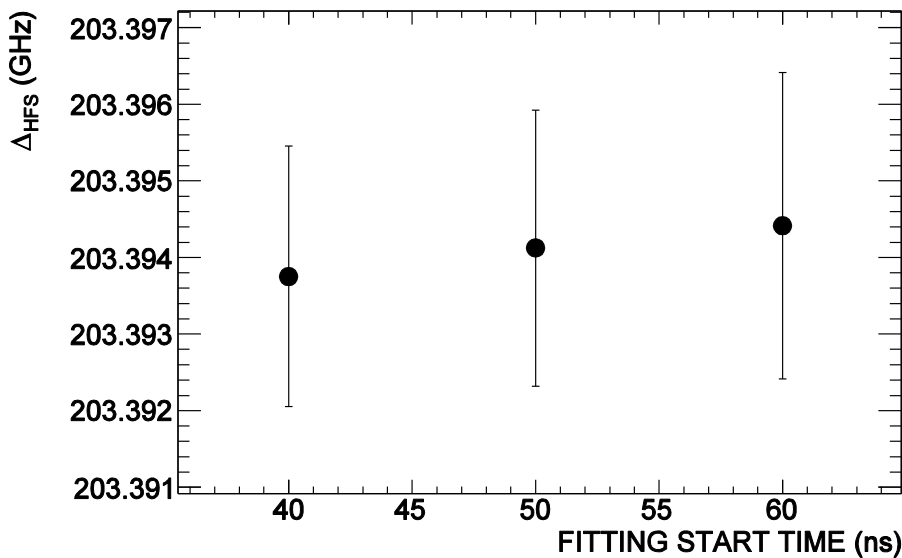
- i-C₄H₁₀ slightly absorbs microwaves
-> heated up -> high temperature (low density)
- This temperature (density) distribution in the RF cavity depends on the position in the RF cavity (RF power distribution)
-> Ps feels different gas density depending on position
- Distributions with an *extreme* condition of no gas convection are calculated.
- Assumed absorbed RF \propto energy density of E-field of TM₁₁₀
 \approx 170 K range distribution
-> shifts D_{HFS} by +2.5 ppm.



Systematic error (choice of timing window)

Timing window of 50–440 ns

1. Ending time of 440 ns is fixed, compared starting time 40 ns, 60 ns
2. Starting time of 50 ns is fixed, compared ending time 260 ns, 620 ns



In both cases, no systematic dependence was observed.

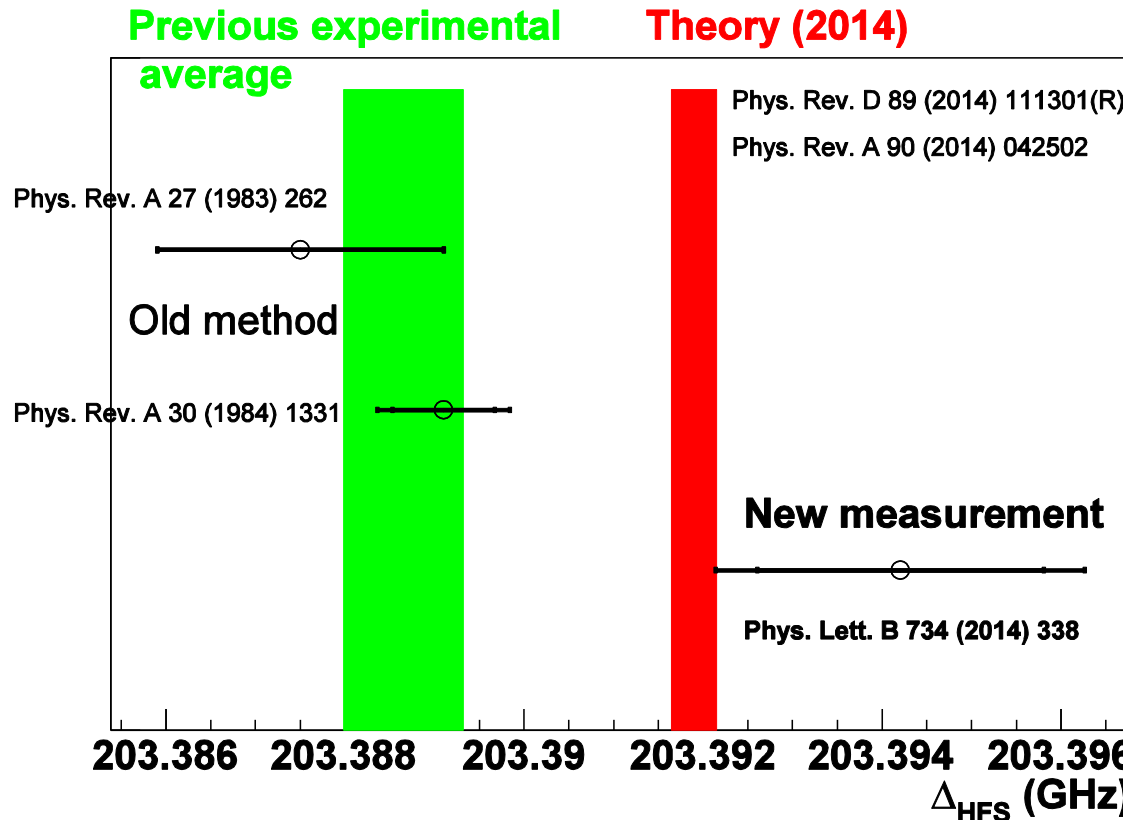
1.8 ppm shift at the maximum → systematic error.

Estimation of non-thermalized o-Ps effect

- In order to evaluate the non-thermalized o-Ps effect on Ps-HFS, fitting without taking into account the time evolution of Δ_{HFS} and pick-off rate was performed. (well-thermalized assumption)
- Other procedures were the same (used 50 – 440 ns timing window)
- Result was:

203.392 2(16) GHz ($\chi^2/\text{ndf}=721.1/592$, $p=2\times 10^{-4}$)
(cf. with time evolution 203.394 2(16) GHz, ($\chi^2/\text{ndf}=633.3/592$, $p=0.12$))
- This value is lower than the fit with time evolution by **as large as 10 ± 2 ppm**. This is comparable to the discrepancy of previous experimental results and theory (16 ppm).
- This effect might be larger if no timing window is applied, since Ps-HFS is dramatically changing in the timing window of 0–50 ns because of the rapid change of Ps velocity.
- It strongly suggests that the reason of the discrepancy in Δ_{HFS} is the effect of non-thermalized Ps.

Result



Favors QED calculation

(Consistent with theory within 1.1σ , disfavors previous experiments by 2.6σ)

Our new result taking into account the Ps thermalization is:

$$\begin{aligned}\Delta_{\text{HFS}} = 203.394 &2 \pm 0.0016 \text{ (stat., 8.0 ppm)} \\ &\pm 0.0013 \text{ (sys., 6.4 ppm) GHz}\end{aligned}$$

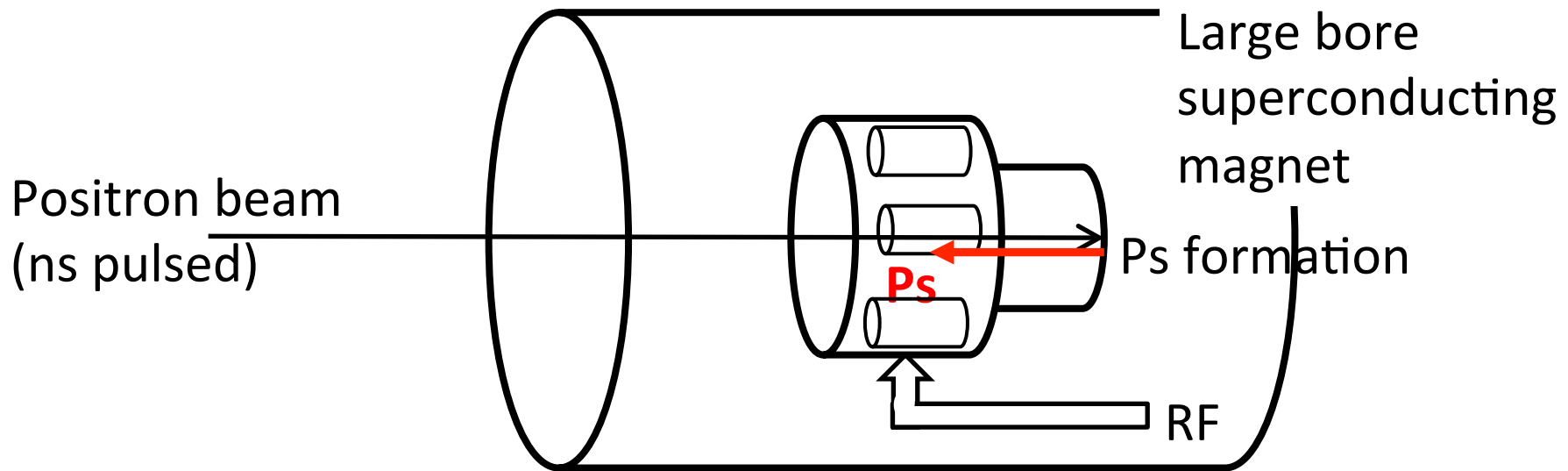
- Positronium Hyperfine Splitting (Ps-HFS)
- Material effect and Ps thermalization
- Our New Experiment
- Analysis and Results
- Prospects & conclusion

Future prospects

Measurement in vacuum using slow positron beam

(hopefully better than 1 ppm result within 4—5 years)

- High statistics (scan in vacuum instead of extrapolation, higher power RF without discharge)
- Completely free from material effect
- Short measurement period reduces systematic errors



Other methods

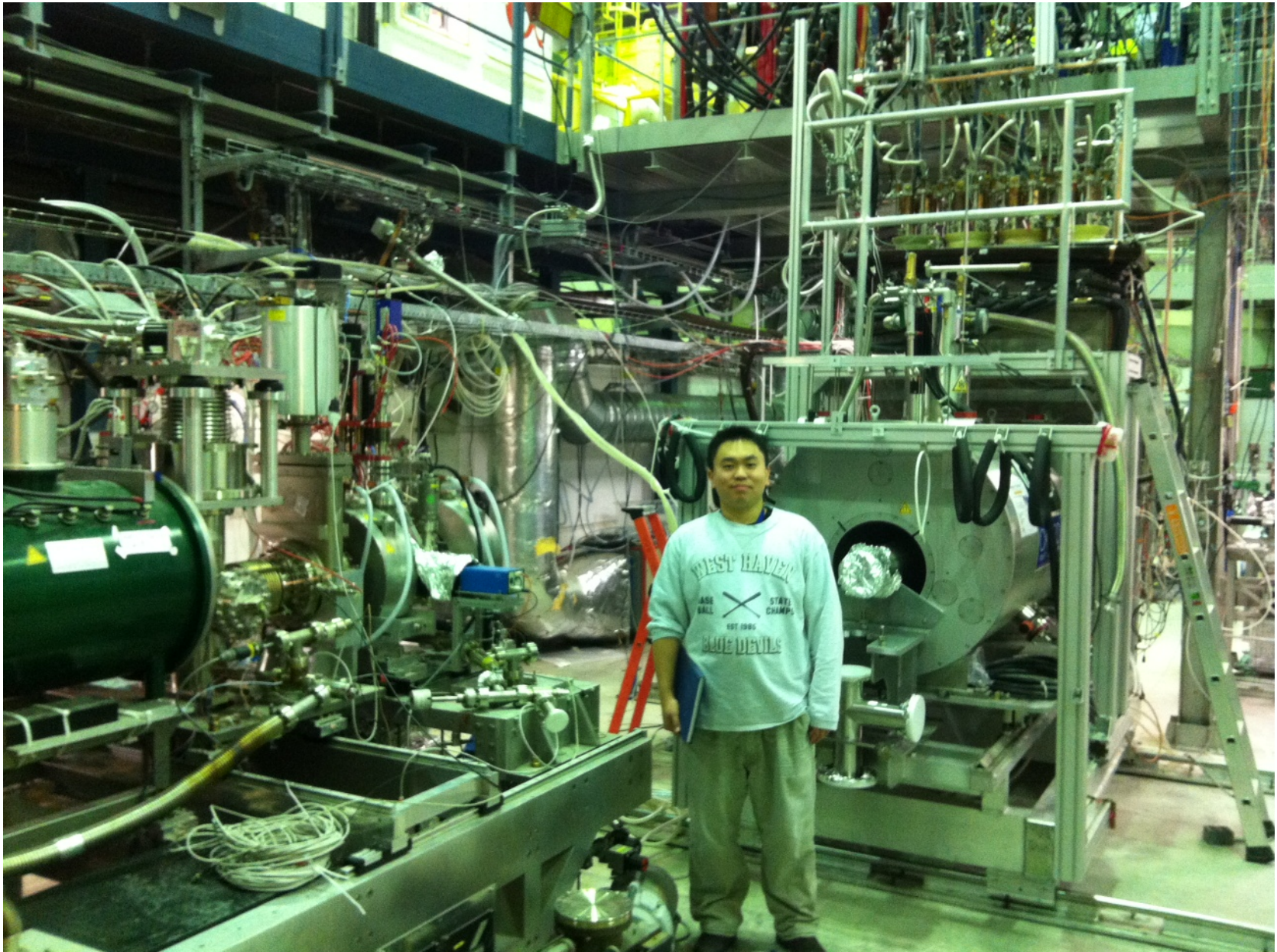
- A. Miyazaki *et al.*, Prog. Theor. Exp. Phys. **2015**, C11C01 (2015).
Direct measurement without static magnetic field (**540 ppm**).
It is mentioned that it can be improved to **< 10 ppm in future**.
- D. B. Cassidy *et al.*, Phys. Rev. Lett. **109**, 073401 (2012).
Saturation absorption spectroscopy between Zeeman-shifted 1S and 2P levels (**2%**).
It is mentioned that it can be improved to **~ ppm in future**.
- Y. Sasaki *et al.*, Phys. Lett. B **697**, 121 (2011).
Quantum oscillation between Zeeman shifted levels (**200 ppm**)
It is mentioned that it can be improved to **15 ppm in future**.

Conclusion

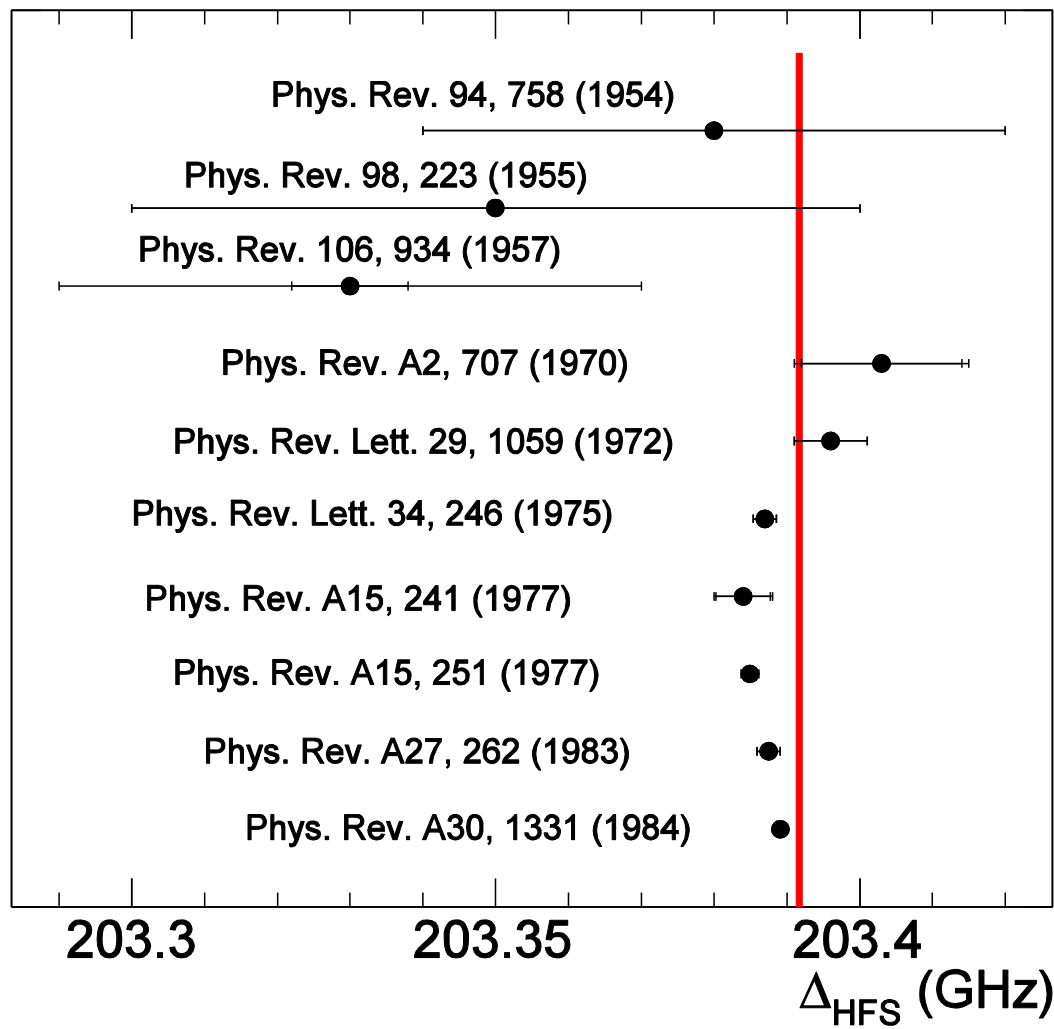
There is a large 4.5σ discrepancy of Ps-HFS between the previous experimental values and theoretical calculation. We performed a new precise measurement which obtains **time information**.

- It reduced possible systematic uncertainties in the previous experiments (Non-thermalized Ps effect and Non-uniformity of magnetic field).
- Ps thermalization function was measured to treat material effect correctly. Time evolution of D_{HFS} and pick-off rate due to Ps thermalization was taken into account.
- **Non-thermalized Ps effect turned out to be as large as 10 ± 2 ppm.** The result taking into account the Ps thermalization effect correctly was $\Delta_{HFS} = 203.3942 \pm 0.0016$ (stat., 8 ppm) ± 0.0013 (syst., 6.4 ppm) GHz, which **is consistent with QED calculation** within 1.1σ , whereas it disfavors the previous measurements by 2.6σ .
- **Our new result shows that the Ps thermalization effect is crucial for the measurement.**

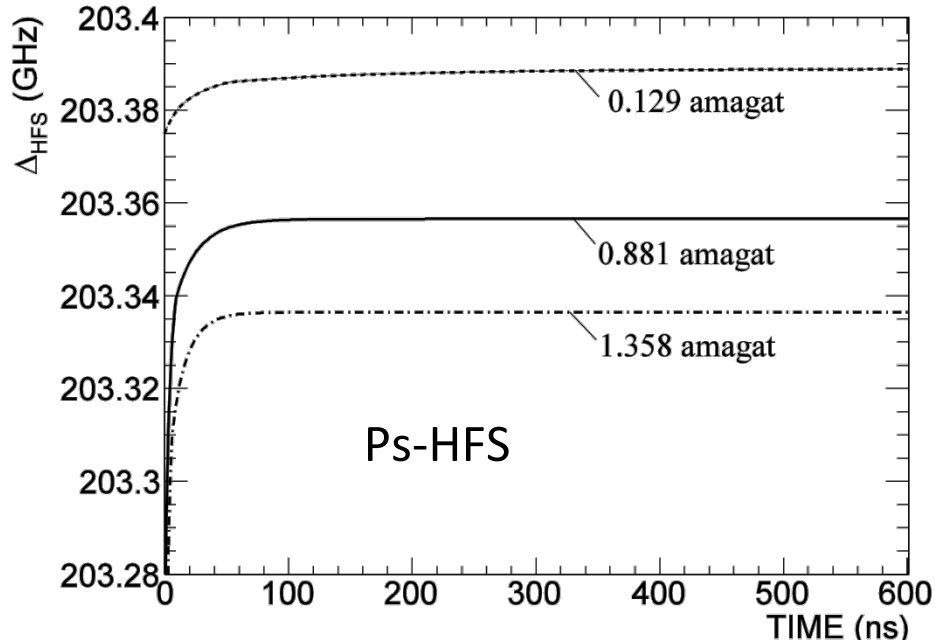
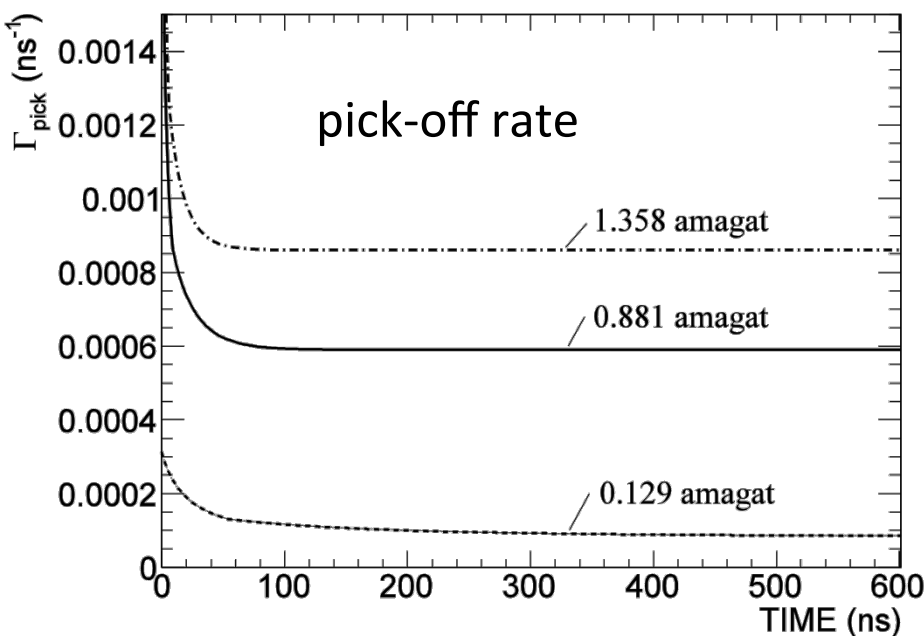
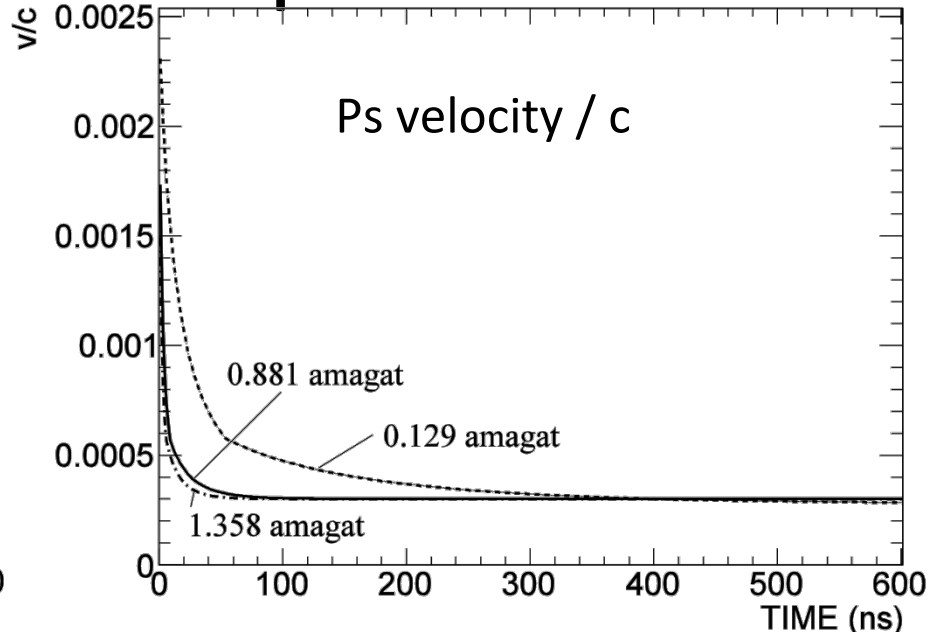
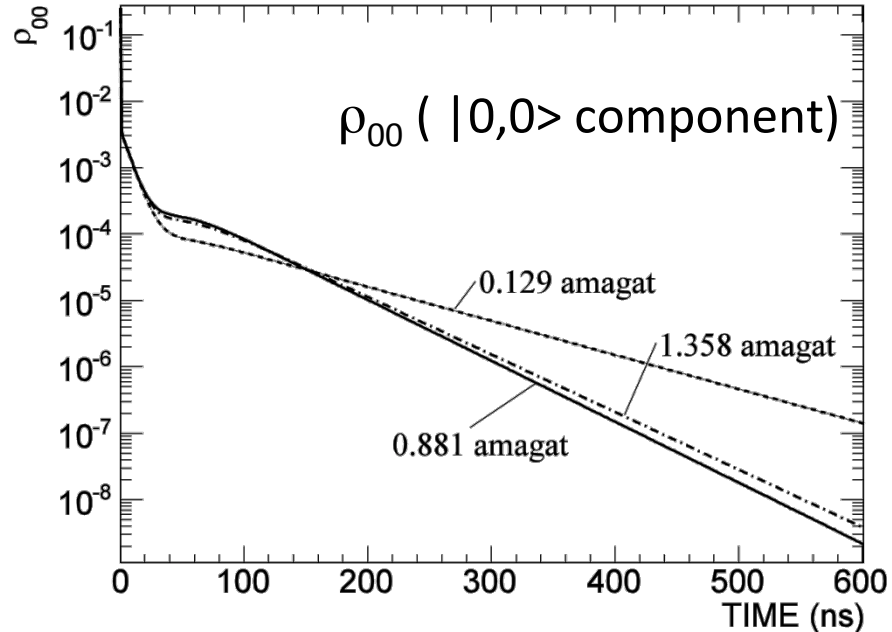
Backup



History plot of Ps-HFS measurements

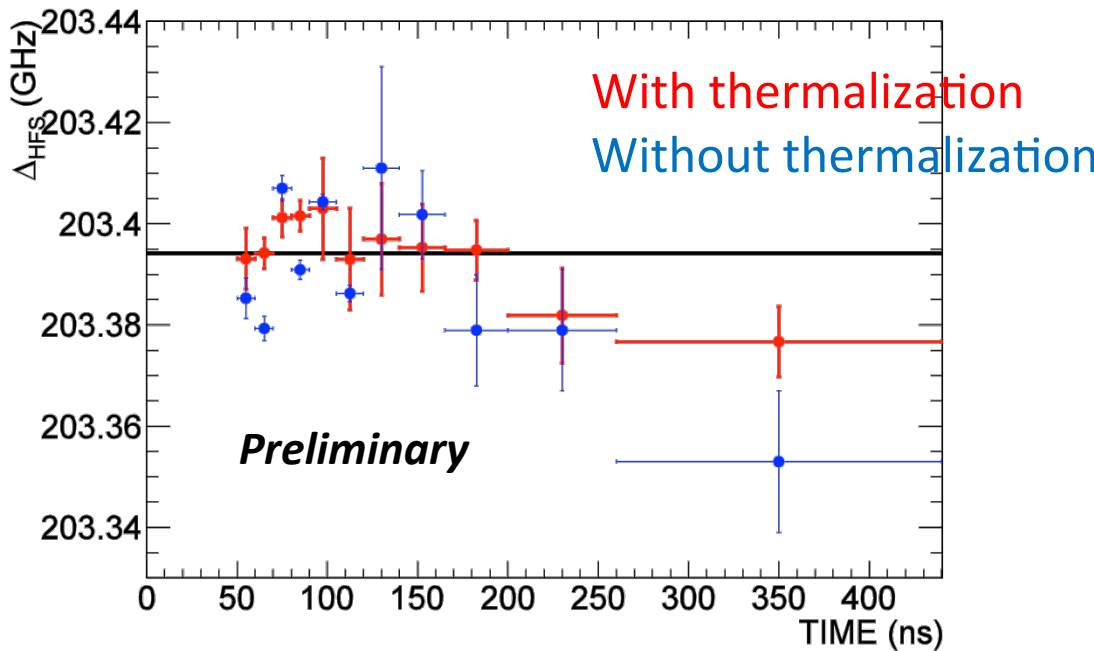


Time evolution of some parameters



Timing window dependence

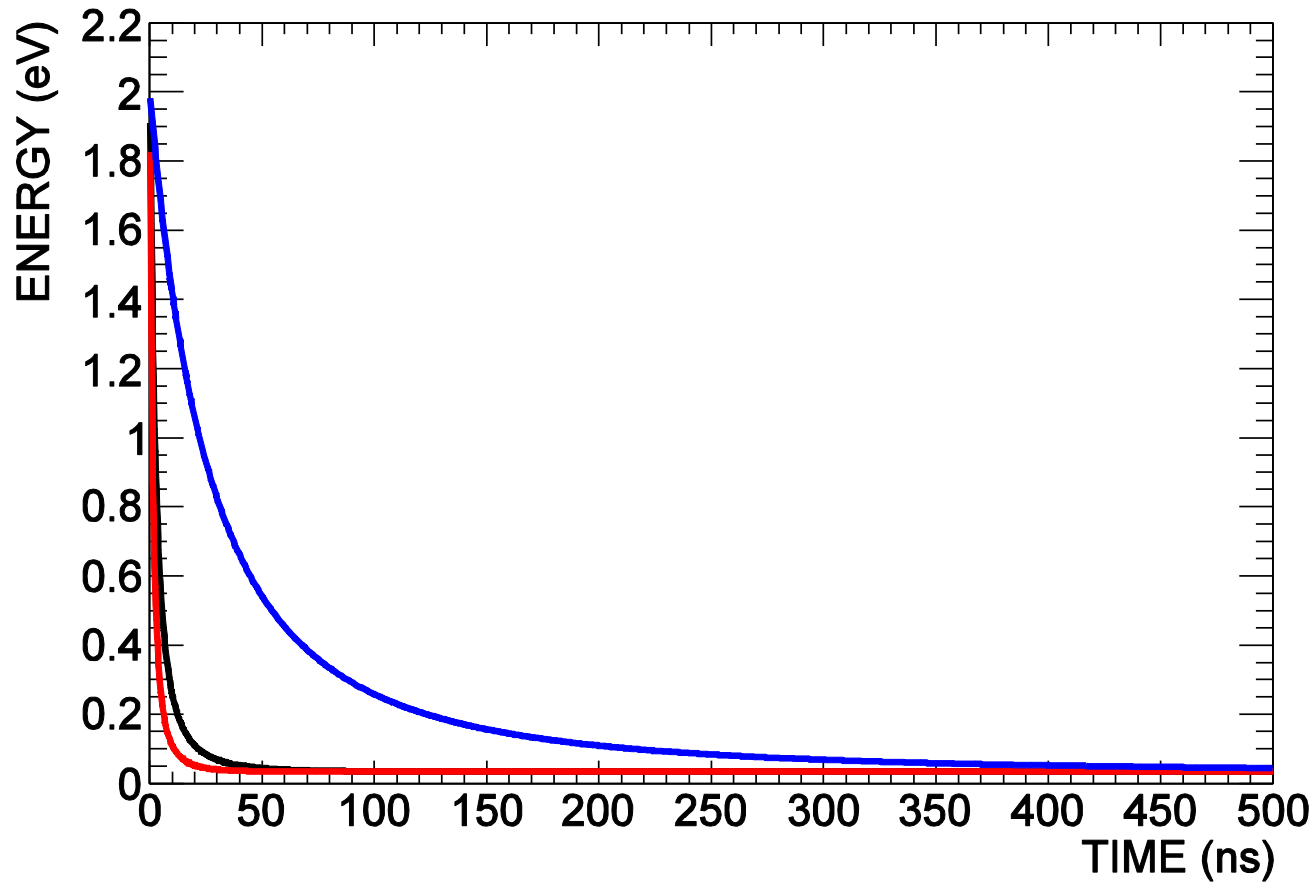
1. Ps-HFS at each timing window has been independently fitted (preliminary). Fitting with thermalization function in the fitting function and without thermalization (well-thermalized assumption) have been compared.



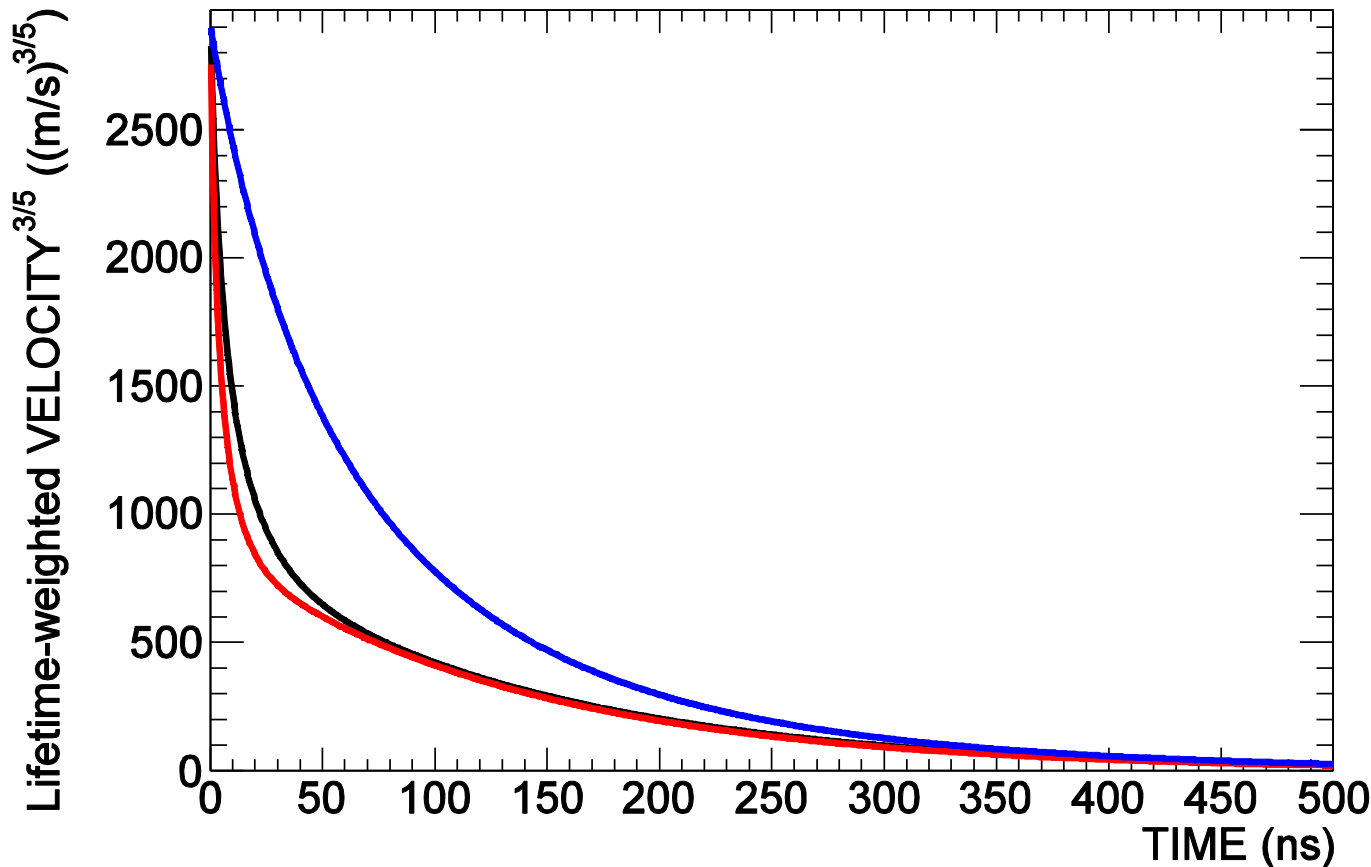
Both of Ps-HFS and C are fitted independently at each TW.

Values without thermalization are smaller.
Larger effect at earlier timing windows.

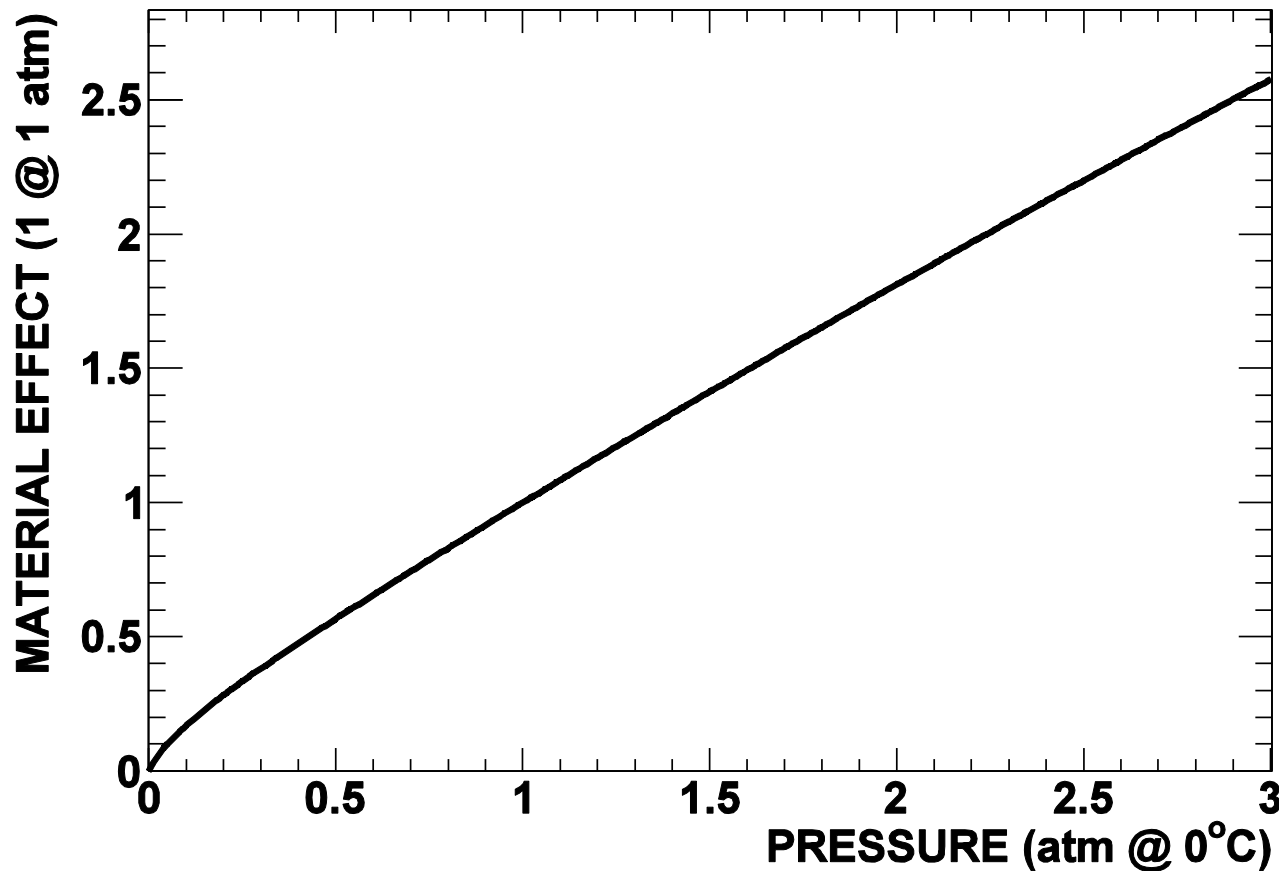
Time evolution of Ps mean kinetic energy in nitrogen gas with an initial kinetic energy of 2 eV and temperature of 273.15 K



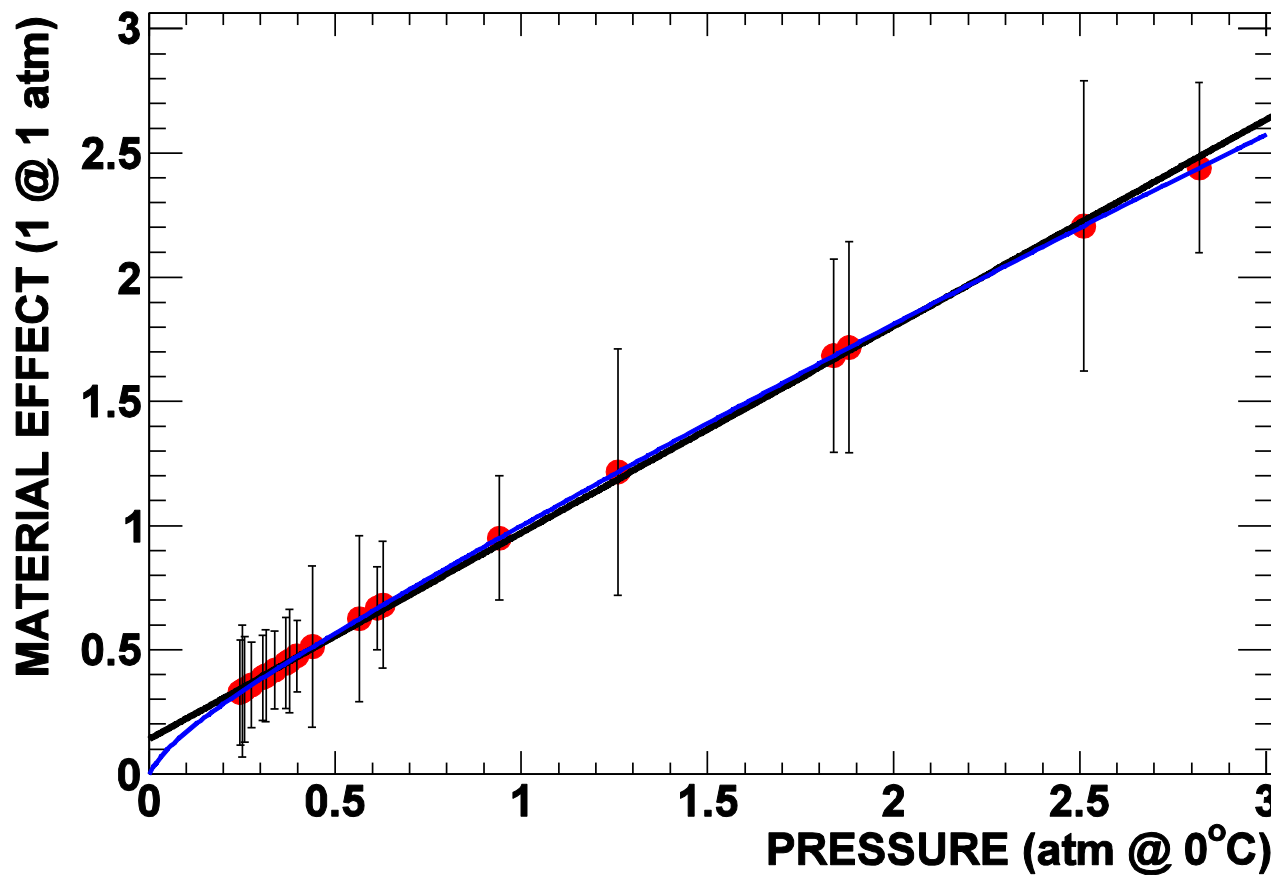
Time evolution of lifetime-weighted Ps mean velocity in nitrogen gas



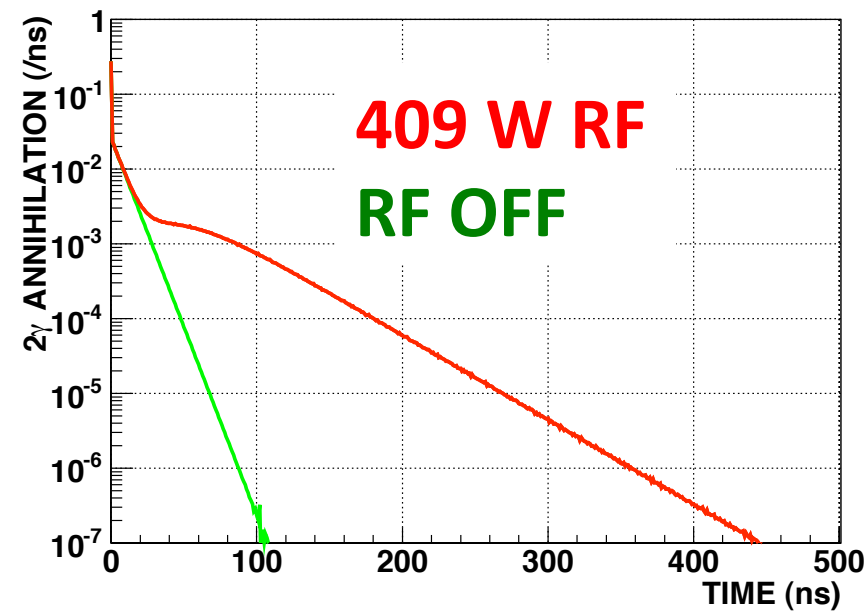
Non-thermalized Ps effect in nitrogen gas



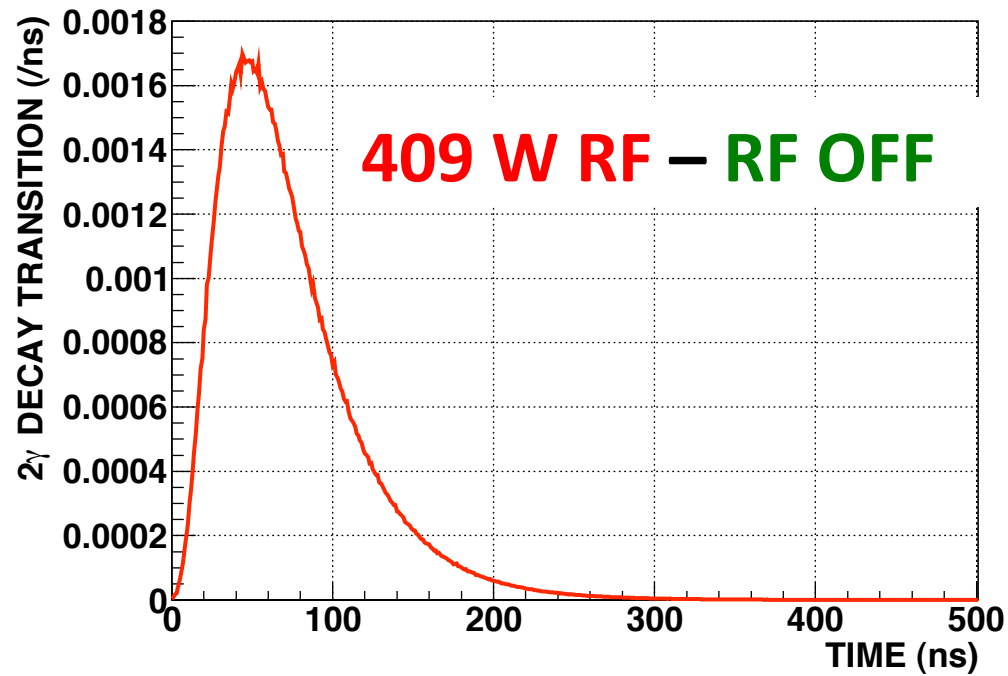
Estimation of the non-thermalized Ps effect on Ps-HFS in nitrogen gas with an initial kinetic energy of 2 eV and temperature of 273.15 K



Timing window



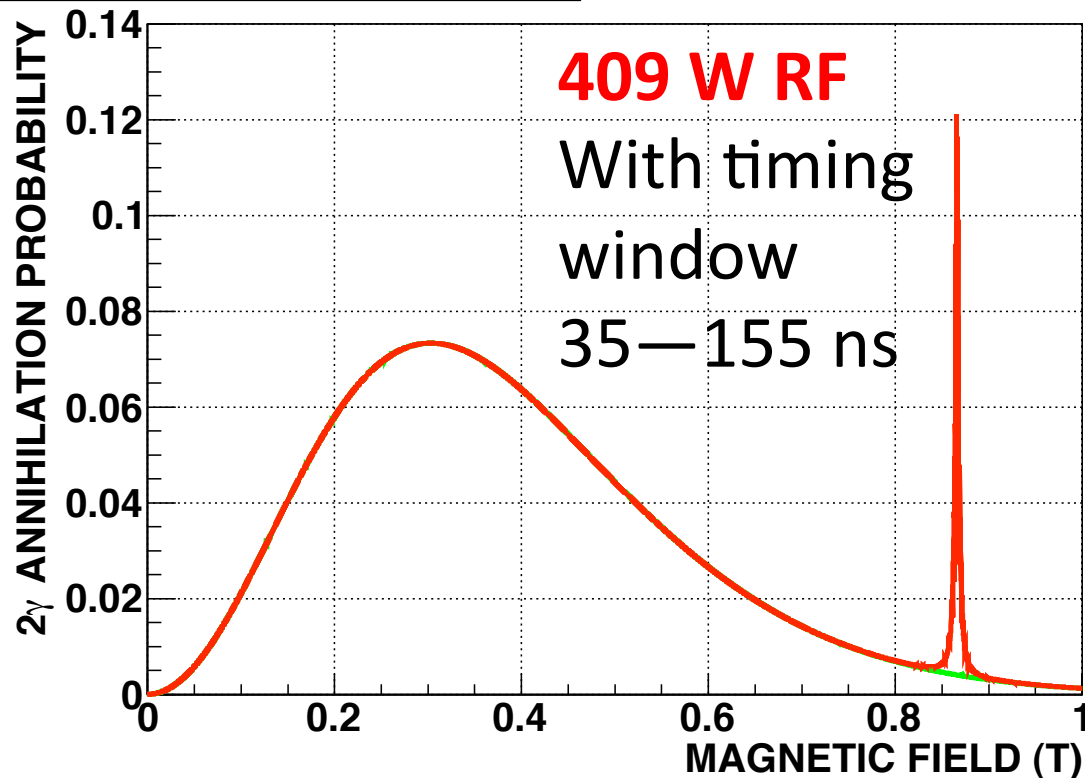
409 W RF
RF OFF



409 W RF – RF OFF

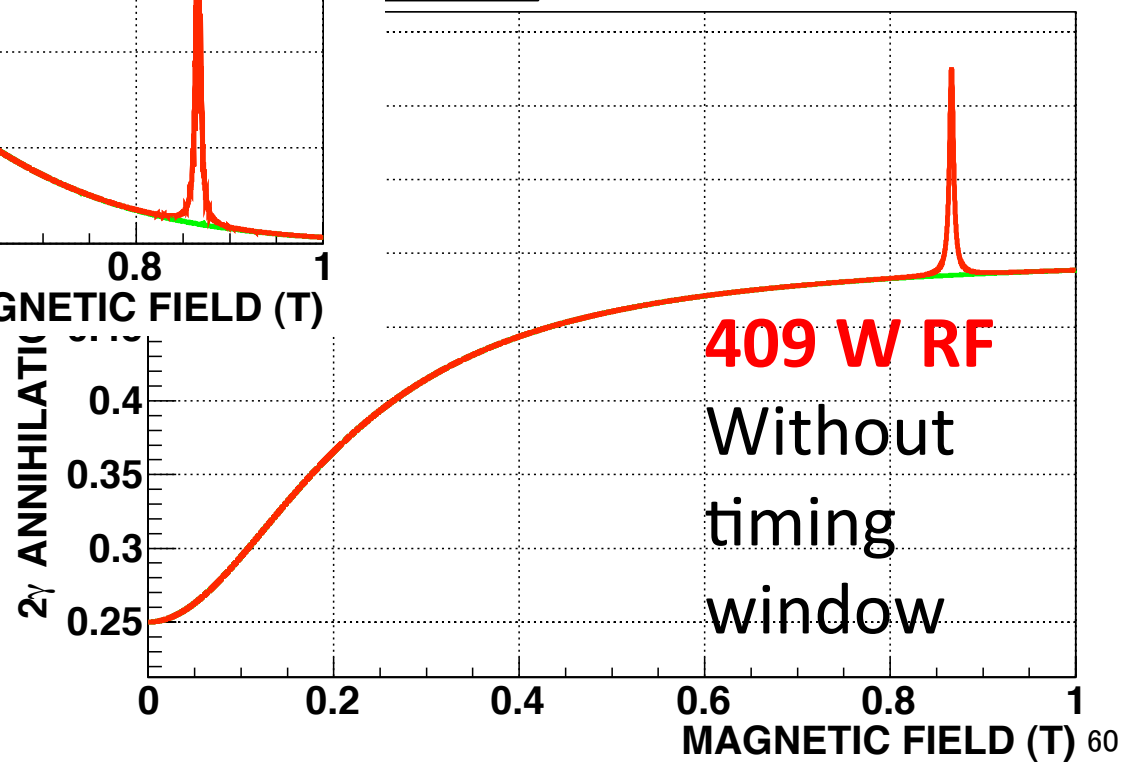
2γ decay rate

WITH TIMING CUT 35--155 ns

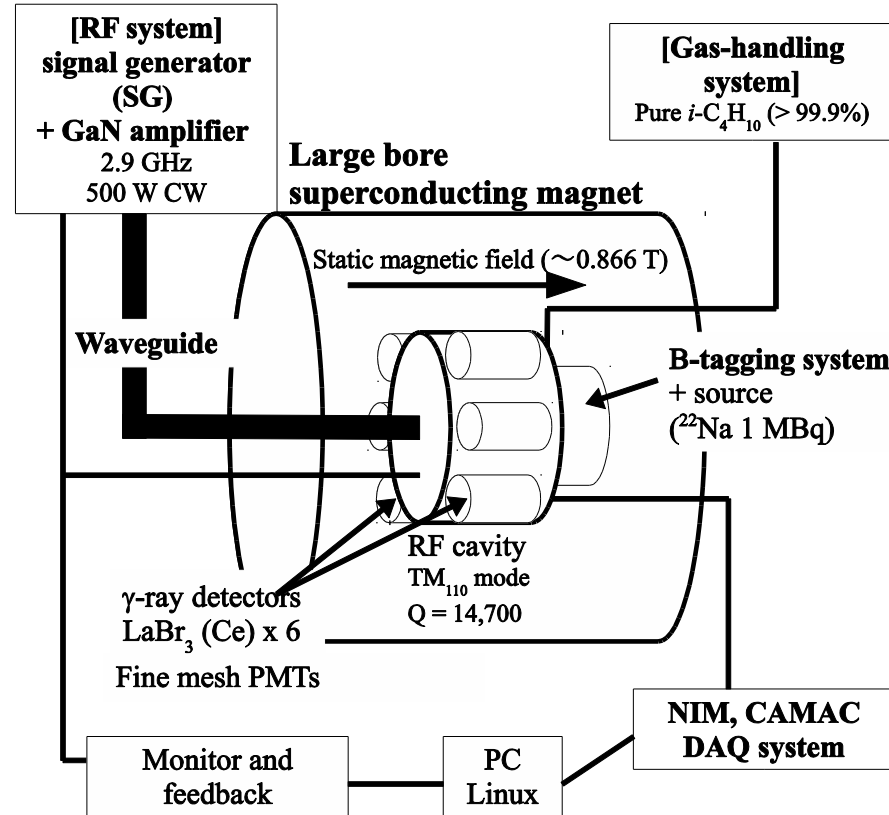


Effect of timing window on 2γ decay rate.
We can decrease BG by timing window
(Figures are theoretical curves at $Q_L=14700$)

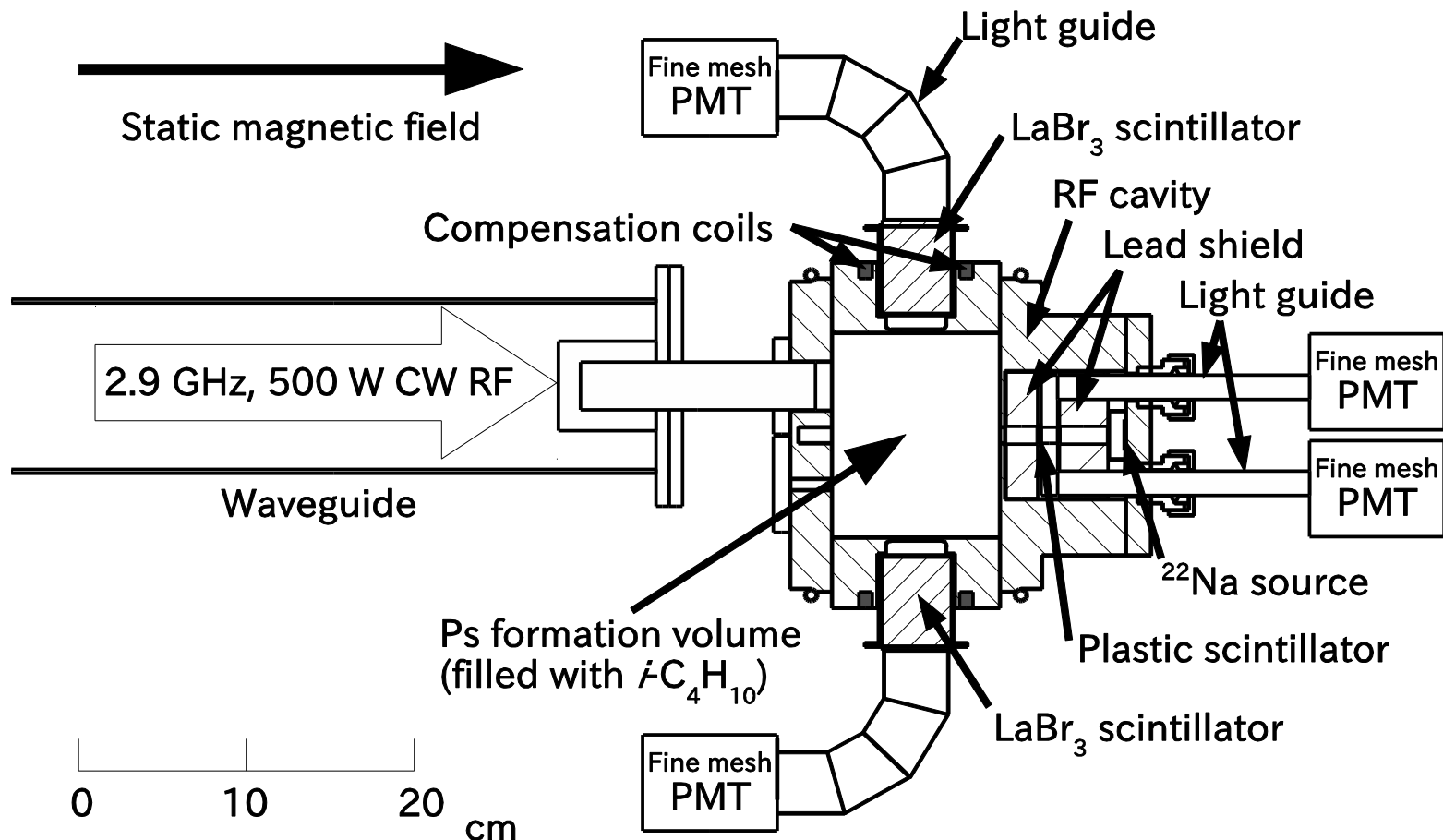
INDOW



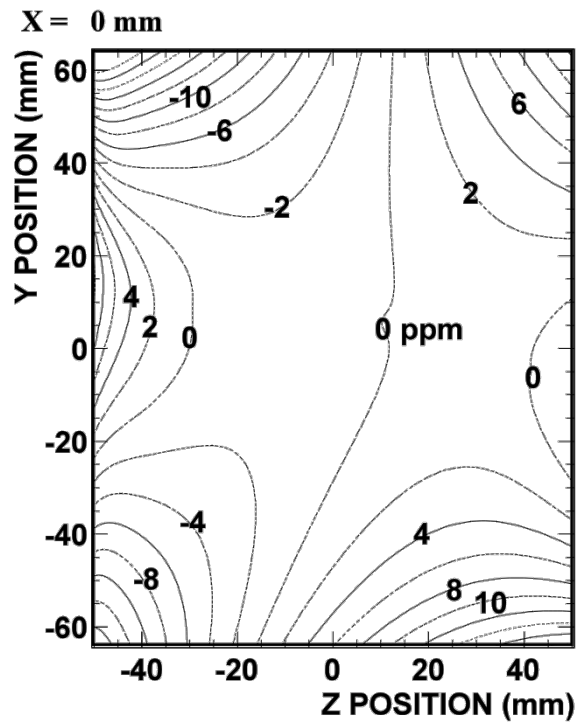
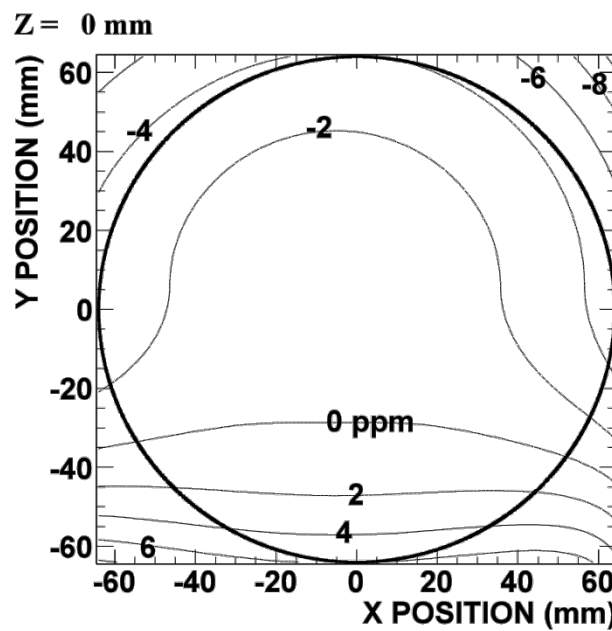
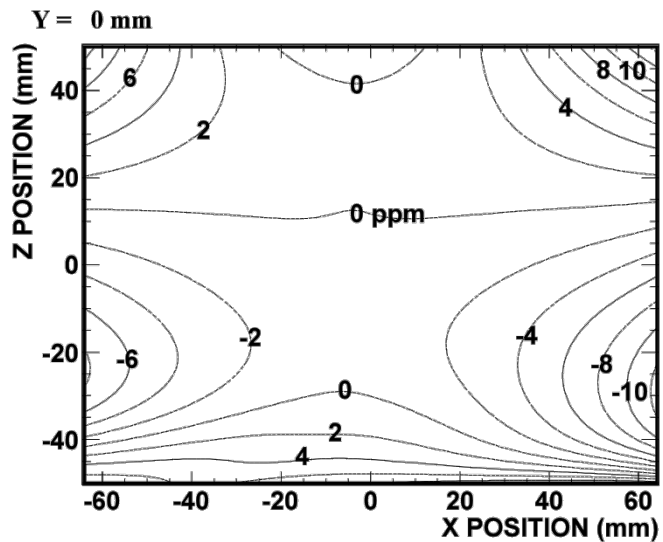
Whole system of our experimental setup



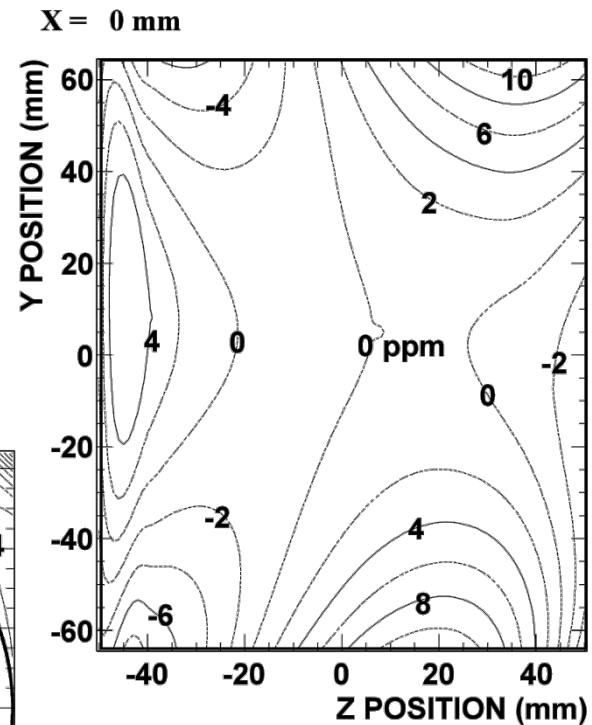
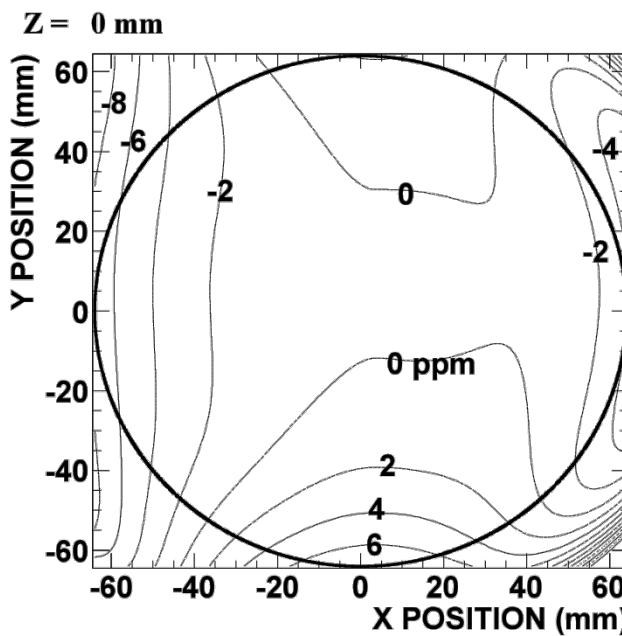
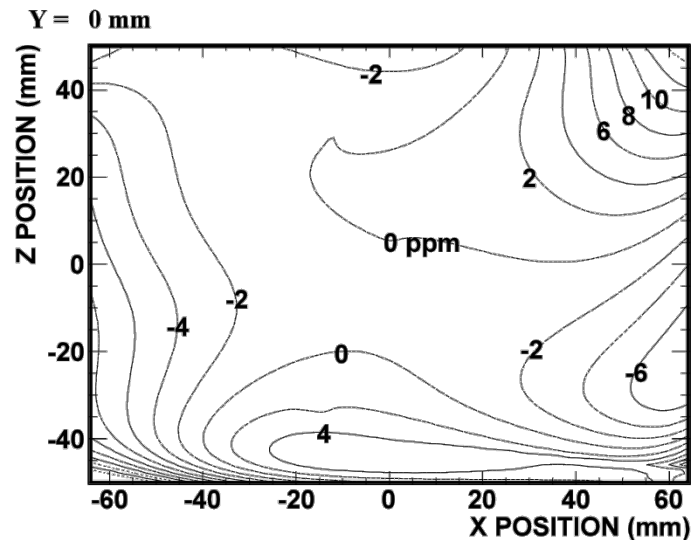
Top view in the magnet



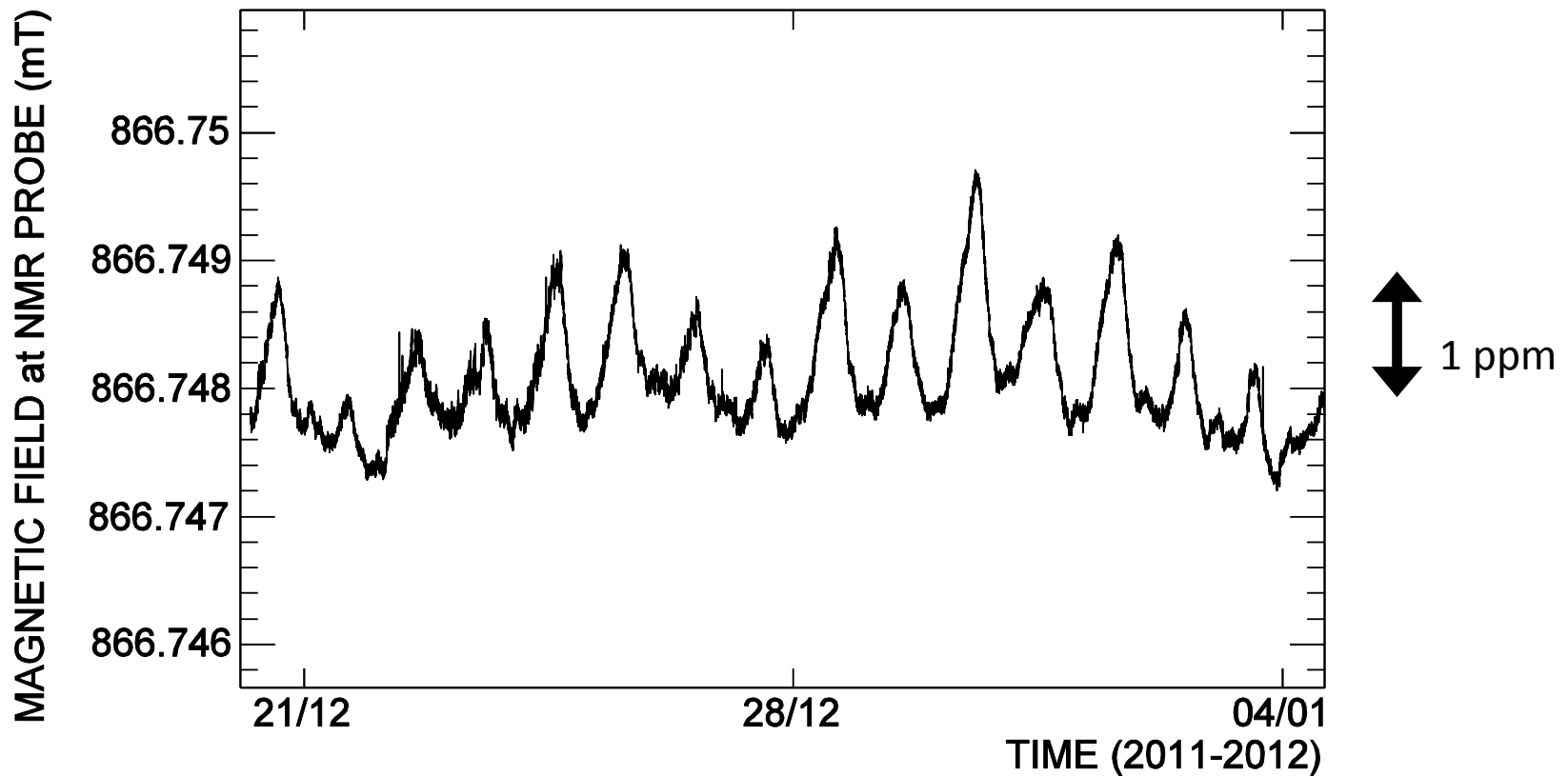
Static magnetic field distribution with compensation magnet (before Ps-HFS measurement)



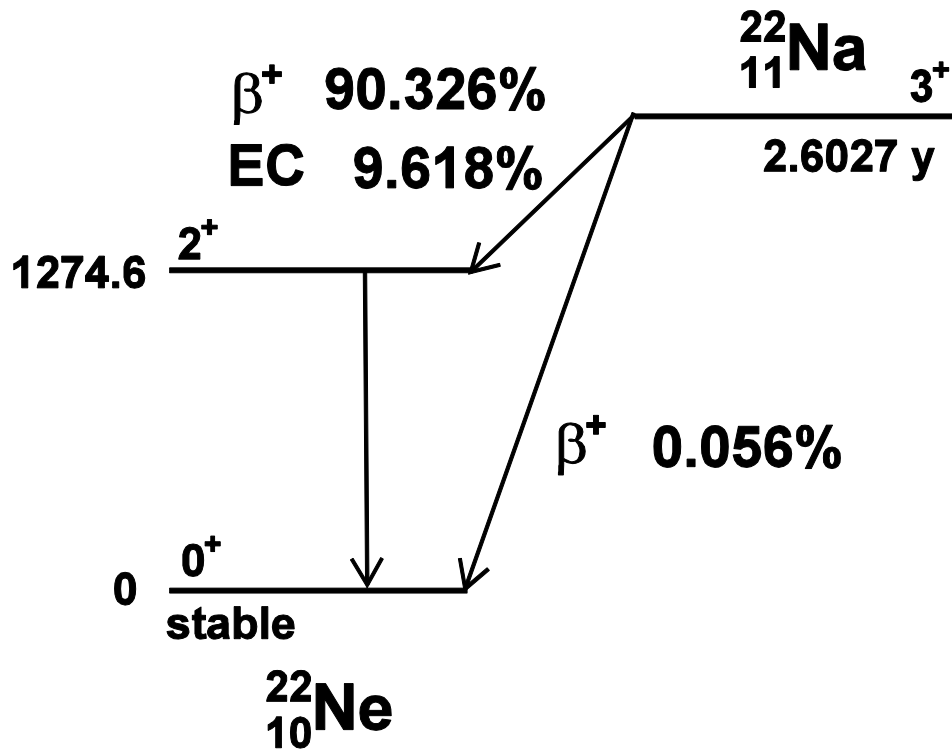
Static magnetic field distribution with compensation magnet (after Ps-HFS measurement)



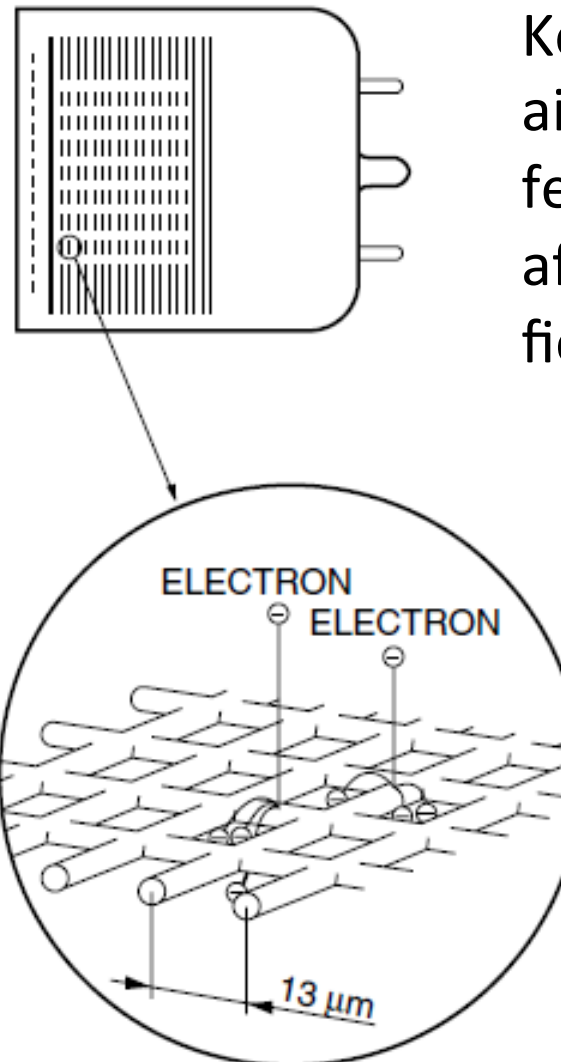
Time fluctuation of the static magnetic field



Decay scheme of ^{22}Na



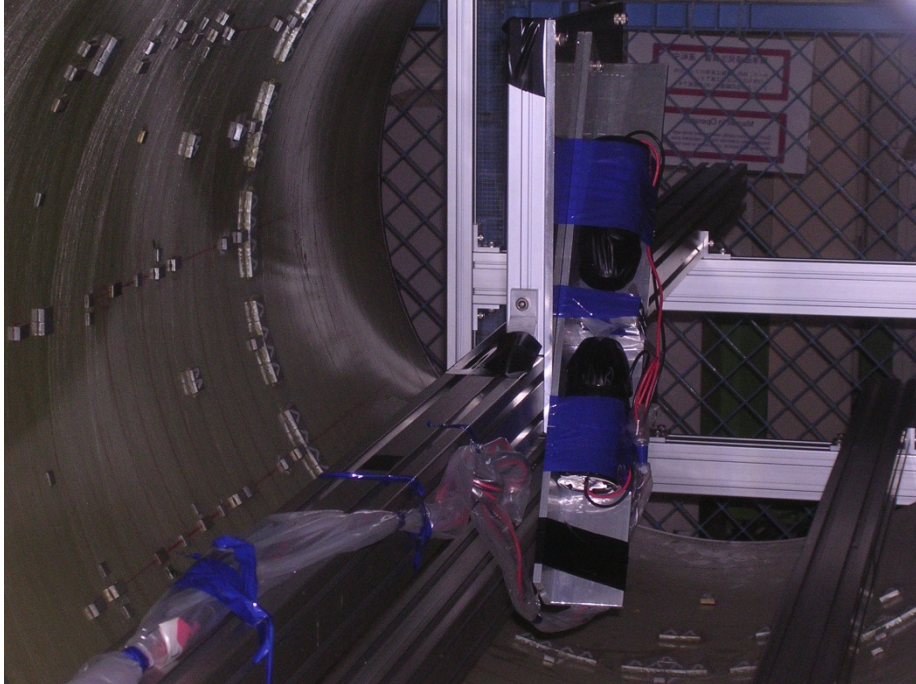
Fine mesh PMT



Kovar (alloy of mainly Fe, Ni, Co. ferromagnetic) affects magnetic field

Measurement at KEK
A few cm from center of mag.
→ 100 ppm
10 cm
→ 10 ppm

Fine mesh PMT in magnetic field



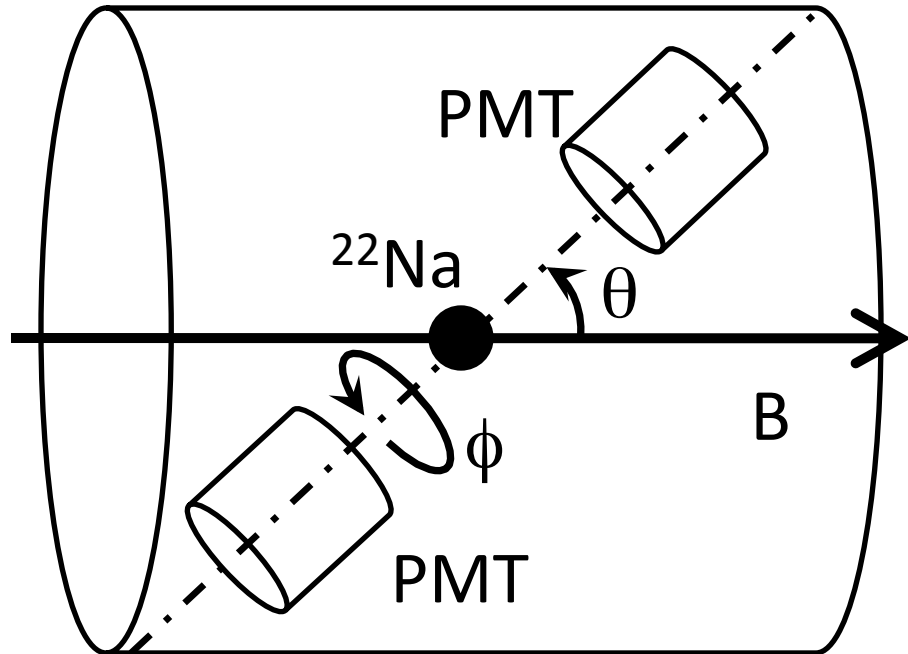
In 0.866 T magnetic field,
 $\text{LaBr}_3(\text{Ce})$ scintillator (1 inch)
and fine mesh PMTs

1.5 inch HAMAMATSU R7761

2.0 inch HAMAMATSU R5924

Put them back-to-back

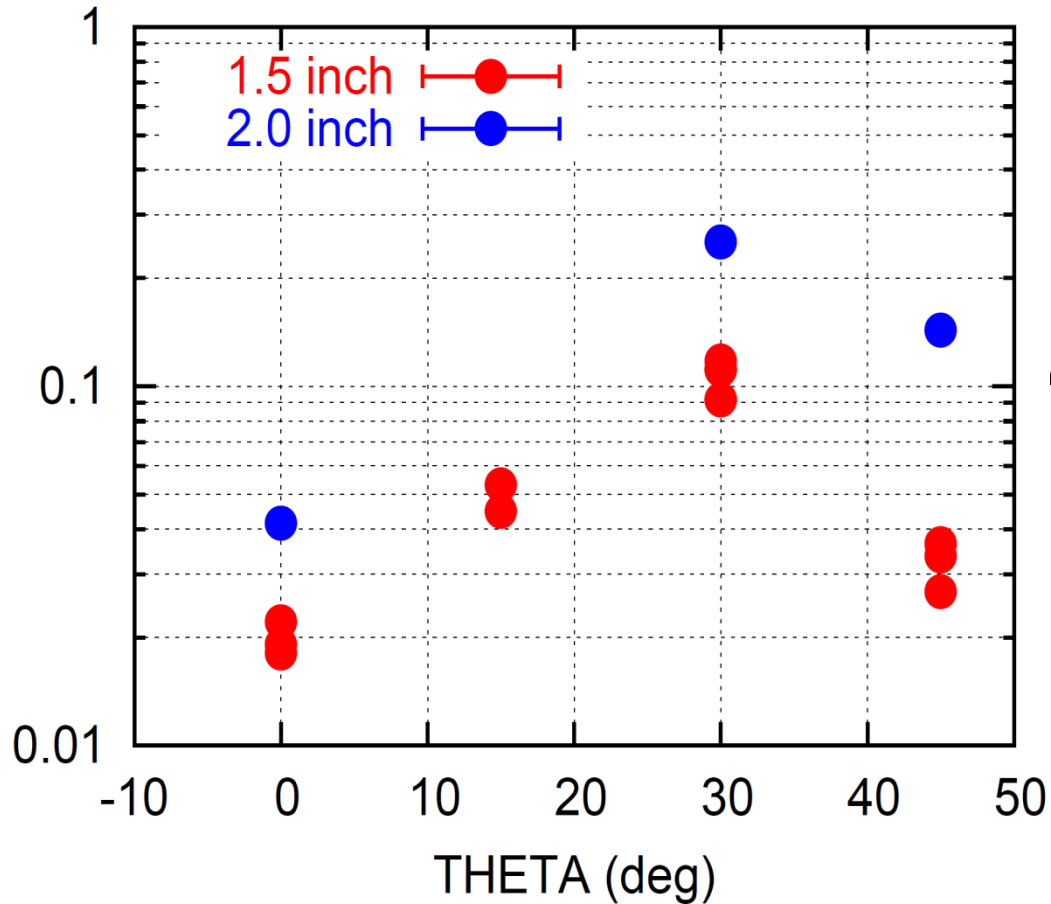
MRI Magnet (@ KEK)



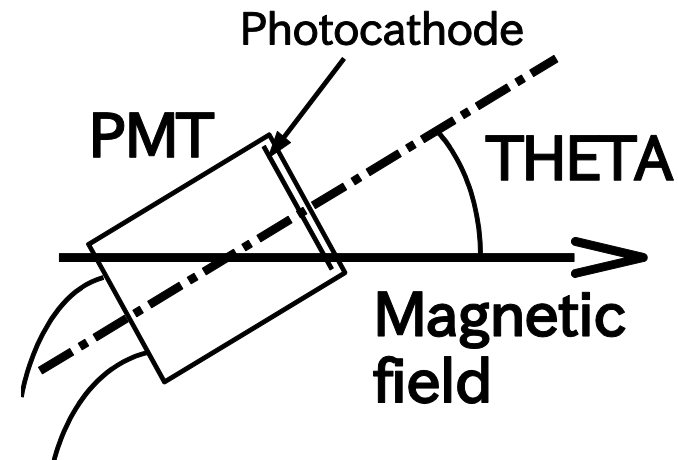
^{22}Na source
(511 keV 2γ back-to-
back, 1275 keV γ)

Angle(θ) dependence of PMT gain

RELATIVE GAIN

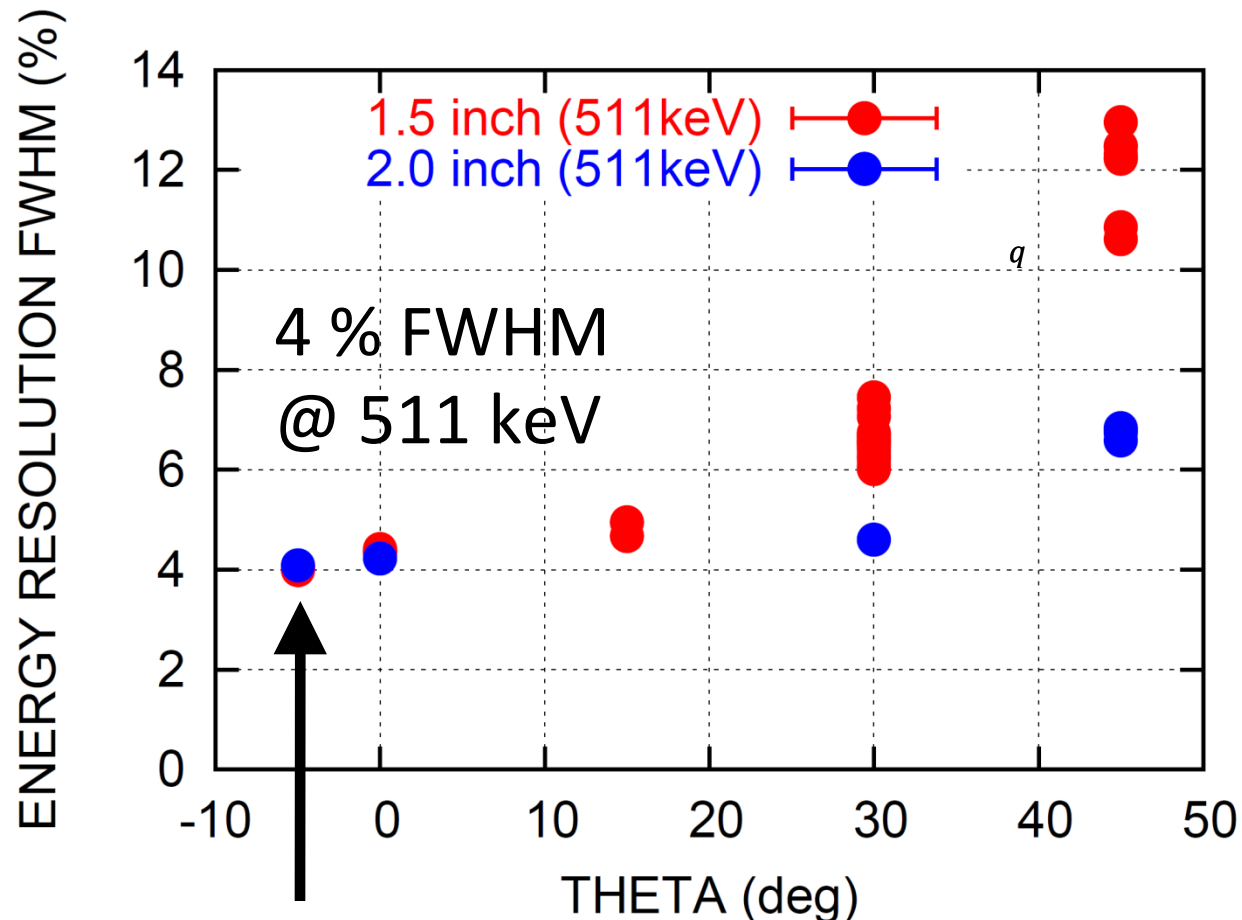


Below 10^{-4} (not possible to measure) over 60°



- Higher effect on 1.5 inch.
- Lowest effect at 30°
- Small effect also at 45° on 2 inch PMT.

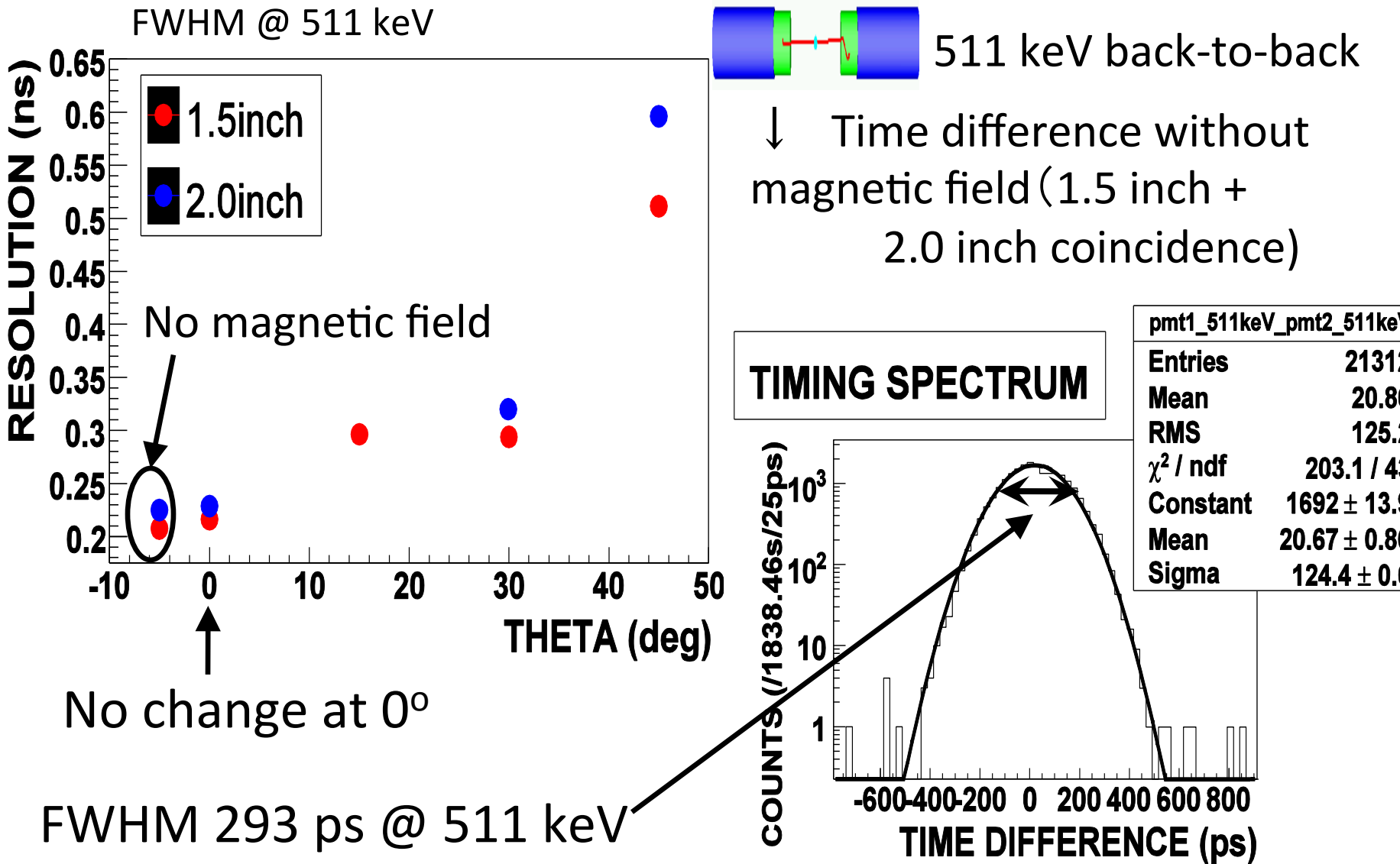
Angle (q) dependence of energy resolution



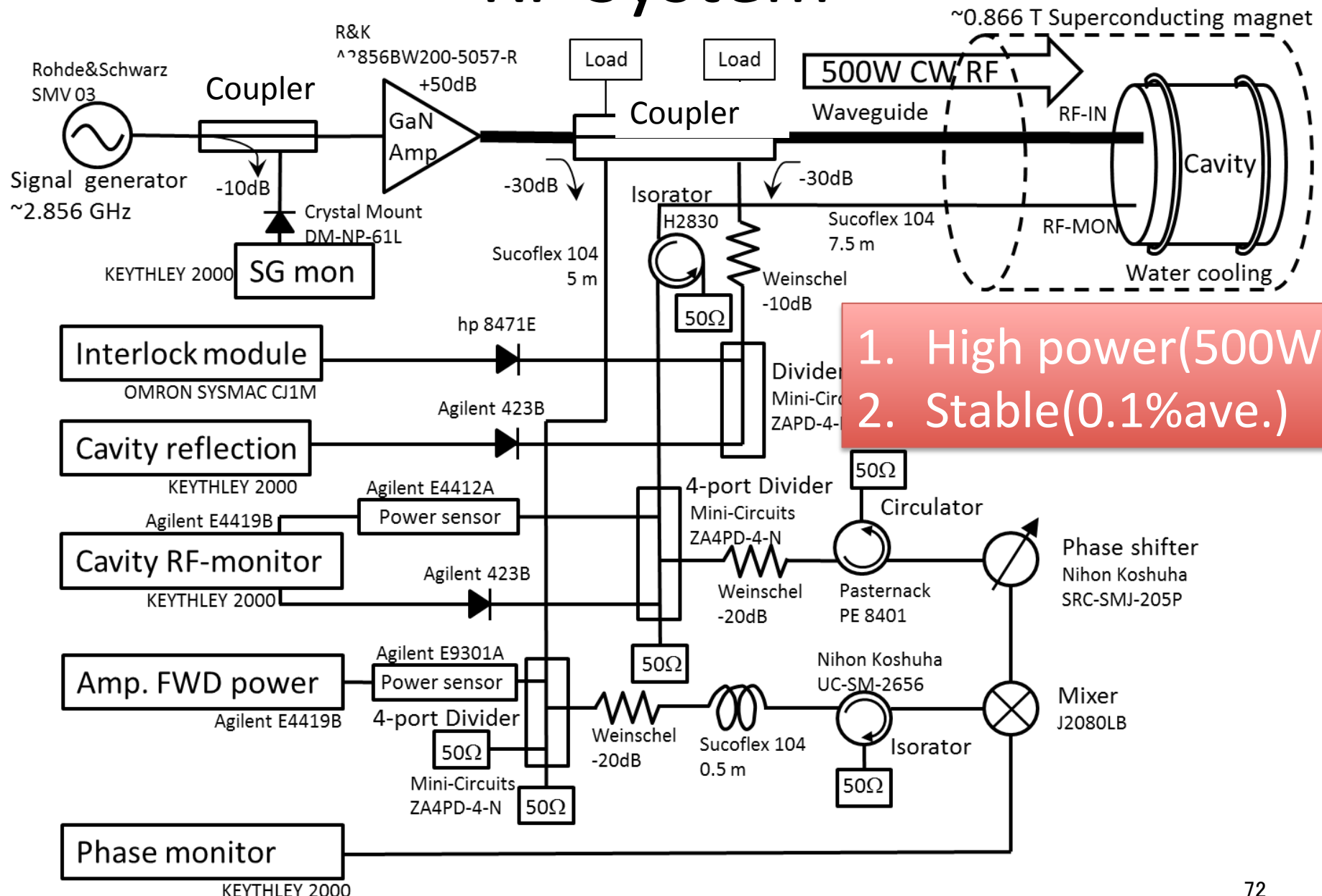
Without magnetic field

- No change at 0°
 - Photoelectrons emitted from photocathode goes to anode spiraling around magnetic field and being gained.
 - 0° is the most efficient at the first diode.
- Good resolution

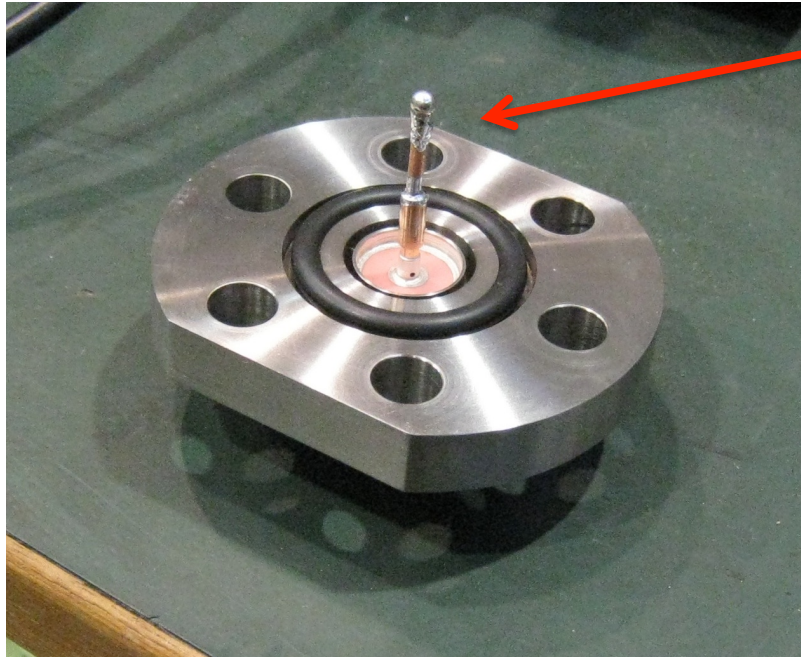
Angle(θ) dependence of timing resolution



RF System



RF input

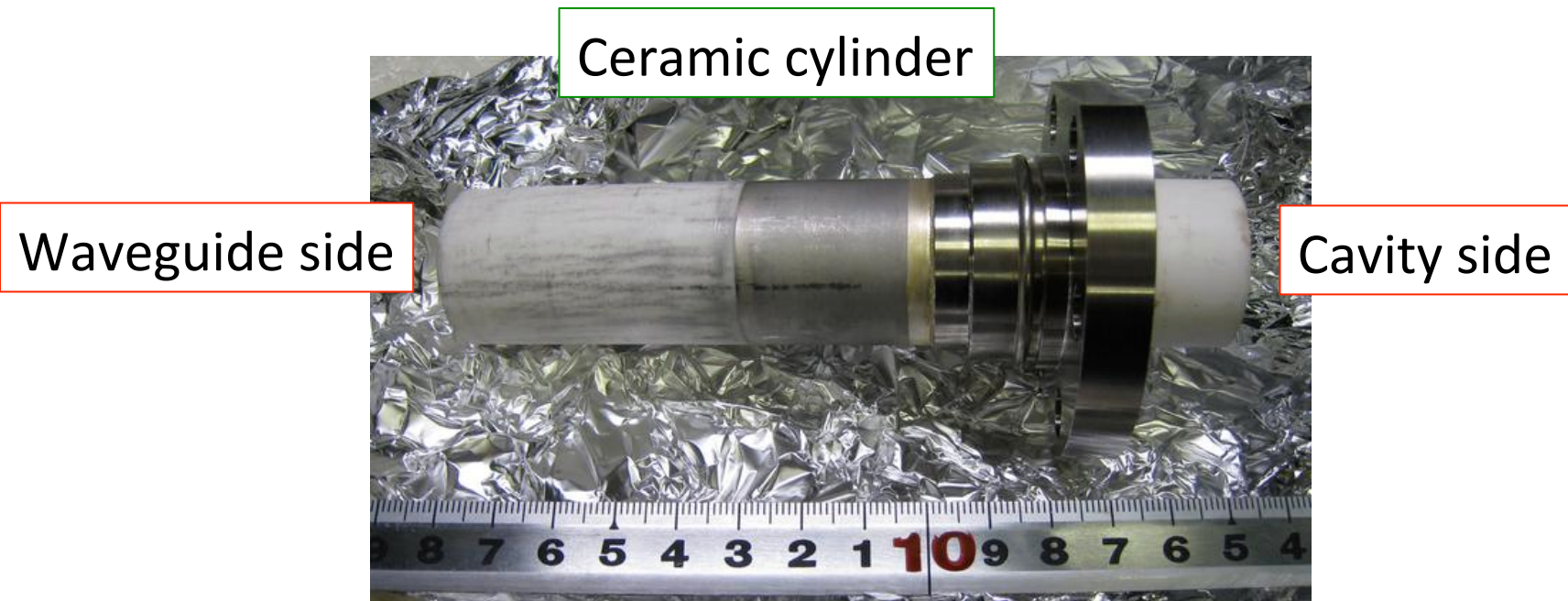


antenna (Cu)

Input microwaves using metallic antenna
→ discharge at low gas density

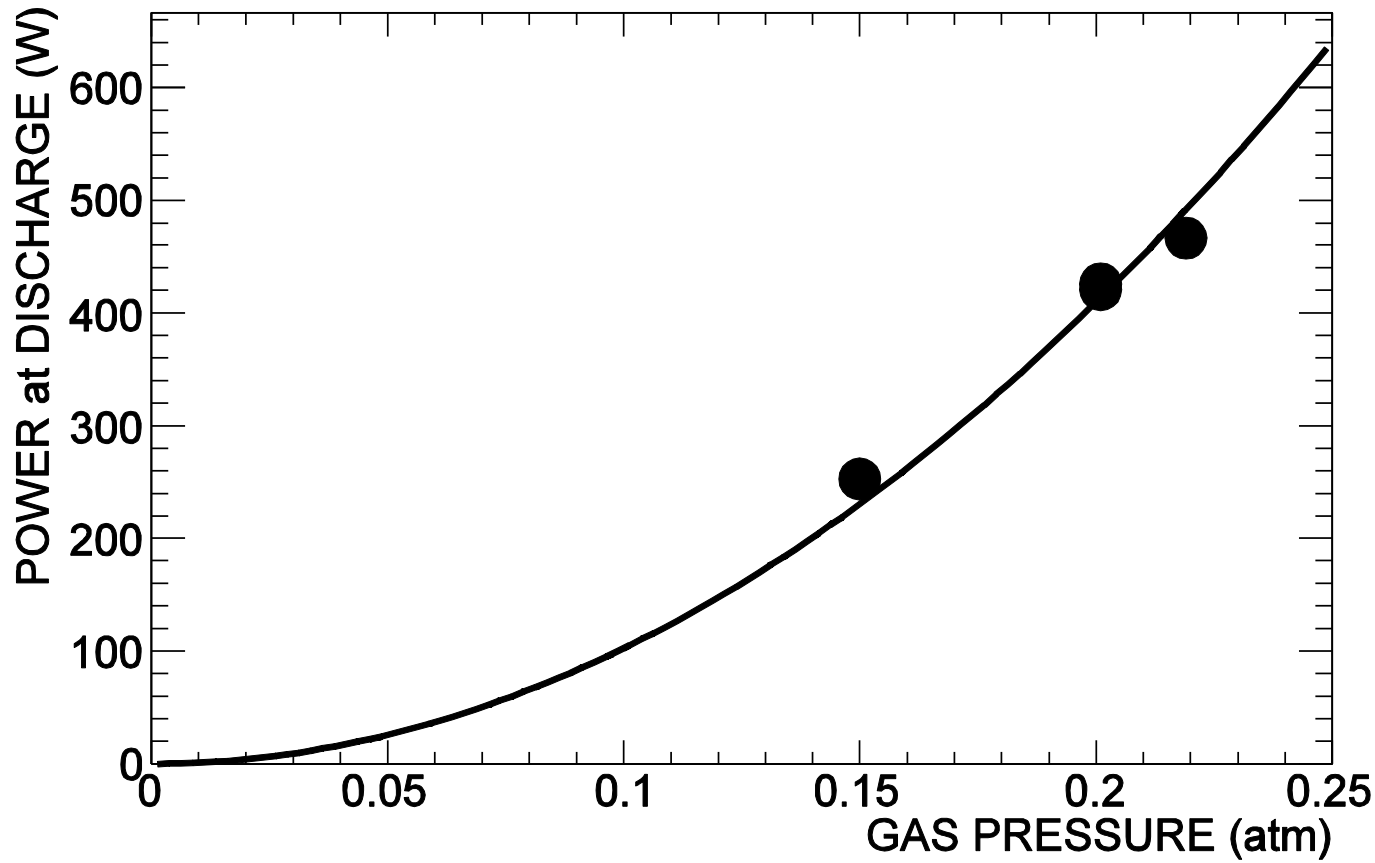
Material effect cannot be evaluated at low gas density

Dielectric (ceramic) feedthrough

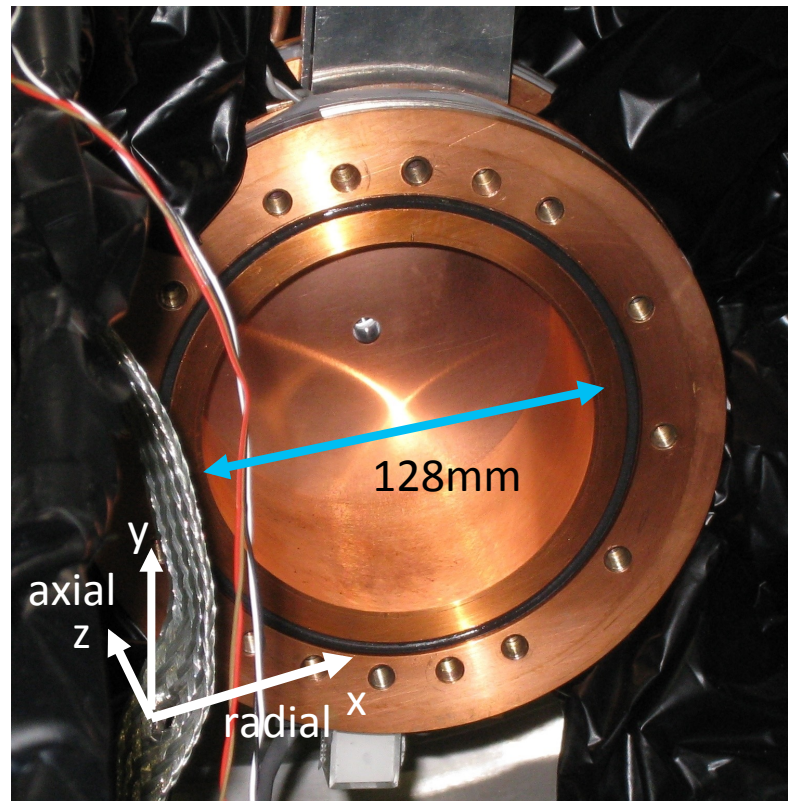
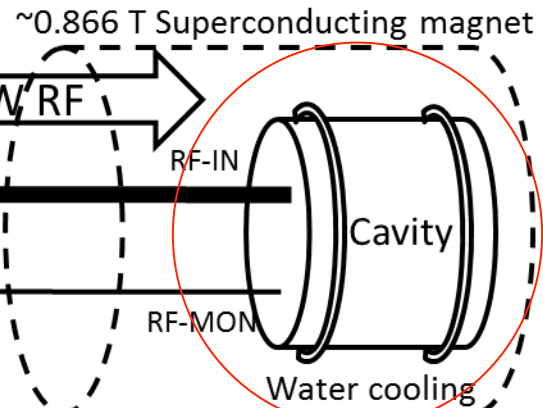
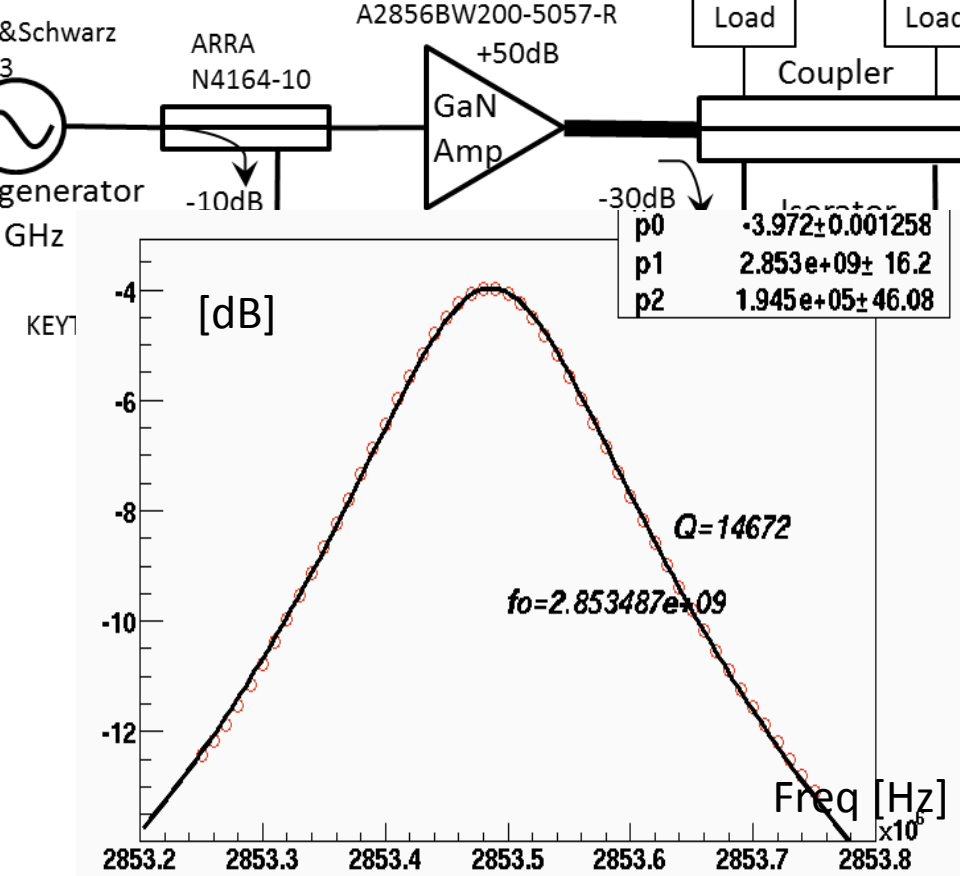


- 500 W CW can be input at the gas density as low as 0.25 atm.
- Measured HFS with low RF power at lower gas densities (ex. 300 W).

Discharge

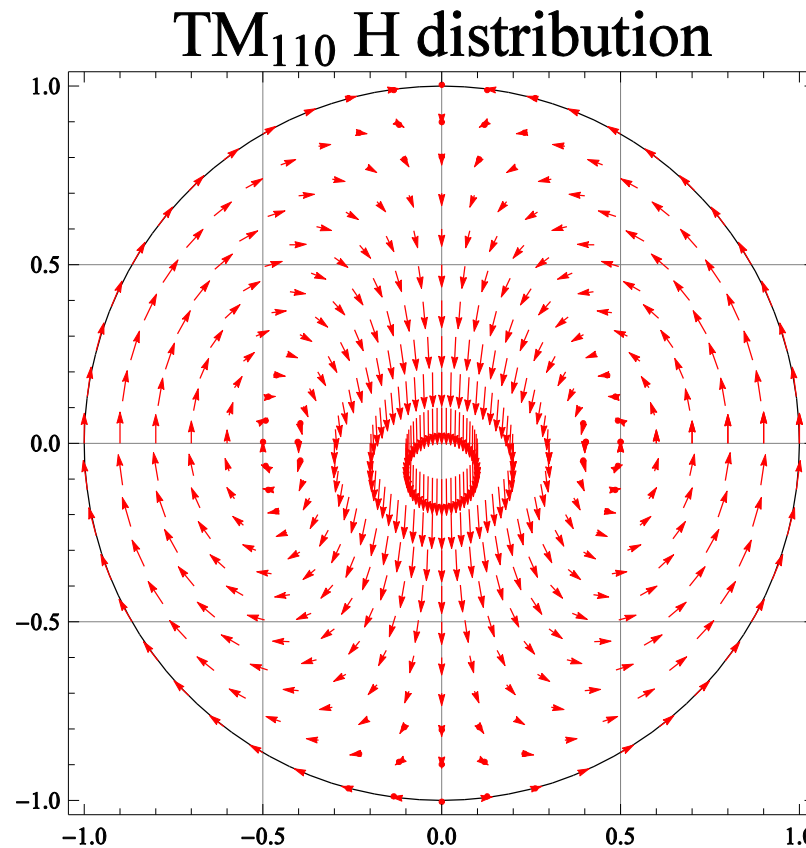


RF Cavity

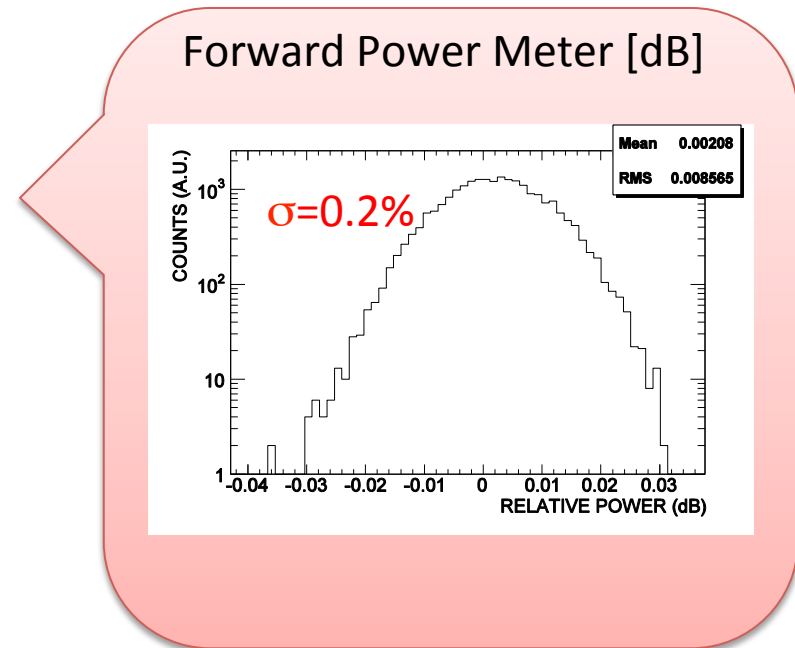
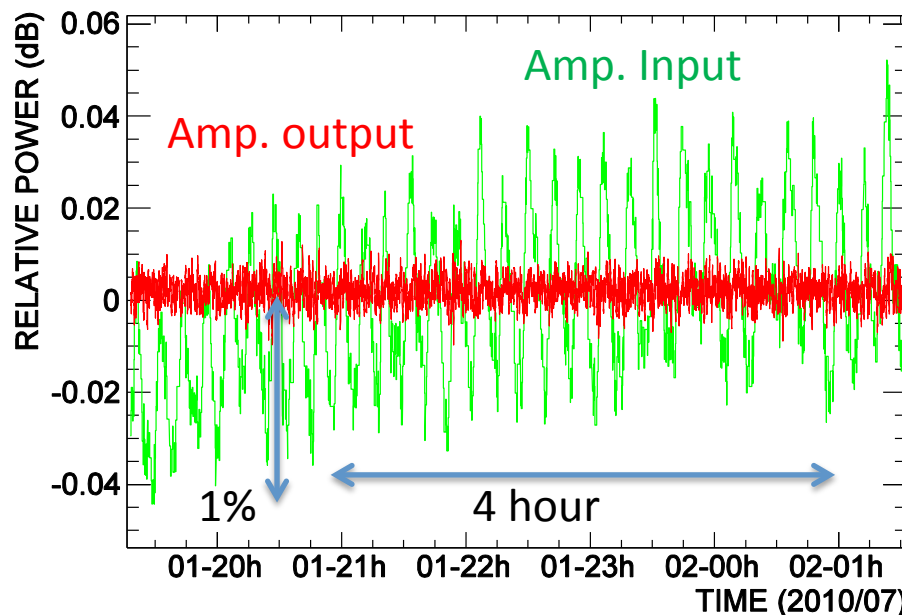


1. Resonant freq.: 2856.6 MHz
2. Mode: TM₁₁₀
3. Max. power: 600W [CW]
4. Wall thickness (Cu): 1.5 mm
5. Q~14,700

Magnetic field of the TM_{110} mode



RF stabilization //Power Feedback

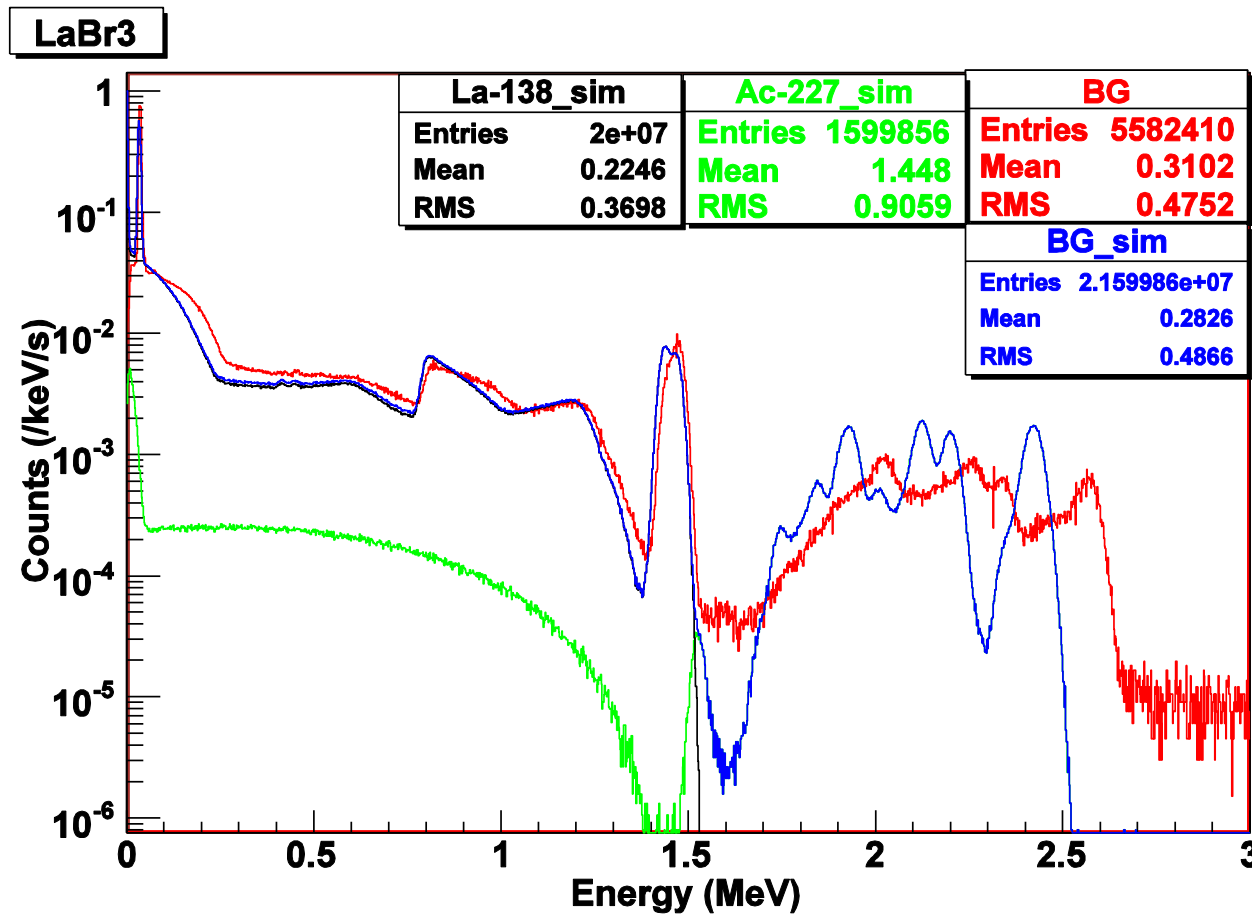


The gain of amplifier fluctuate due to fluctuation of the room temperature. The instability of RF power causes the precision of Ps-HFS to be poor. Power feedback on SG output (Amp. Input) RF can be used to stabilize the Amp. output power. Stable RF power was obtained for the long measurement period. Short-time fluctuation was **0.2%**, and 1-hour averaged power had only **0.08%** fluctuation.

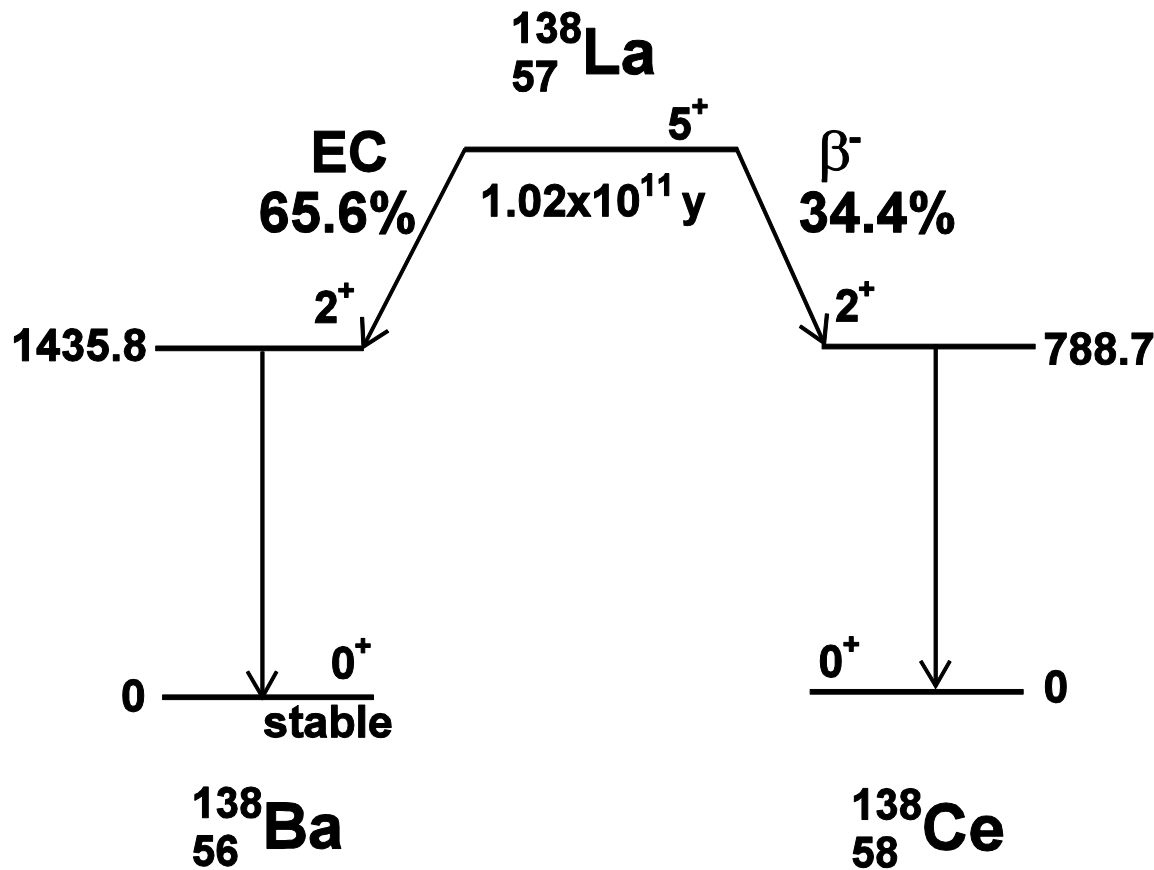
Spec of scintillators

scintillator	density	reflective index	Photons per MeV	Max. intense wavelength	decay time	Radiation Length
	g / cm ³			nm	ns	cm
Nal (Tl)	3.67	1.85	38000	415	230	2.59
CsI (Tl)	4.51	1.79	59000	565	1000	1.86
LYSO	7.25	1.81	32000	420	40	1.15
YAP (Ce)	5.55	1.93	19700	347	28	2.7
LaBr ₃ (Ce)	5.08	1.9	63000	380	16	1.88

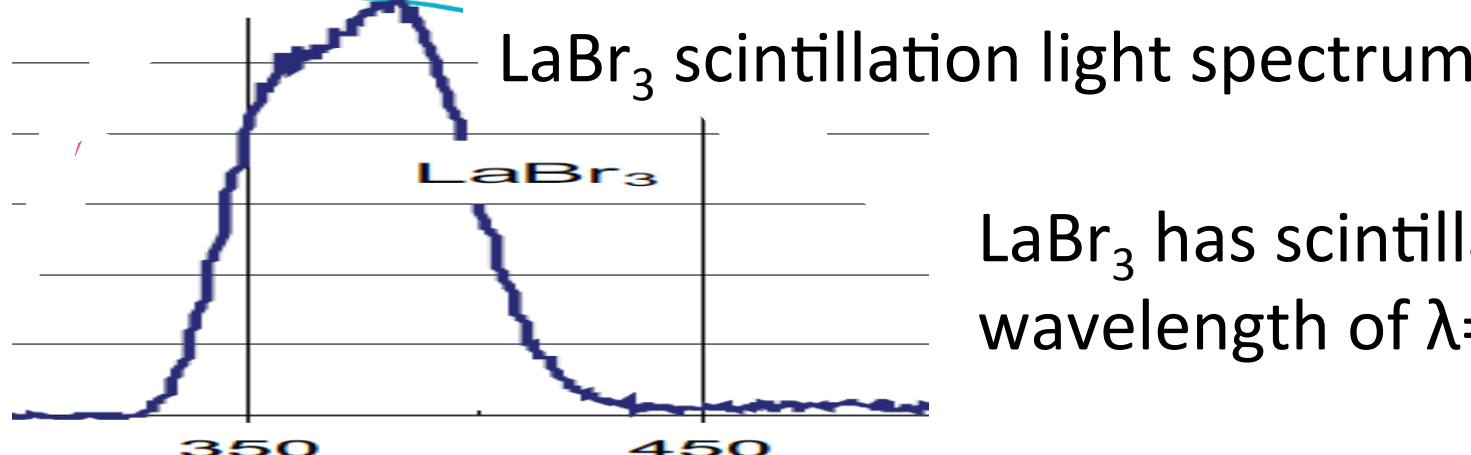
Background energy spectra of LaBr₃(Ce)



Decay scheme of ^{138}La



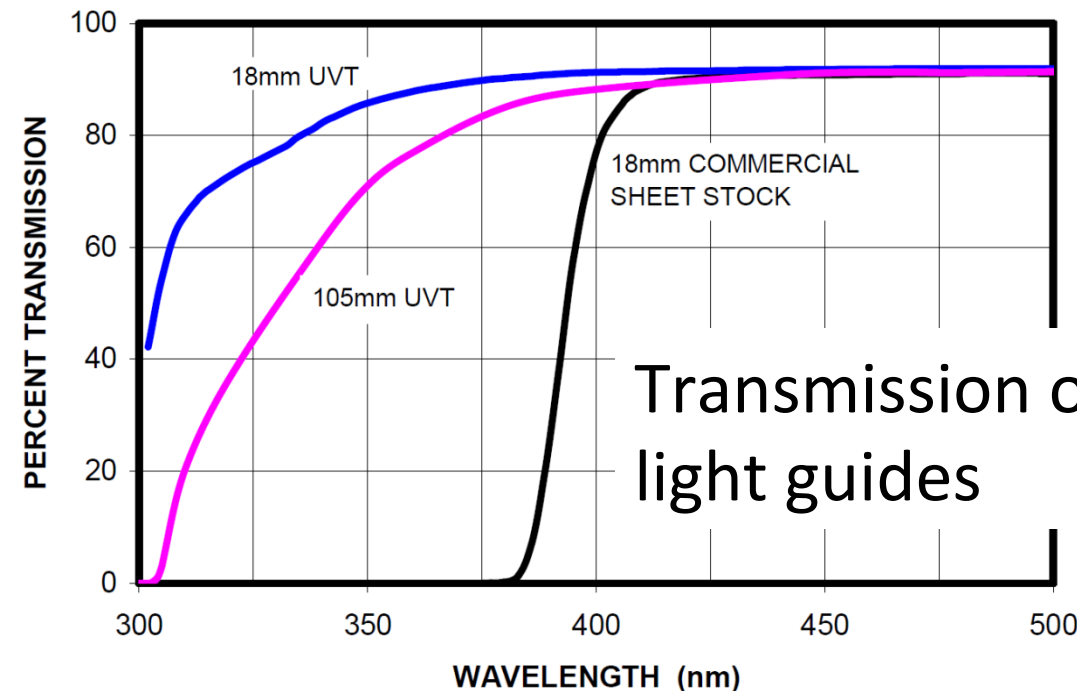
UVT light guide



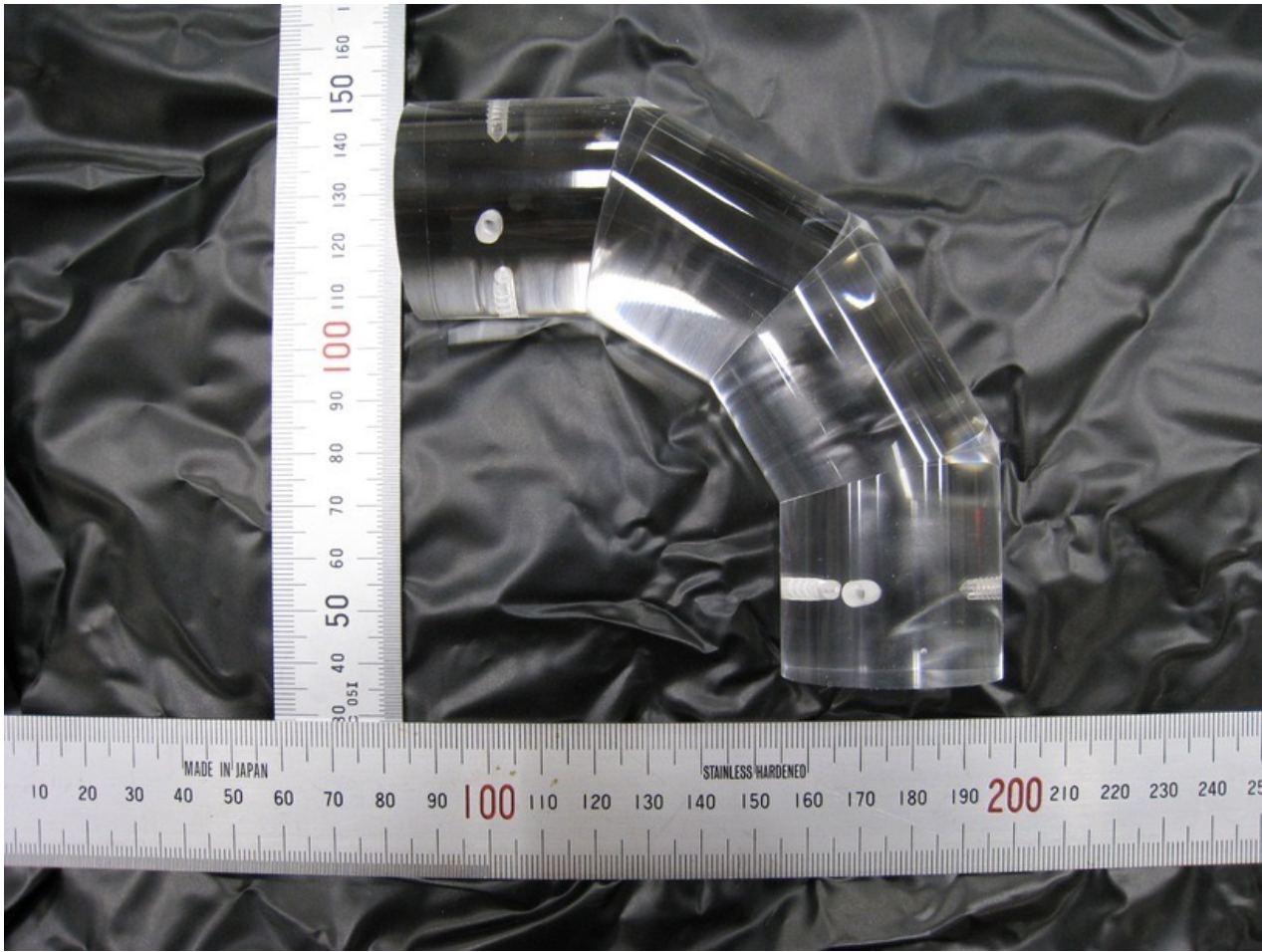
LaBr_3 has scintillation light wavelength of $\lambda=380 \text{ nm}$

UVT
(Ultra-Violet Transmitting)
light guides were used.

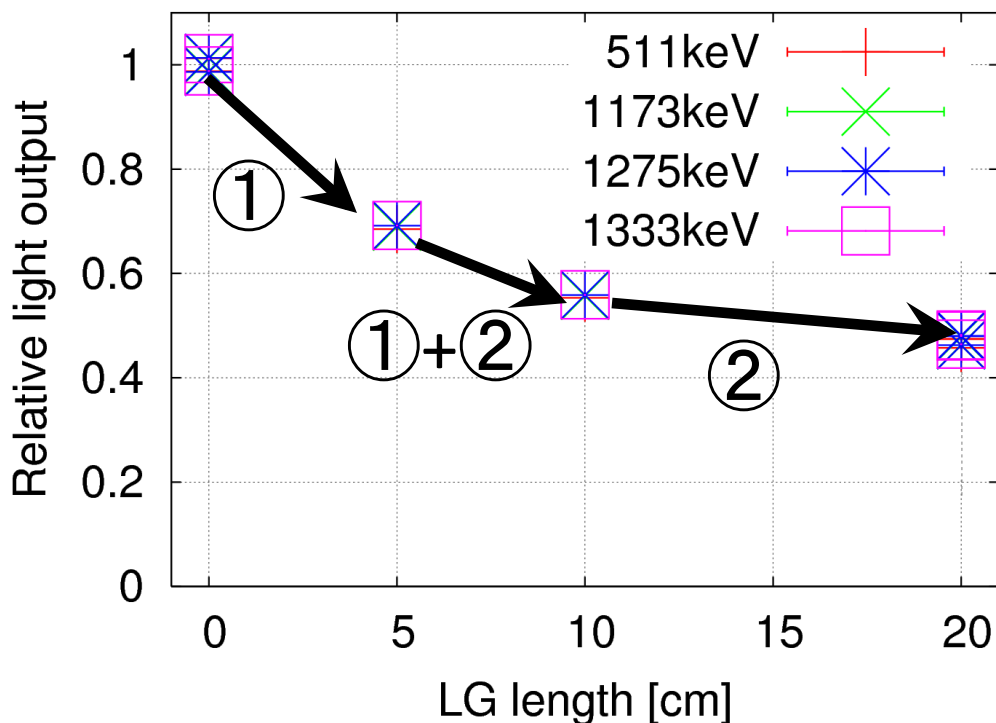
Transmission of UVT
light guides



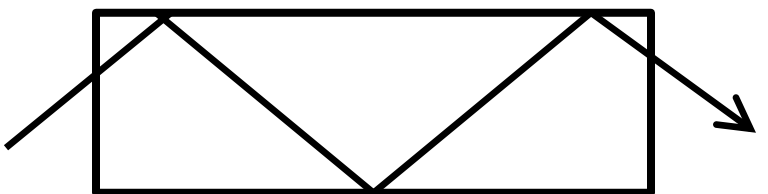
UVT light guide



Light guide length dependence of output light amounts



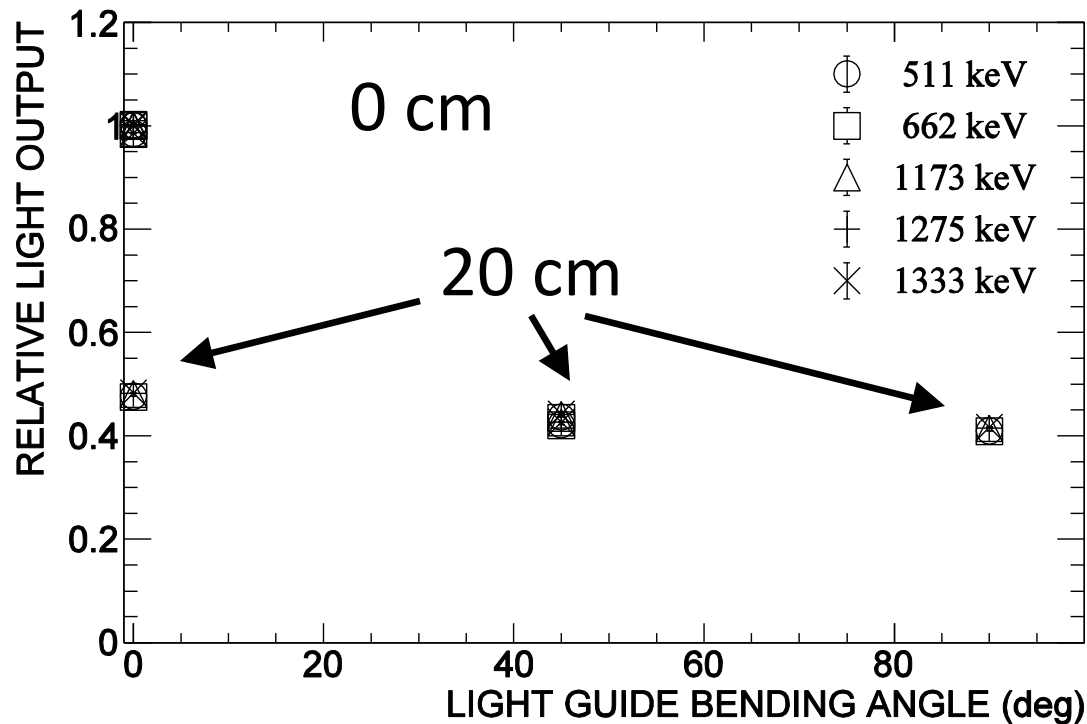
① Lose lights which do not satisfy total reflection condition



② Absorption
(relatively small effect)

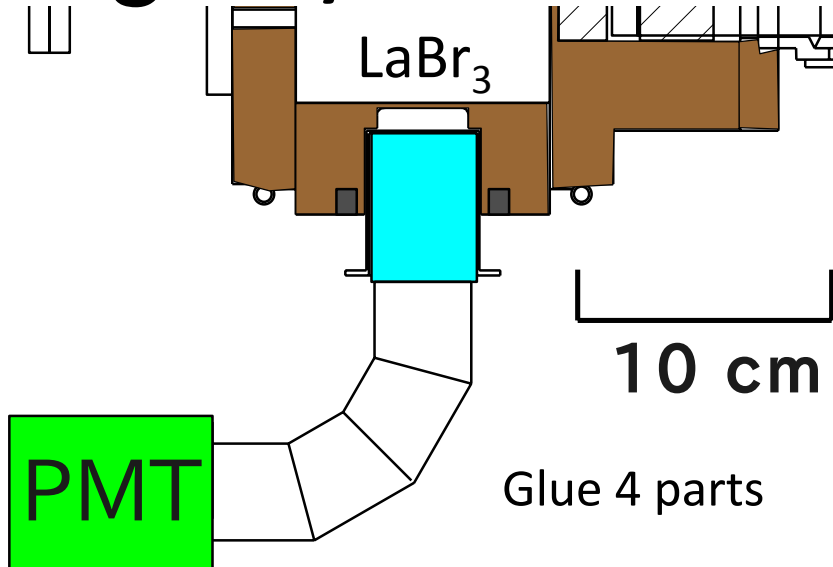
About half at 20 cm, no more large decrease

Angle dependence

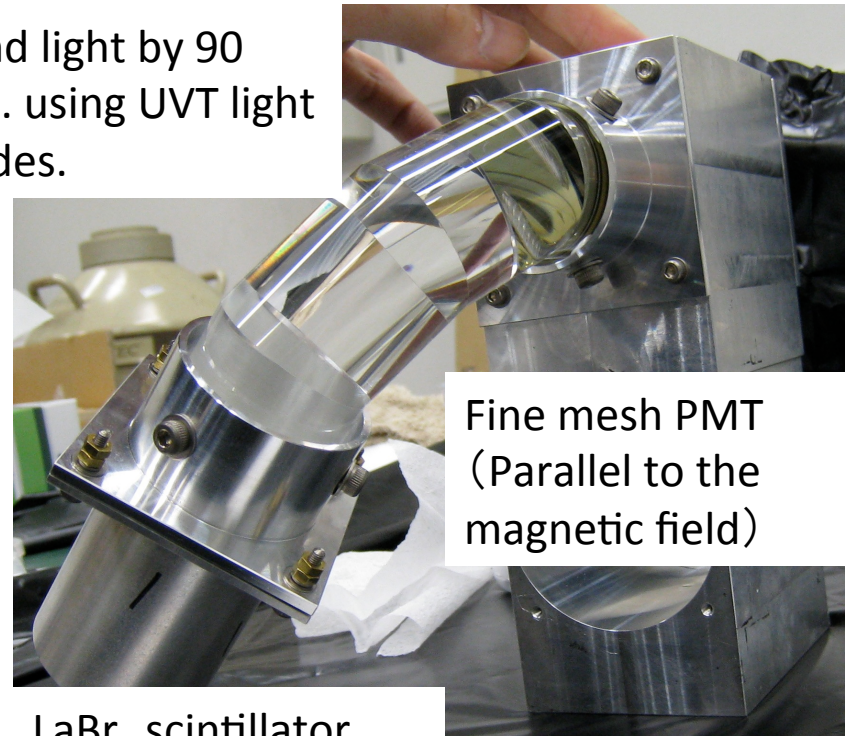


- No big change at 20 cm (similar at 0° , 45° , and 90°)
- Almost no effect by bending.

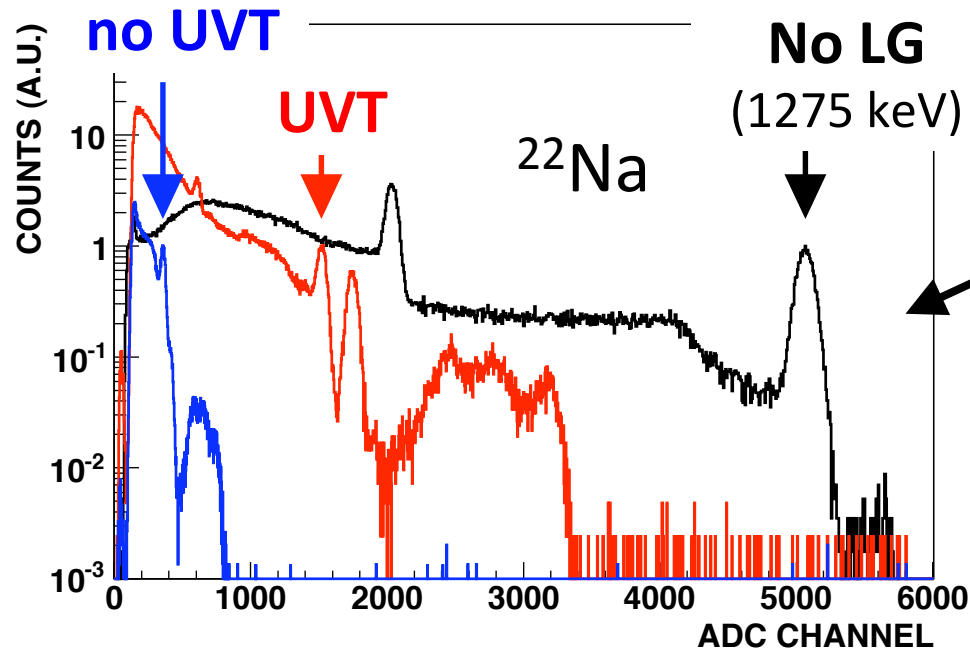
γ -ray detector ~UVT light guide~



Bend light by 90
deg. using UVT light
guides.

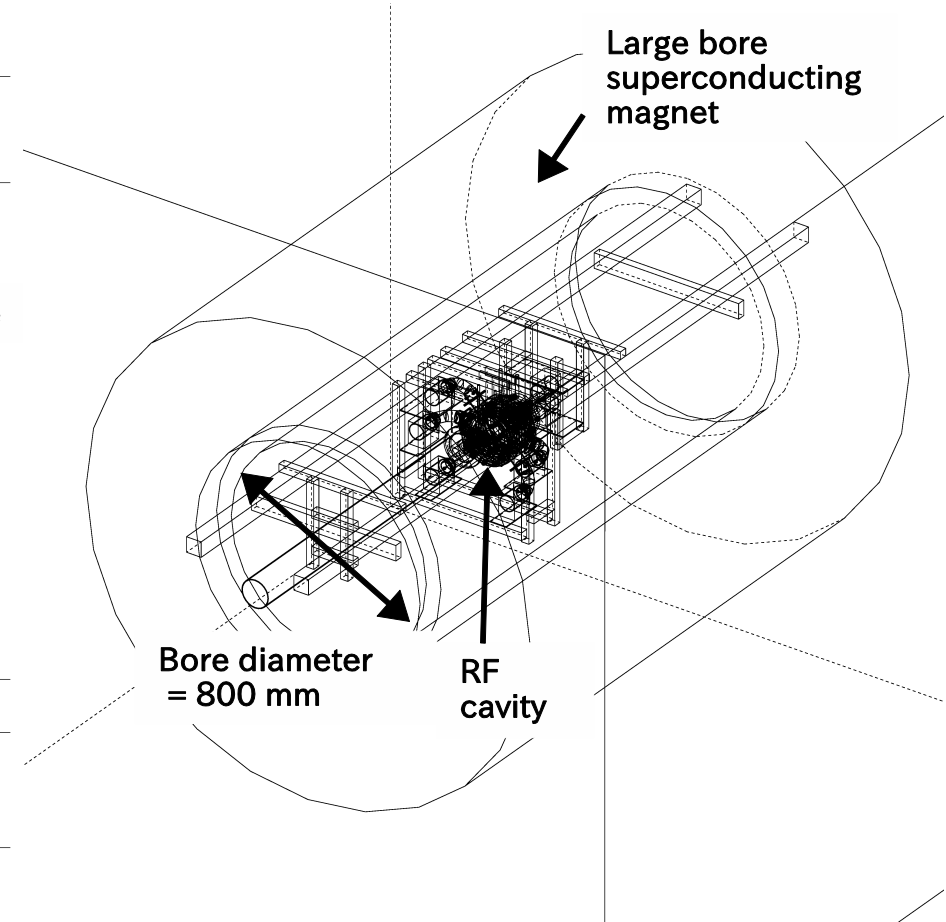
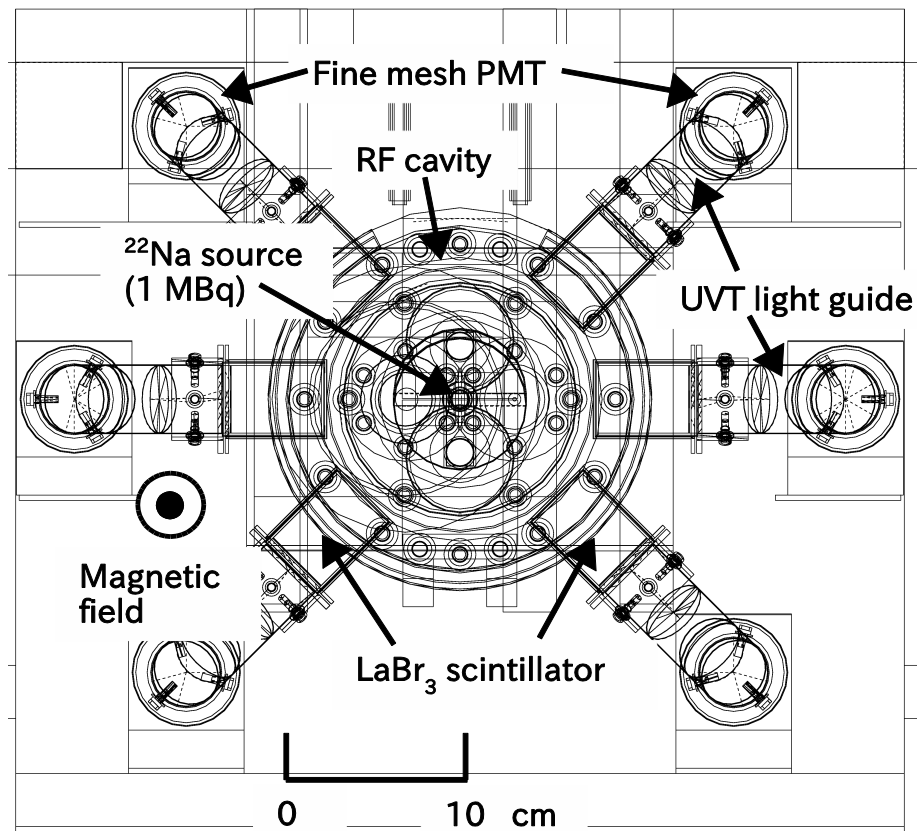


Fine mesh PMT
(Parallel to the
magnetic field)

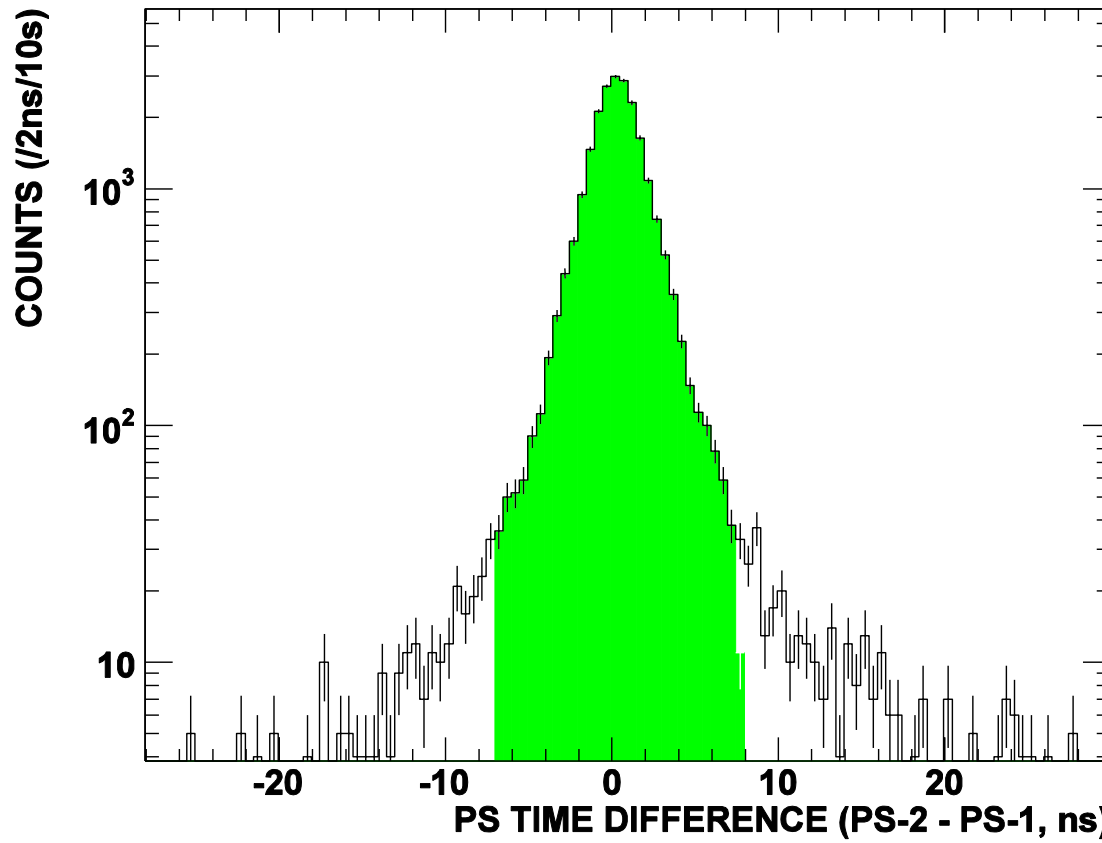


Decrease of light by LG.
Compared to light output without
light guide,
it is decreased to 30% with UVT light
guide.
(7% with no-UVT light guide)

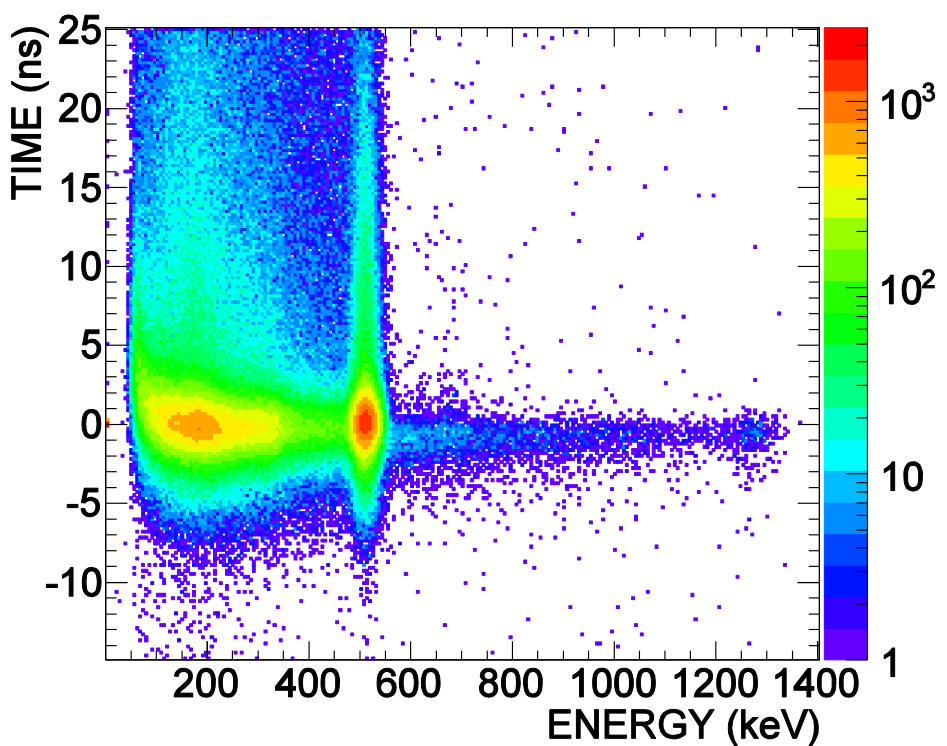
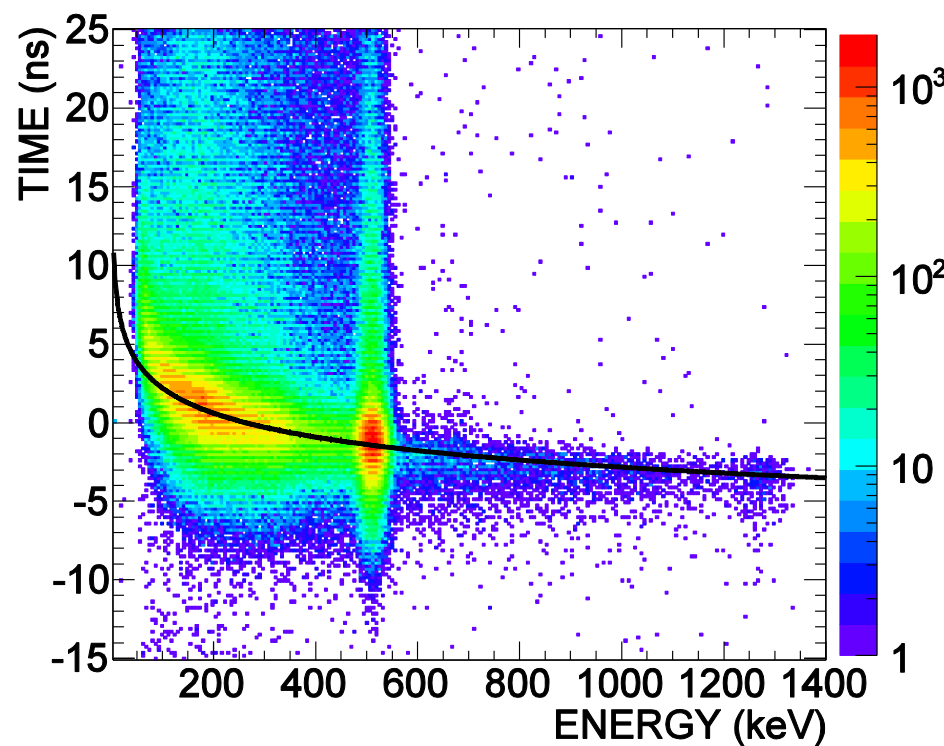
MC geometry



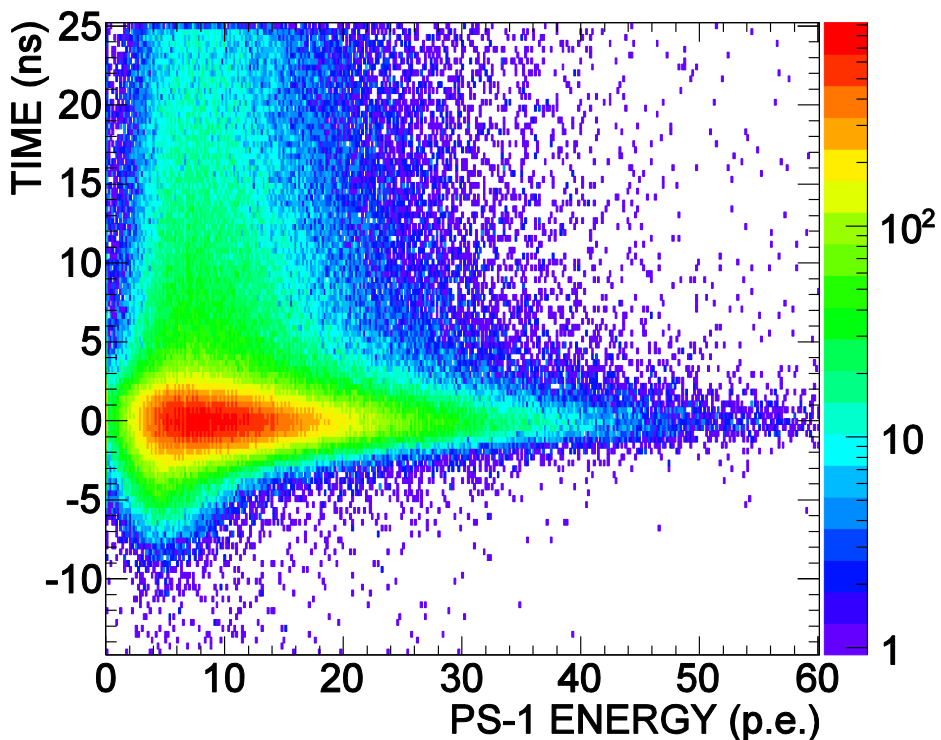
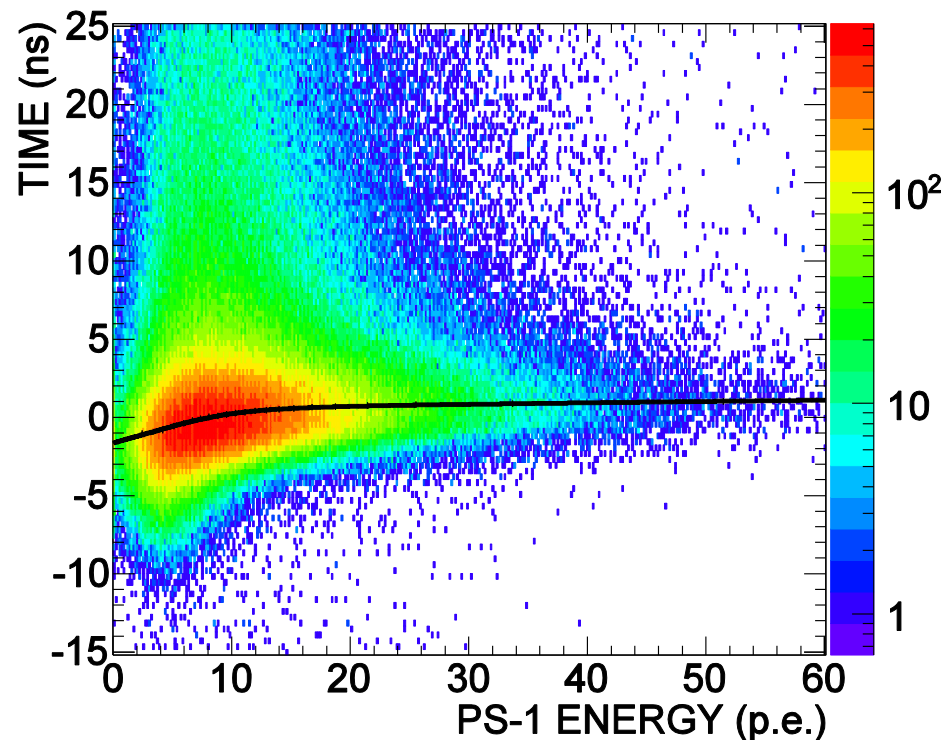
Time difference of the PMTs of the plastic scintillator



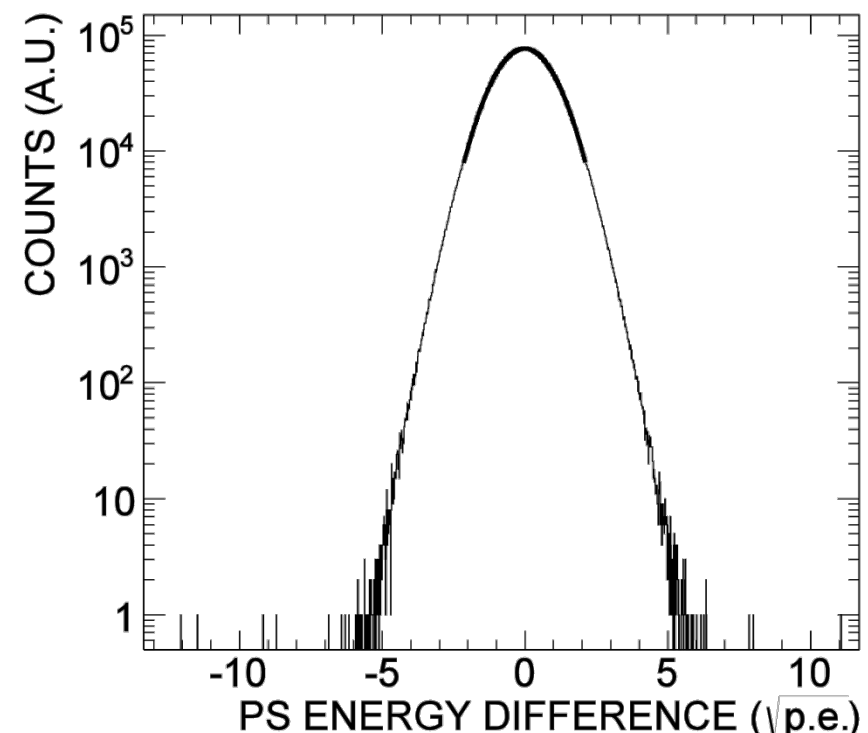
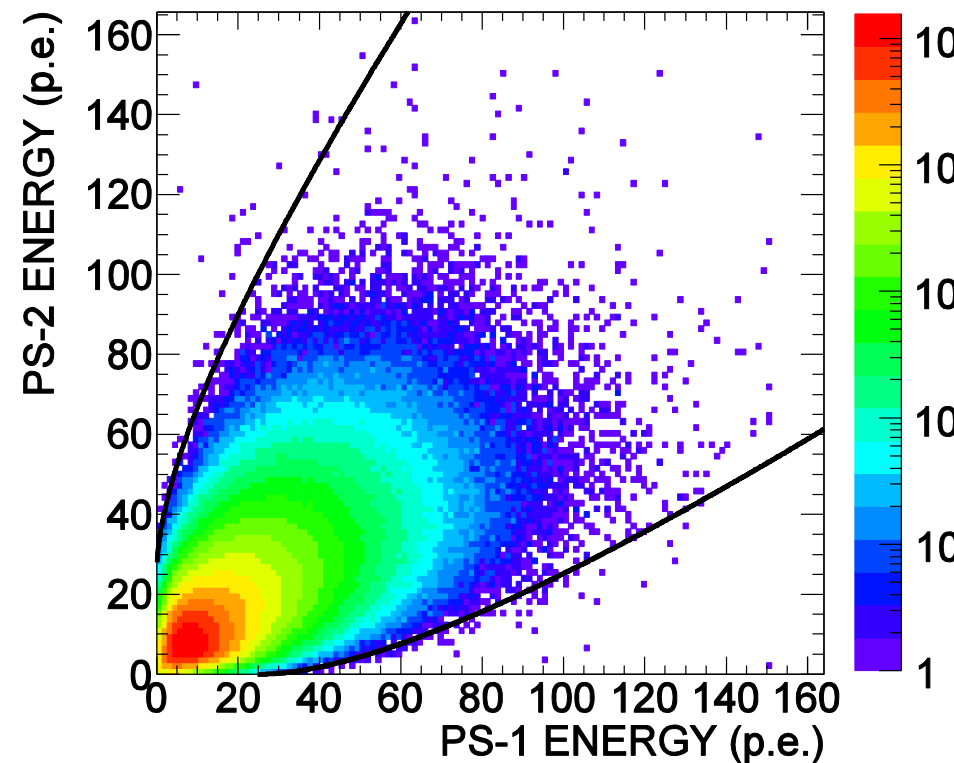
Time walk correction of LaBr₃(Ce)



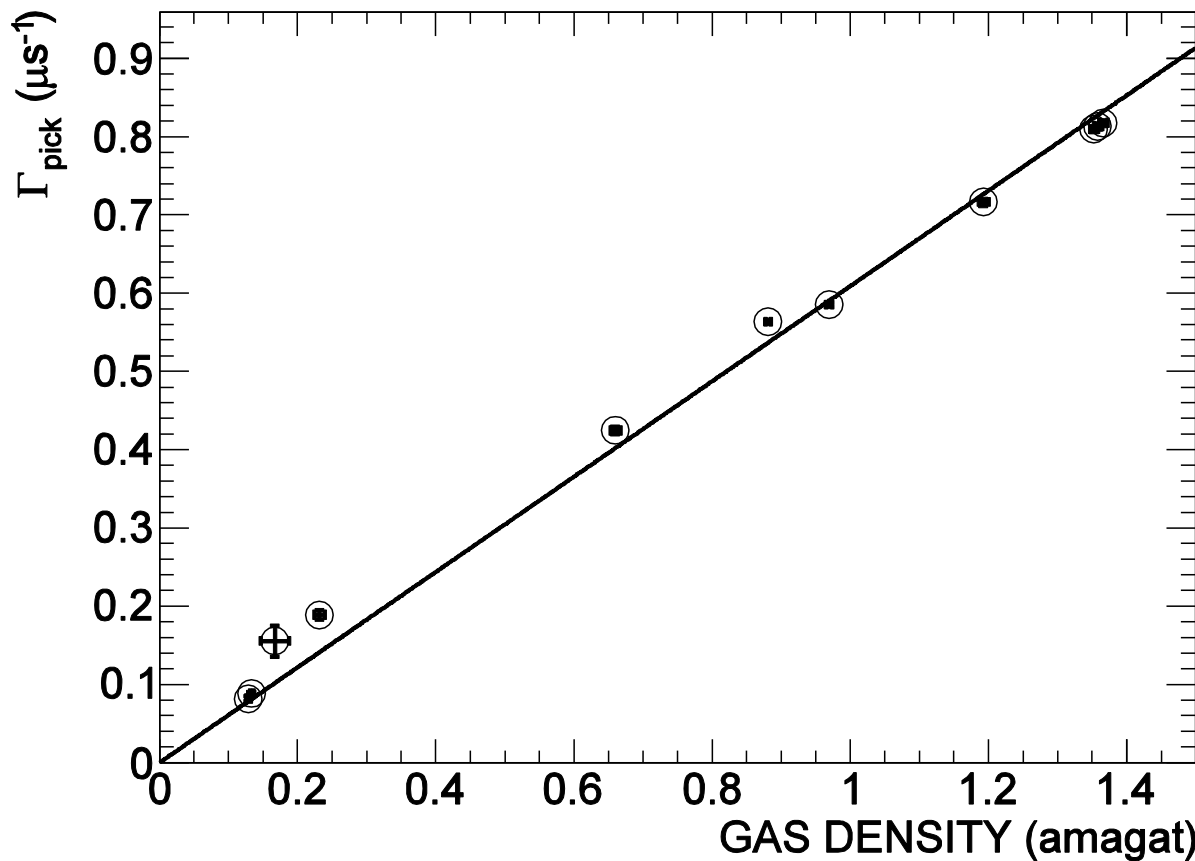
Time walk correction of the plastic scintillator



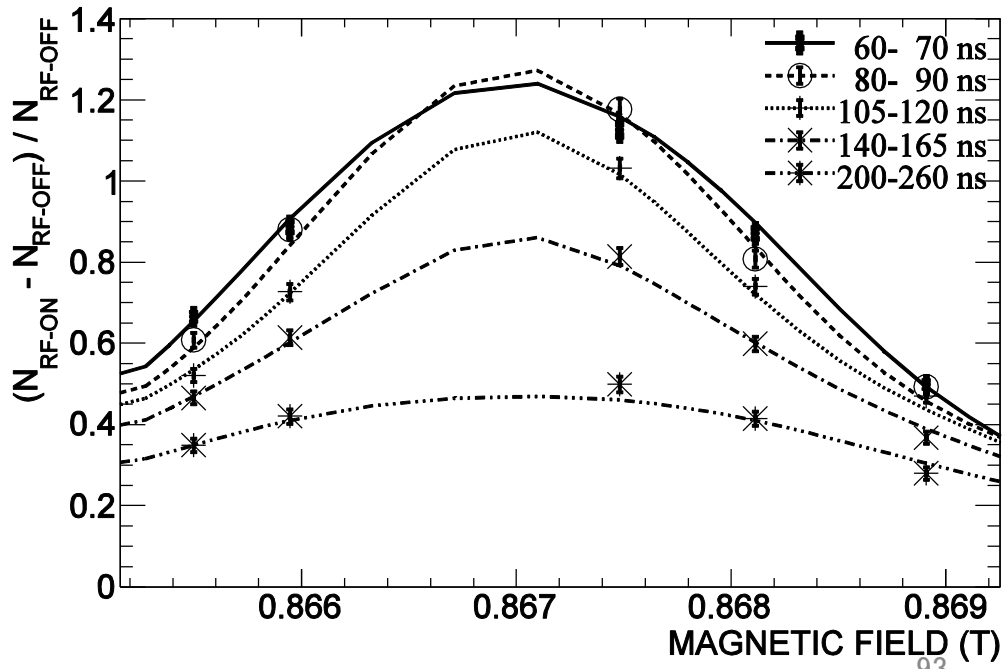
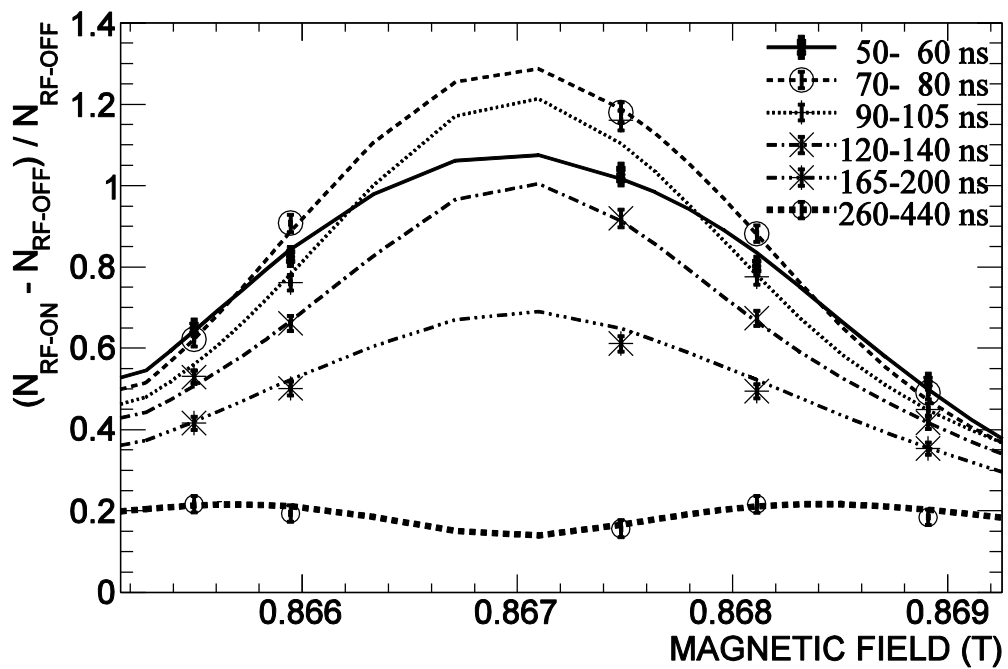
Energy balance cut of the plastic scintillator



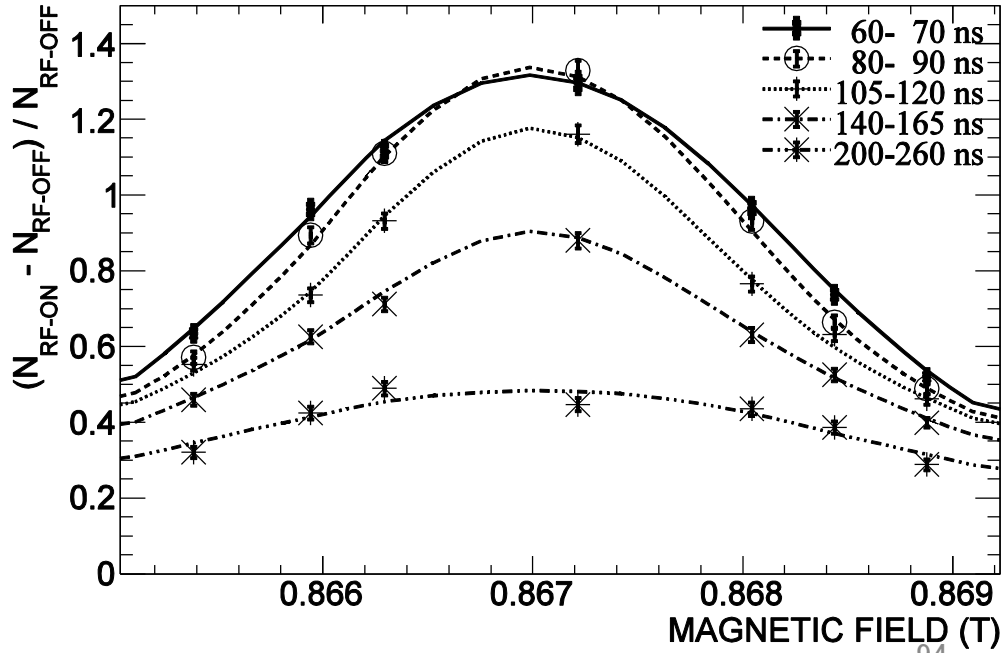
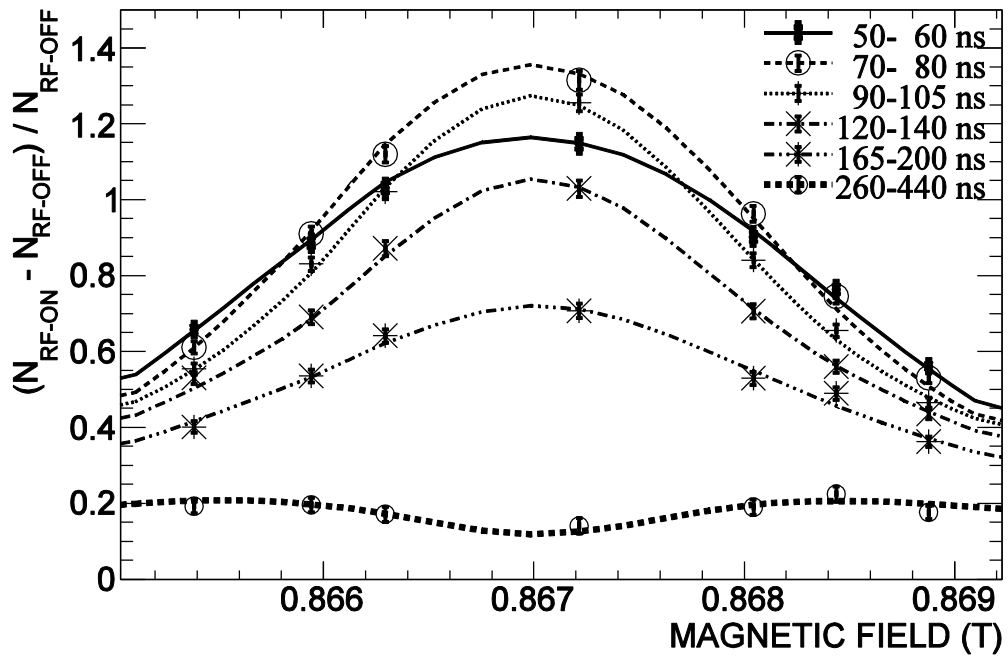
$$\Gamma_{\text{pick}}(n, \infty)$$



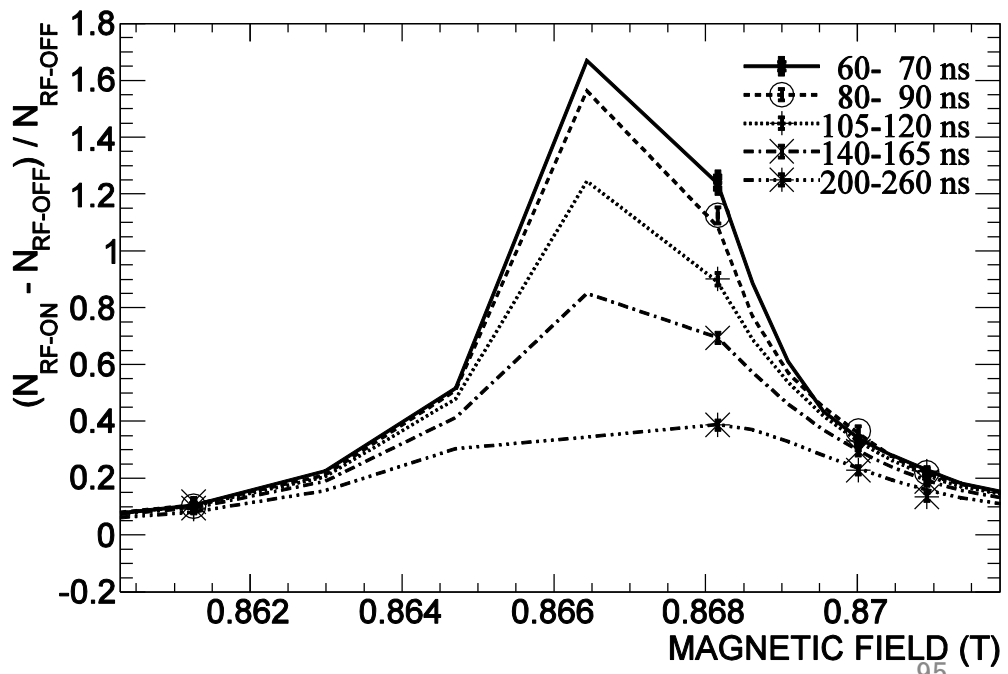
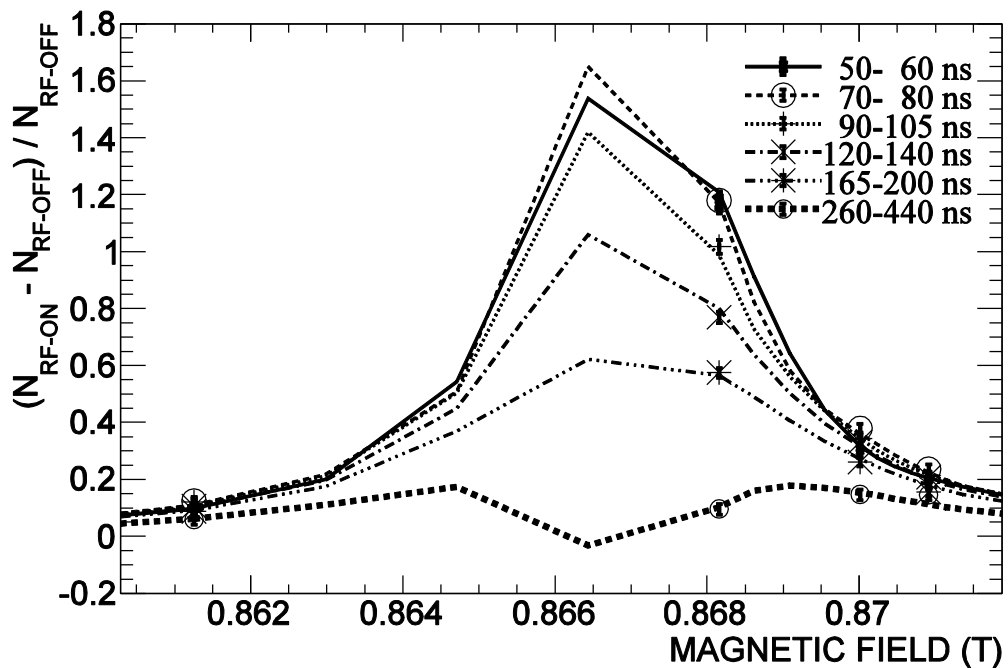
Resonance lines (0.129 amagat)



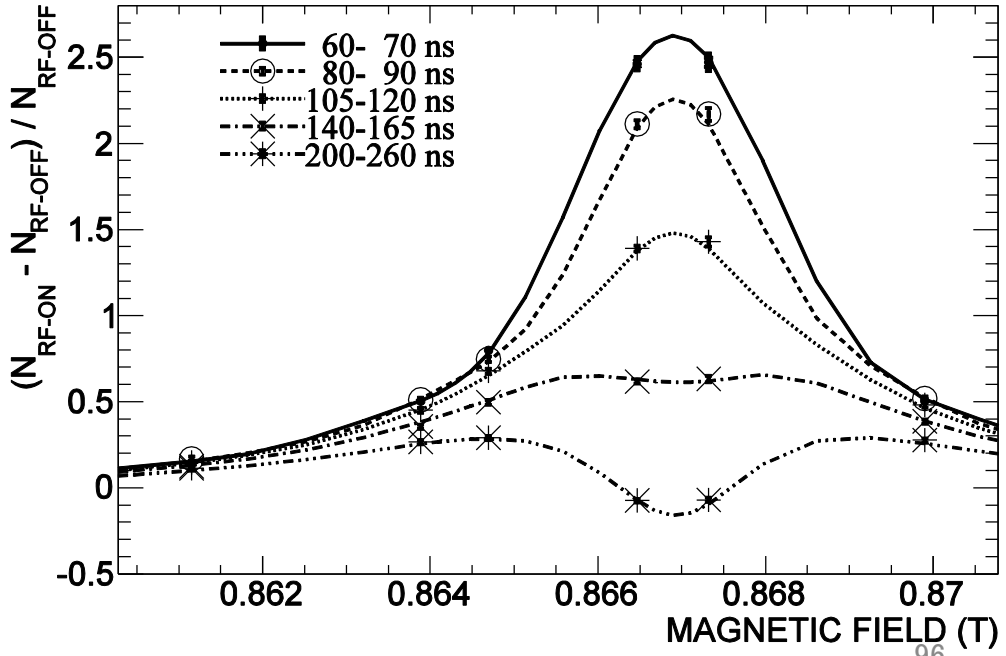
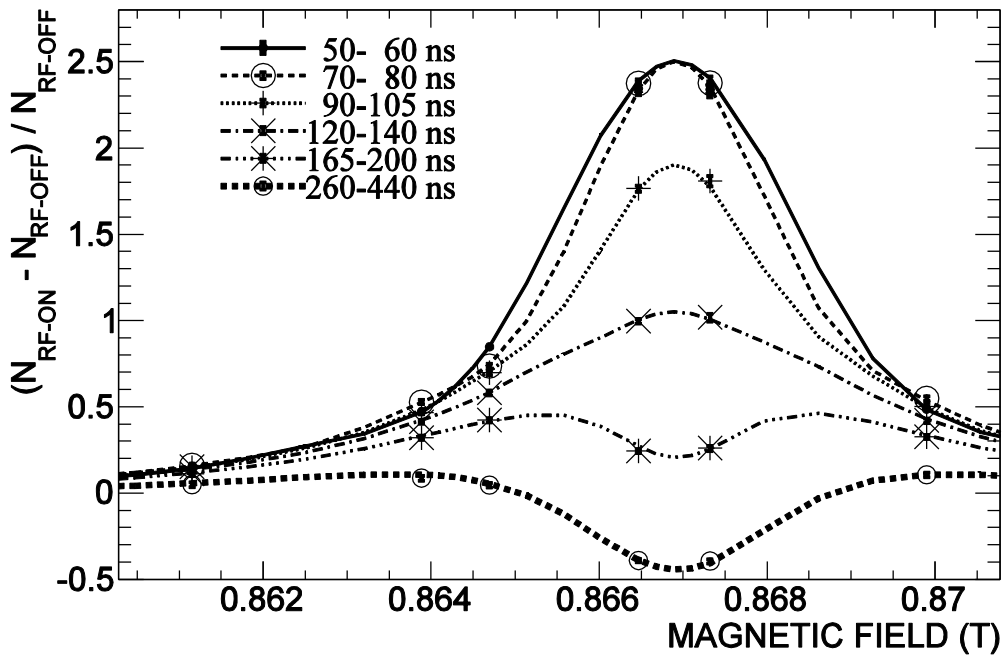
Resonance lines (0.133 amagat)



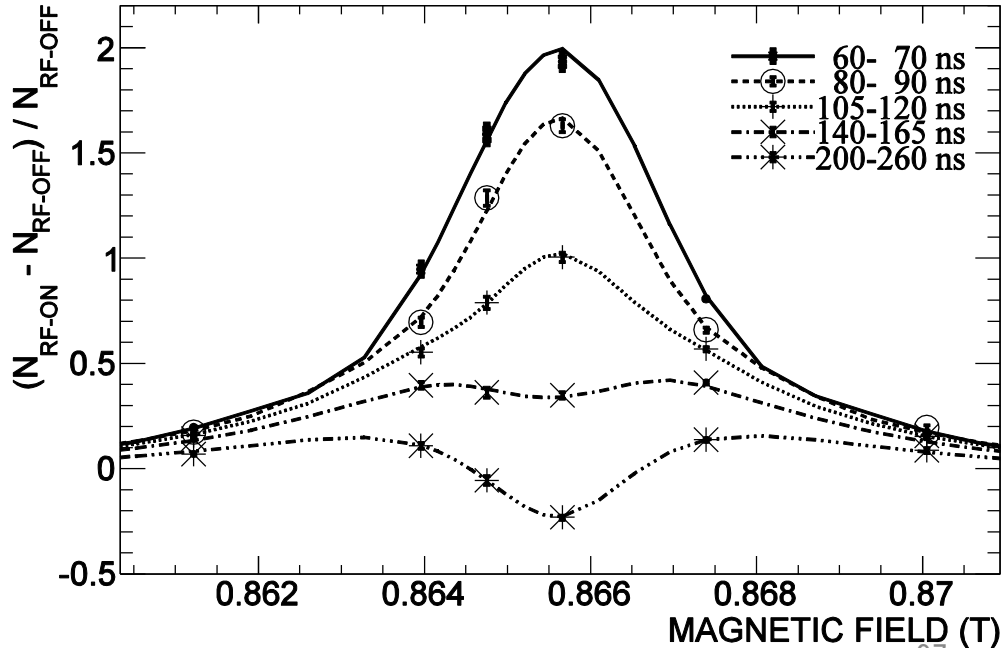
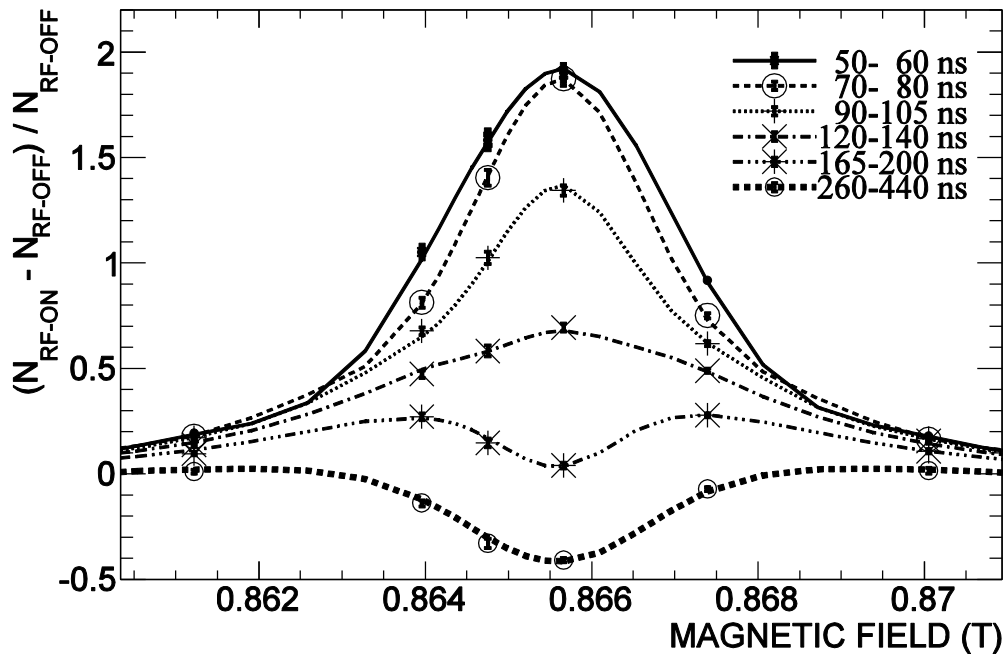
Resonance lines (0.167 amagat)



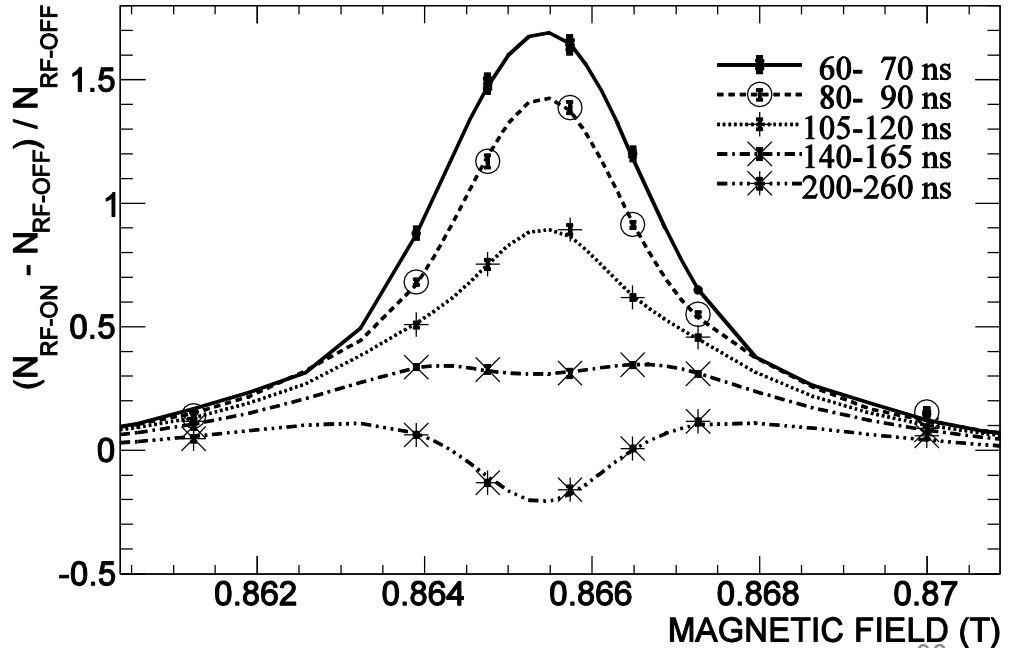
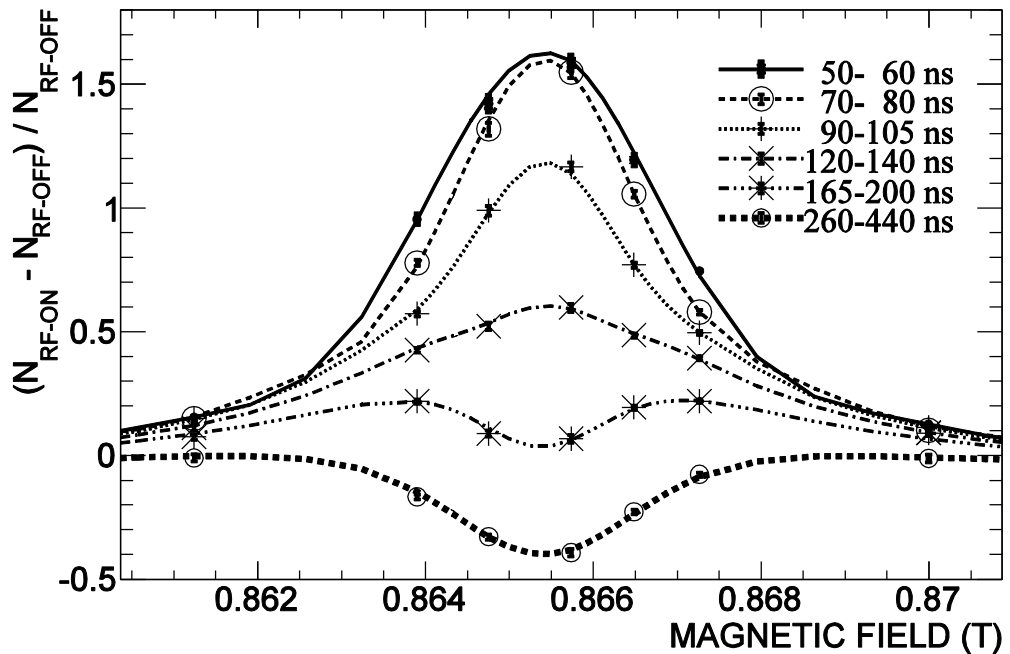
Resonance lines (0.232 amagat)



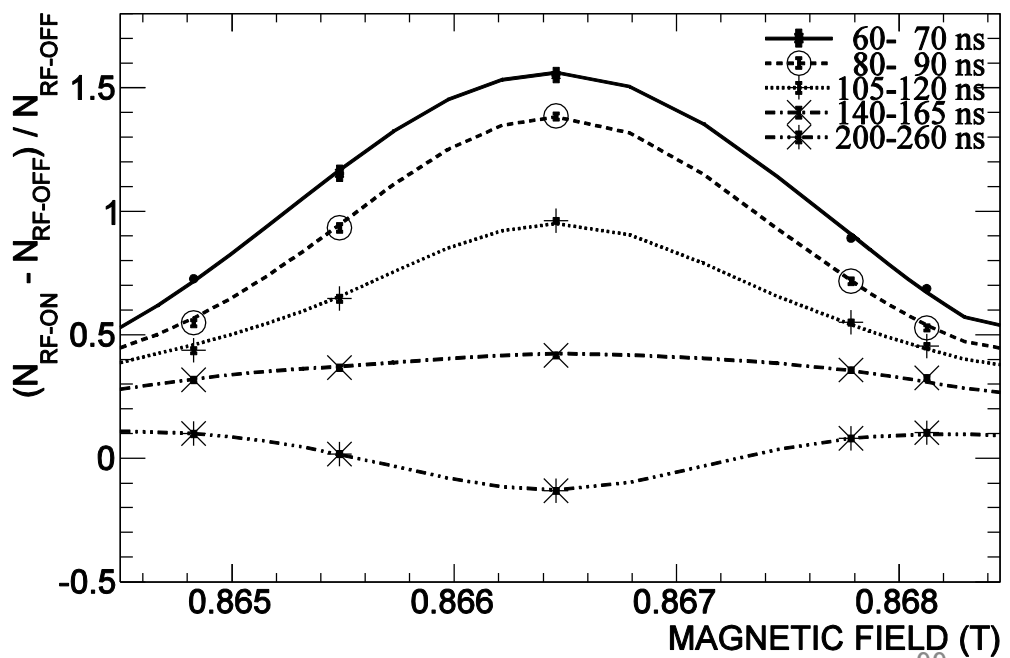
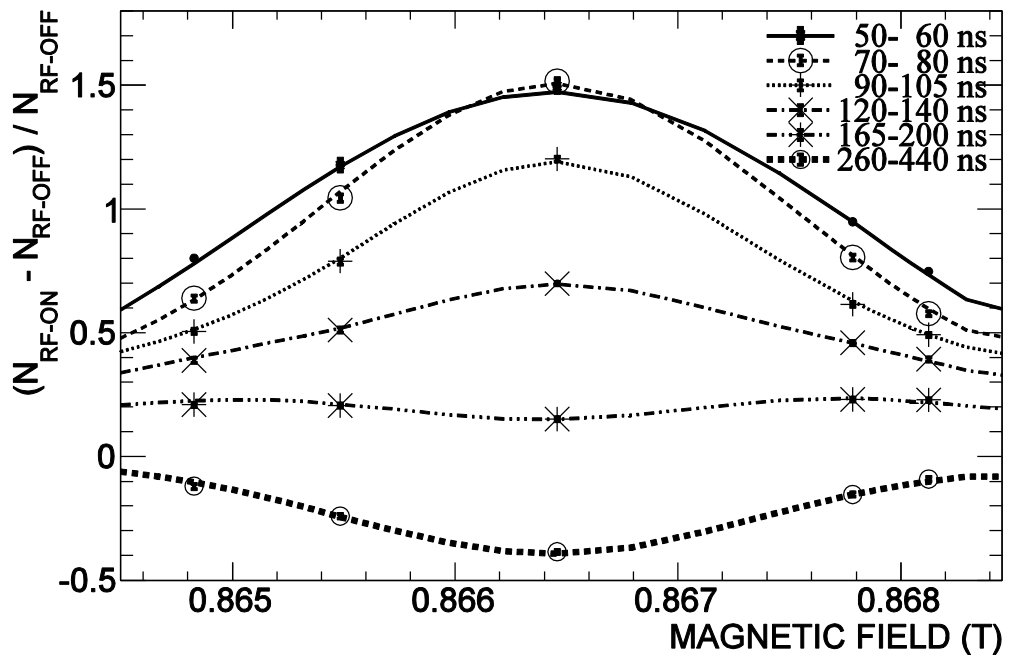
Resonance lines (0.660 amagat)



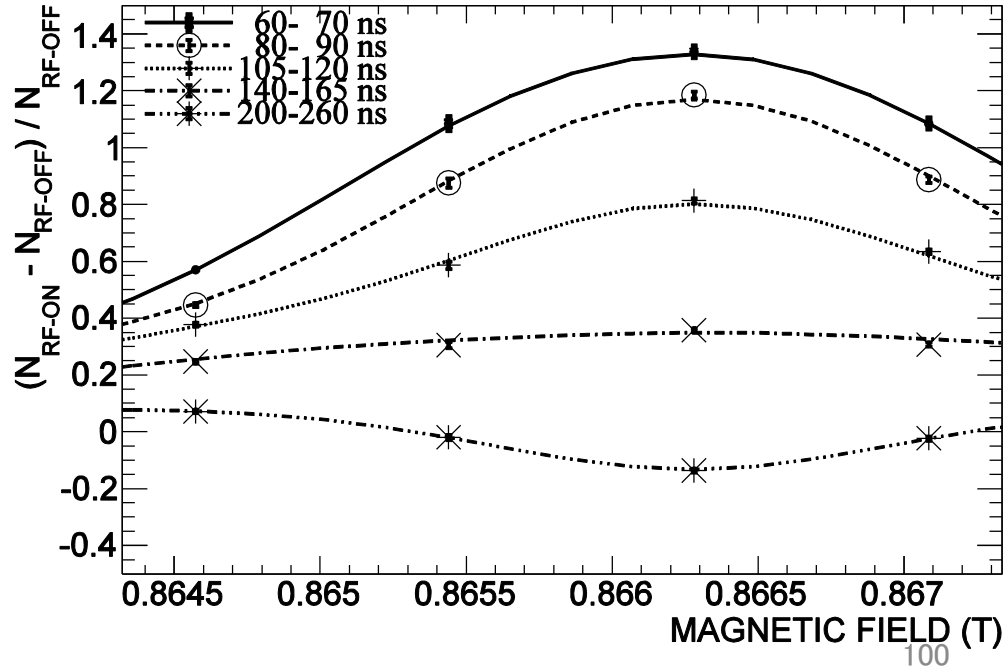
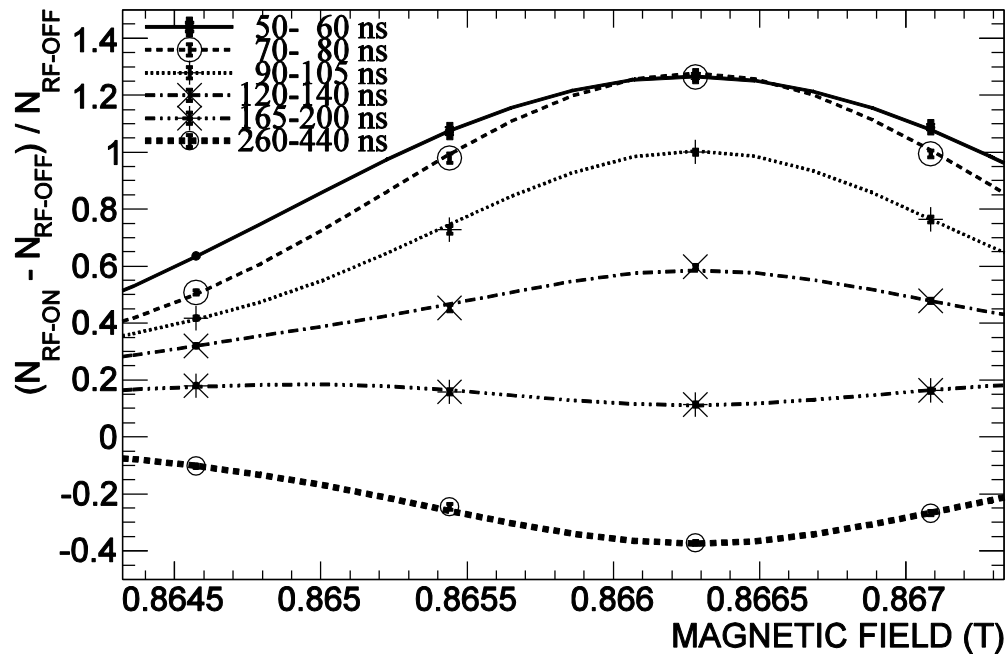
Resonance lines (0.881 amagat)



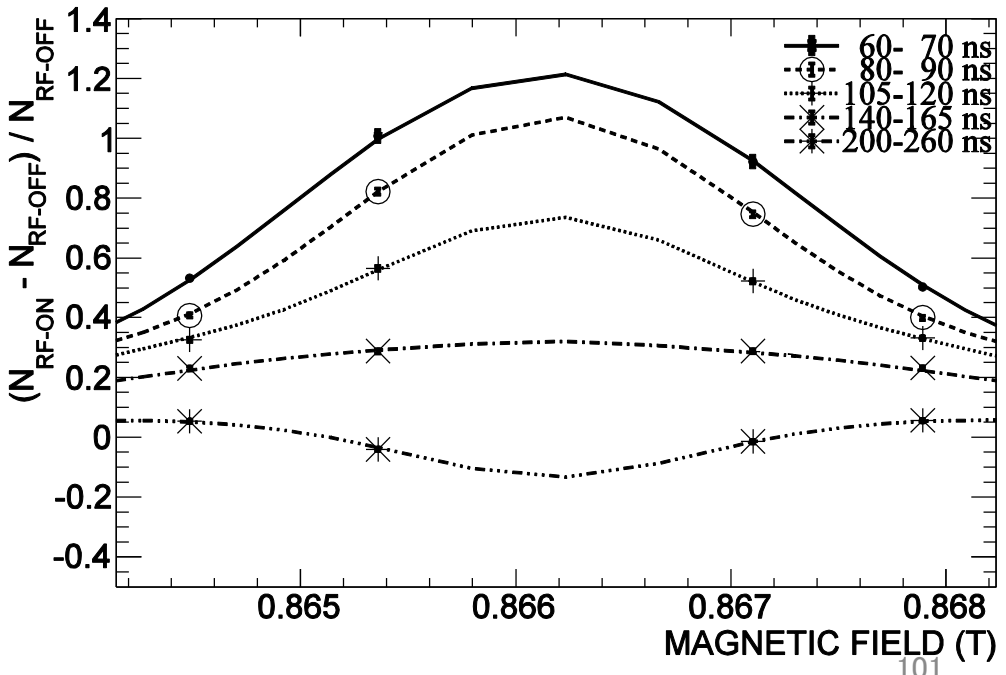
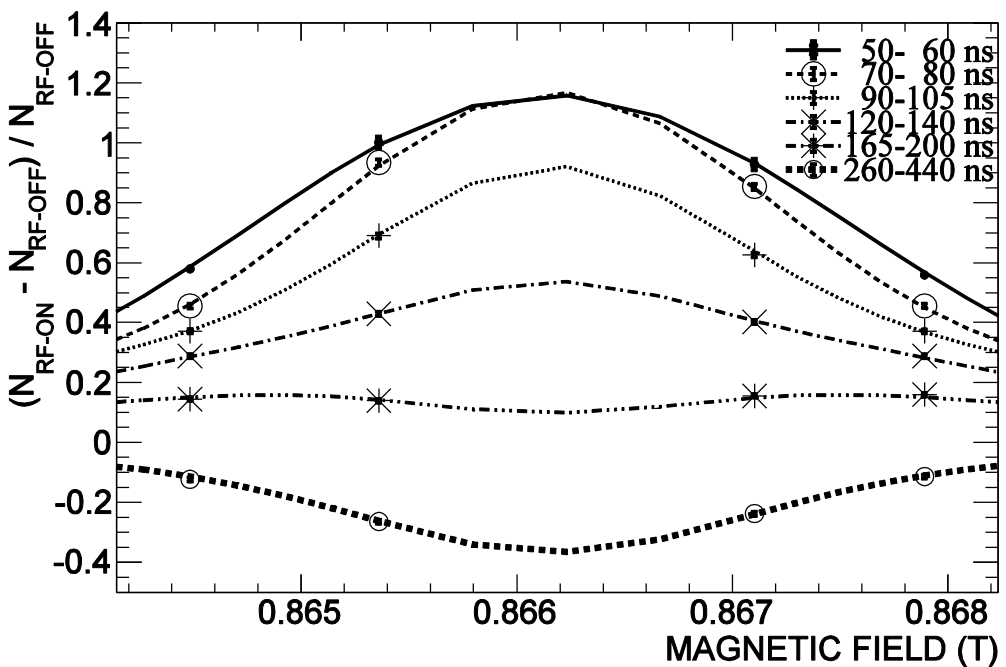
Resonance lines (0.969 amagat)



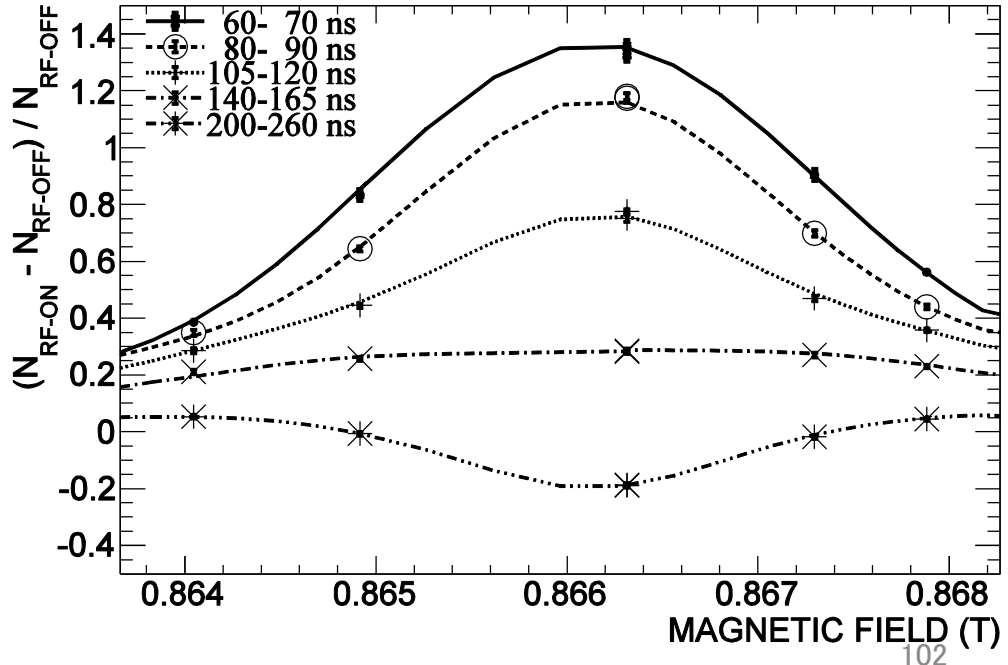
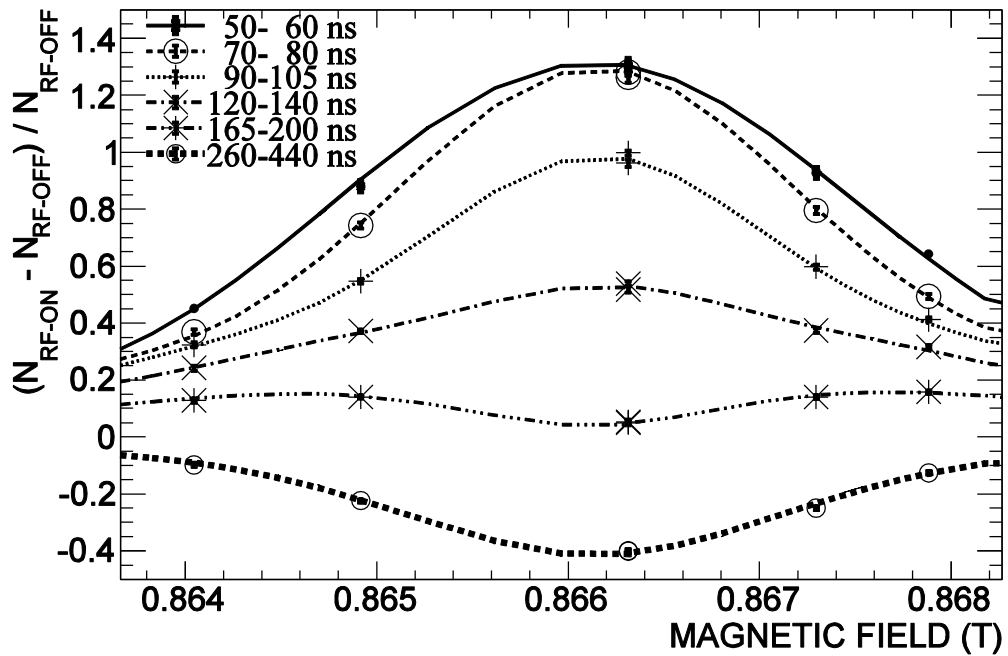
Resonance lines (1.193 amagat)



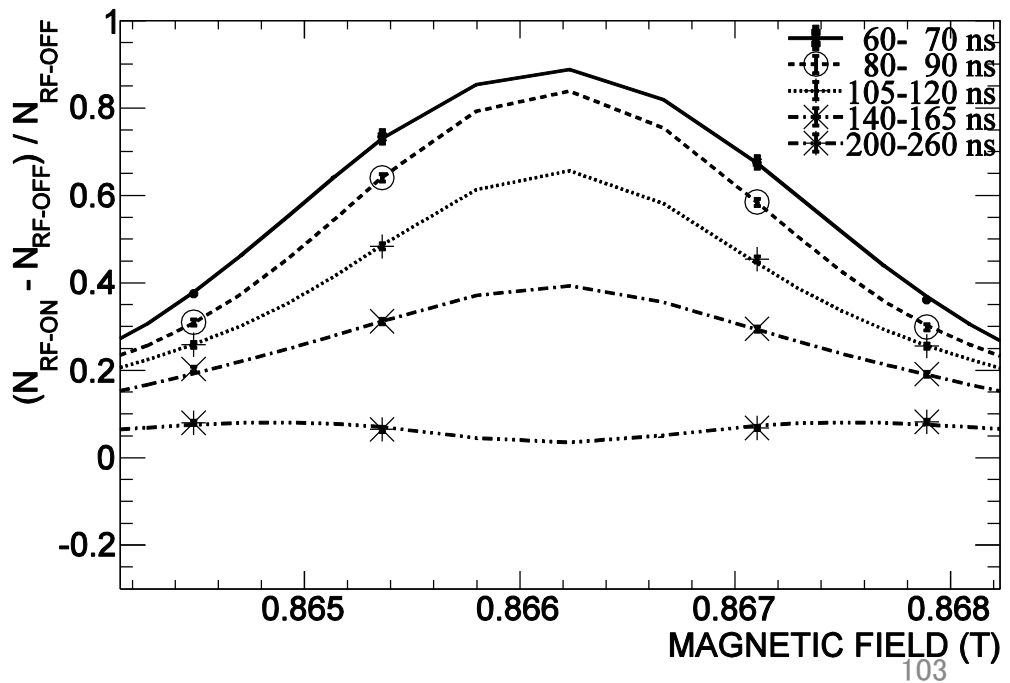
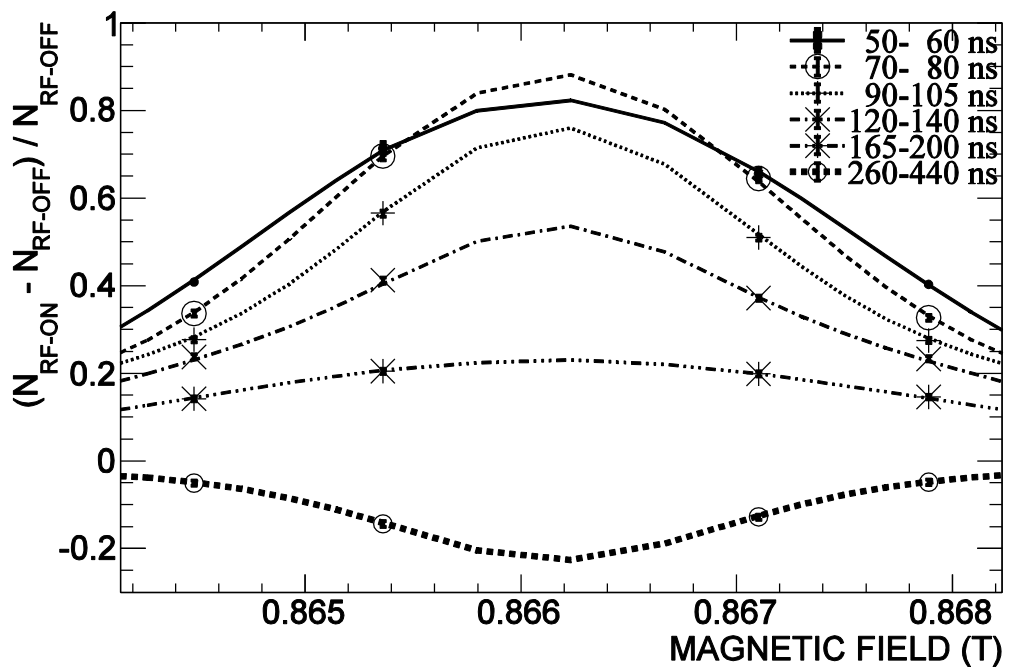
Resonance lines (1.353 amagat)



Resonance lines (1.358 amagat)



Resonance lines (1.366 amagat)



Systematic errors

Table 5.1: Summary of systematic errors. (Reproduced from Ref. [1])

Source	Errors in Δ_{HFS} (ppm)
<i>Material Effect:</i>	
o-Ps pick-off	3.5
Gas density measurement	1.0
Temperature measurement	0.1
Spatial distribution of density and temperature inside the RF cavity	2.5
<i>Thermalization of Ps:</i>	
Initial kinetic energy E_0	0.2
DBS result σ_m	0.5
pick-off result σ_m	1.8
<i>Magnetic Field:</i>	
Non-uniformity	3.0
Offset and reproducibility	1.0
NMR measurement	1.0
<i>RF System:</i>	
RF power	1.2
Q_L value of RF cavity	1.2
RF frequency	1.0
Power distribution in the cavity	< 0.1
<i>Others:</i>	
Choice of timing window	1.8
Choice of energy window	0.6
Polarization of e^+	< 0.2
Phase of microwaves	< 0.1
o-Ps lifetime	< 0.1
p-Ps lifetime	< 0.1
Quadrature sum	6.4 ¹⁰⁴

Systematic errors in the previous experiment

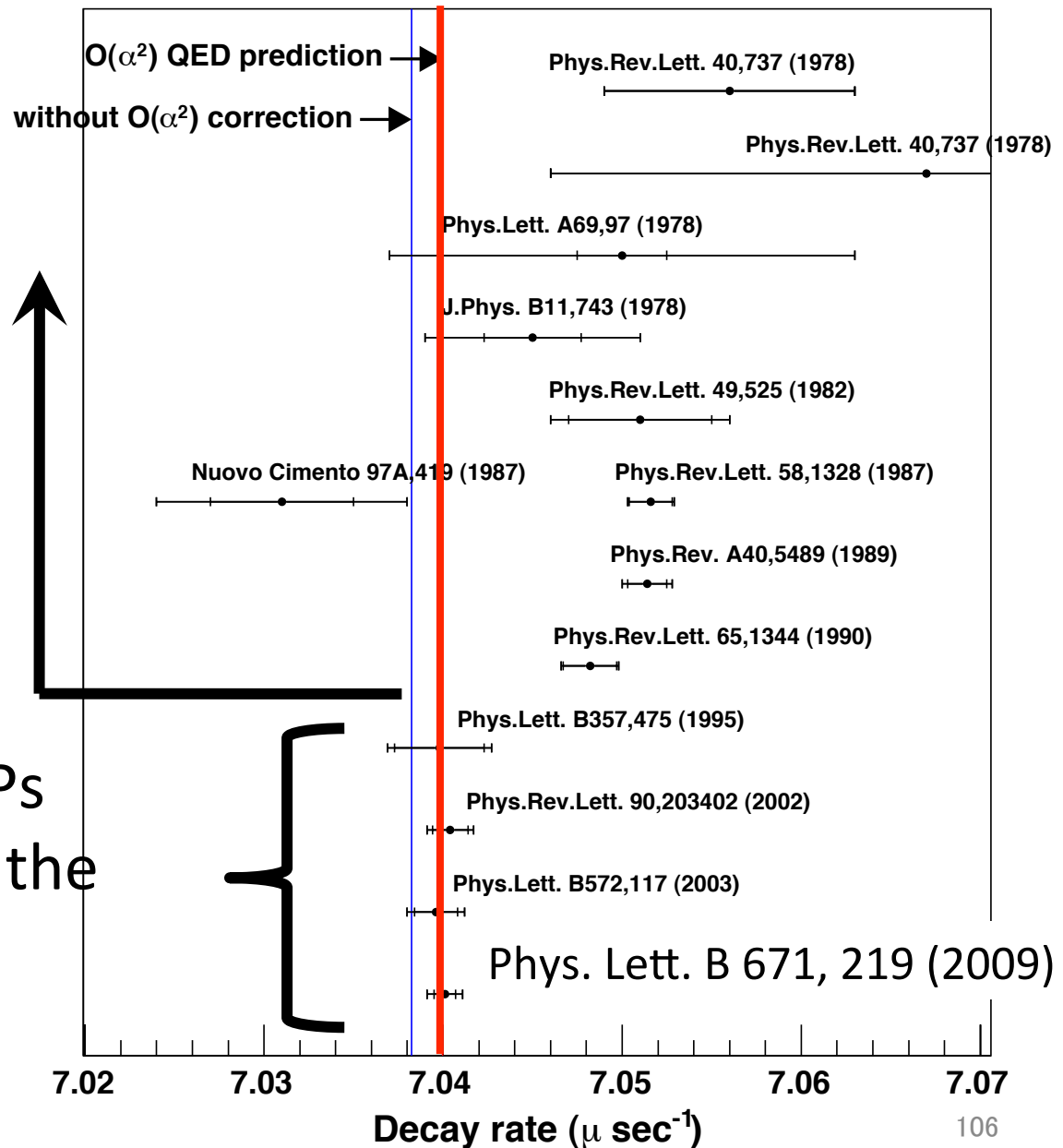
TABLE III. Uncertainties in $\Delta\nu$ measurement (ppm).

	1977	1983	All
Counting statistics	5.0	4.4	2.8
Magnetic field inhomogeneities	2.4	1.0	1.6
Magnetic field offset and reproducibility	1.4	0.8	1.0
Nuclear magnetic resonance (NMR) calibration	0.4	0.4	0.4
Microwave power and frequency uncertainty	0.5	0.5	0.5
Density uncertainty	0.3	0.3	0.3
Line-shape corrections	1.1	0.6	0.7
Quadrature sum	5.9	4.7	3.6

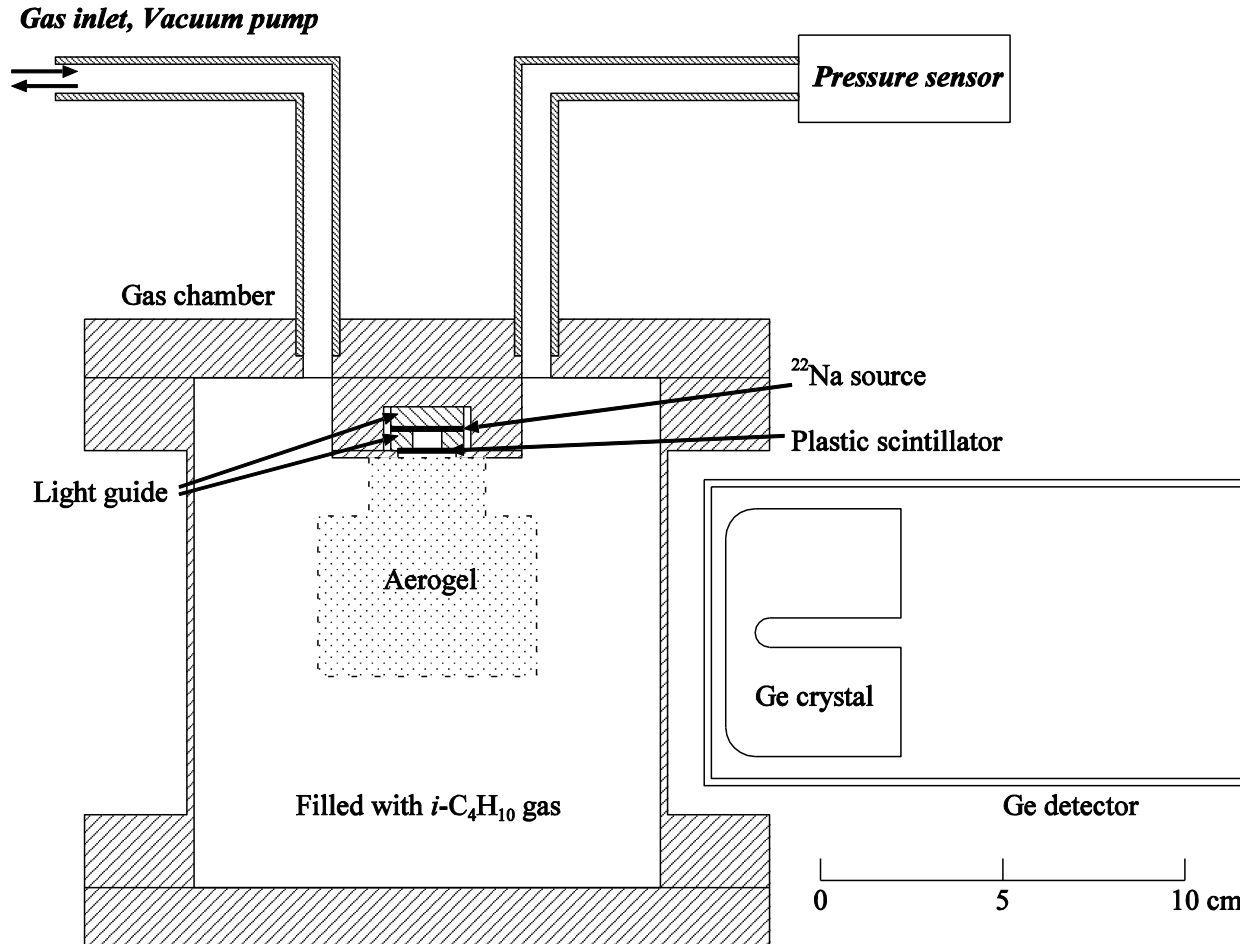
“o-Ps lifetime puzzle” solved!

Ps thermalization was not considered correctly. There was a significant discrepancy.

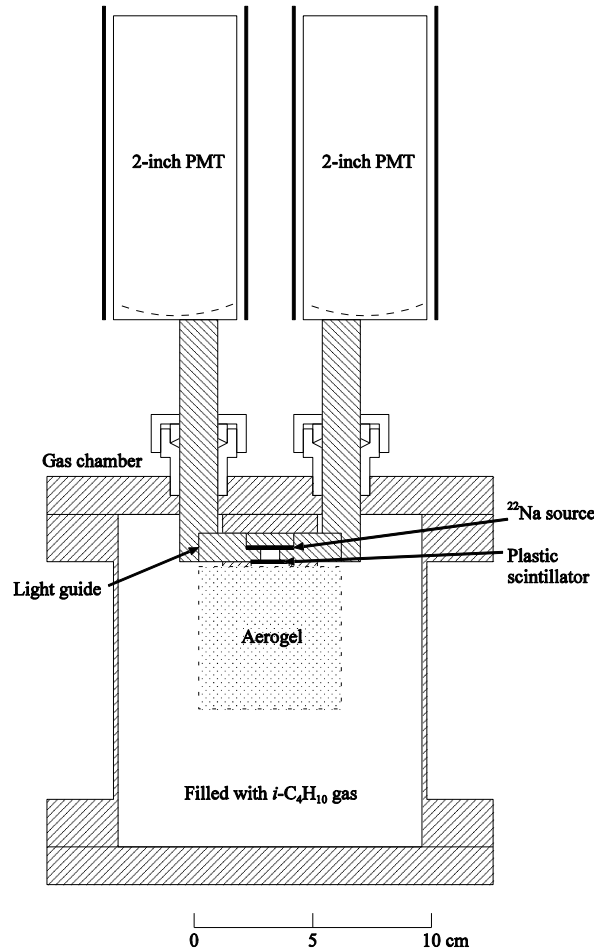
Correct treatment of Ps thermalization solved the discrepancy.



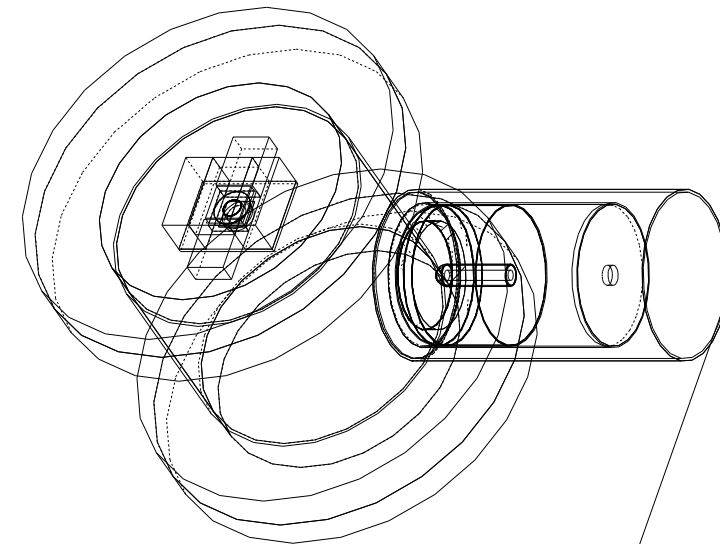
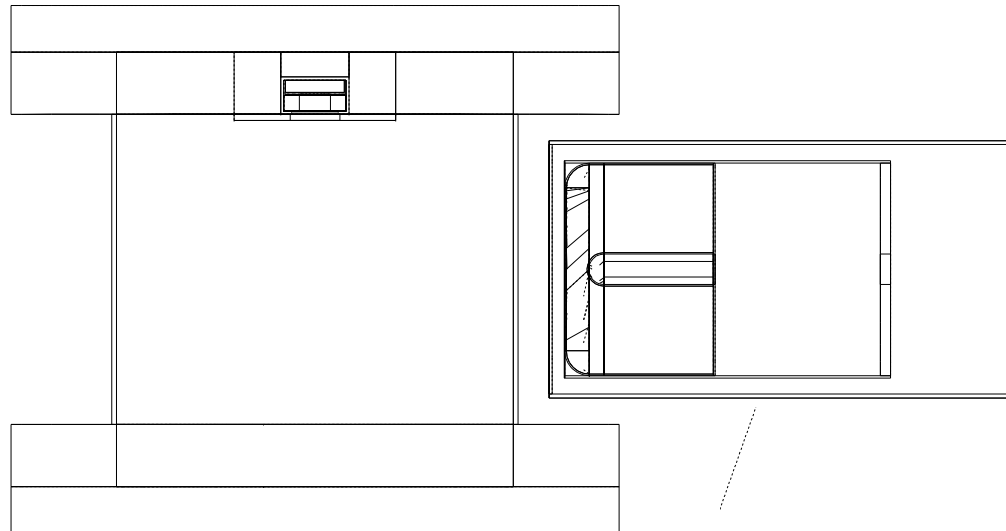
Thermalization Setup (Side view)



Thermalization Setup (Front view)

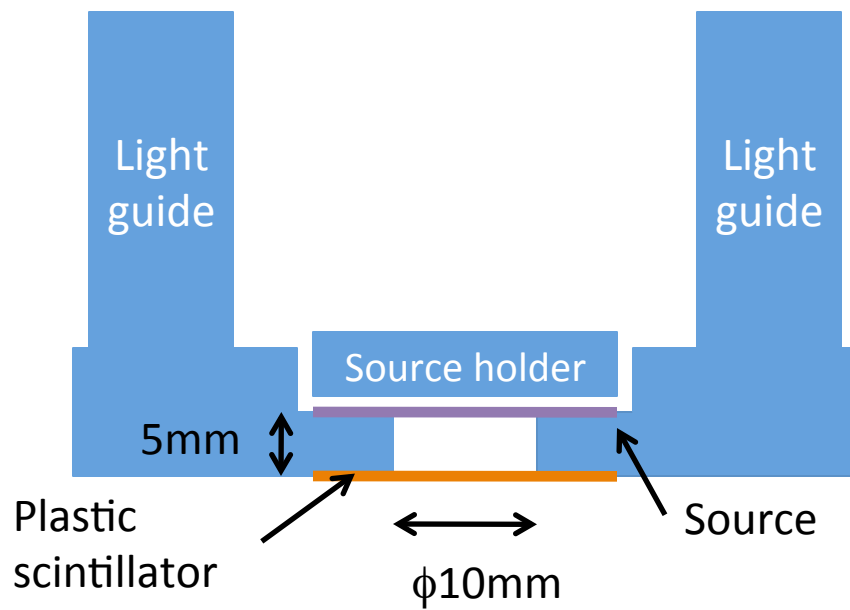
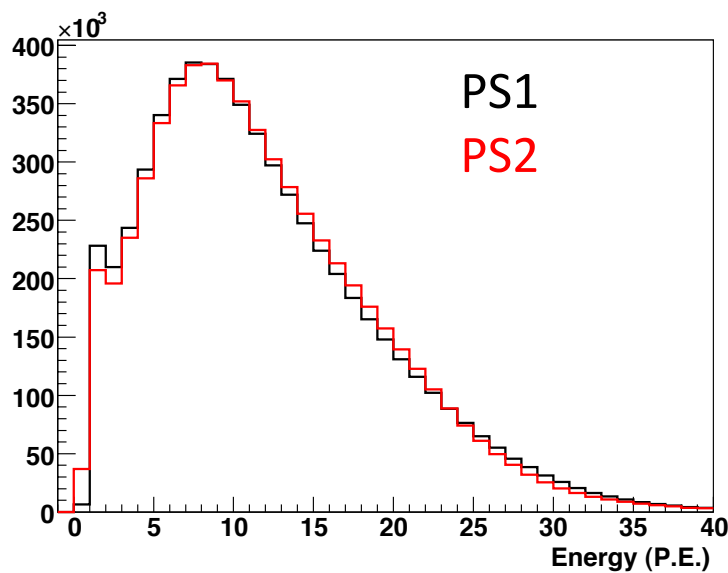
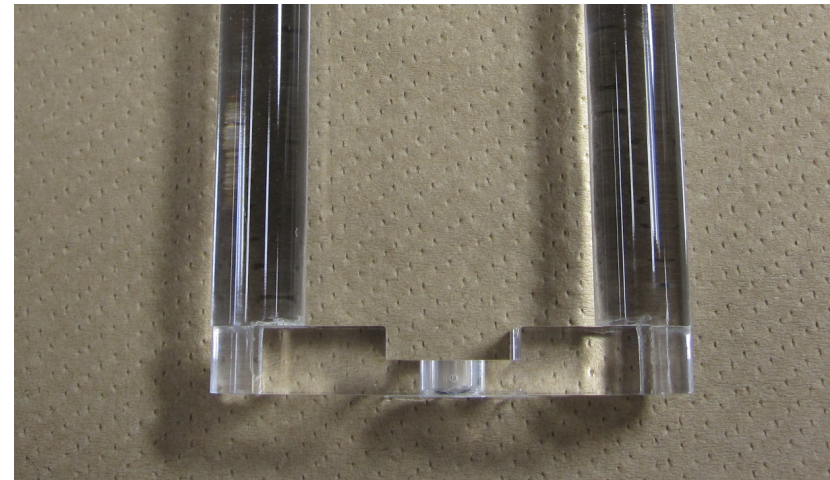


Thermalization MC



Ps thermalization measurement setup (β^+ system)

- Source: ^{22}Na (30 kBq, Ti foil)
 - β^+ : detect by a plastic scintillator (200 μm thick)
 - Scintillation photons are guided to PMTs through the light guides.
- Start timing is the coincident of two PMT signals.



ACAR

Angular Correlation of Annihilation Radiation

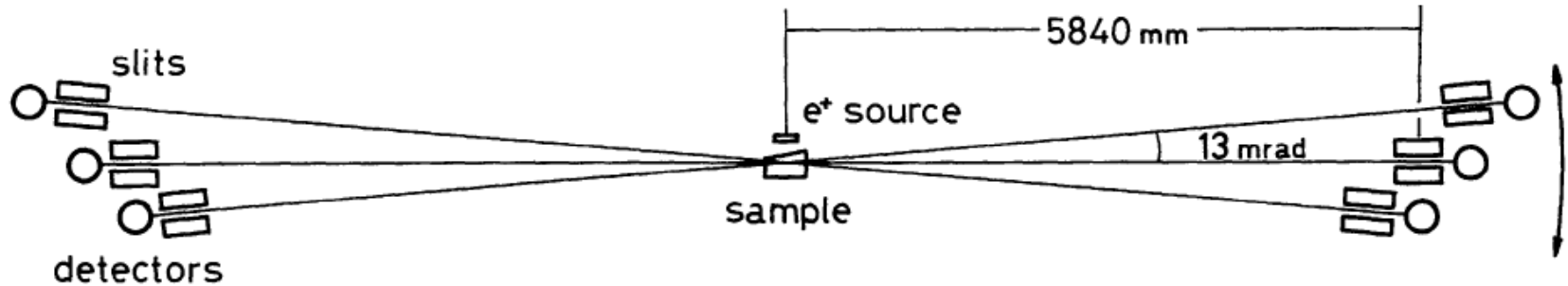


Fig. 1. One dimensional angular correlation apparatus having three pairs of long (800 mm) NaI(Tl) scintillation detectors. Adjacent pairs are separated by 13 milliradians.

Phys. Rev. A 52, 258 (1995)
 J. Phys. B 31, 329 (1998)
 J. Phys. B 36, 4191 (2003)

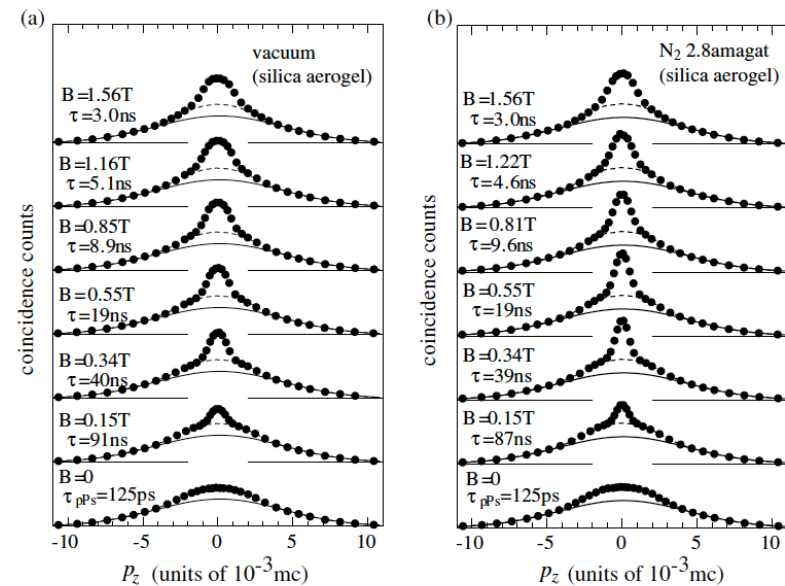


Figure 1. ACAR data for silica aerogel (a) in vacuum and (b) in 2.8 amagat of N_2 . The full and broken curves indicate the broad component and the $p\text{-Ps}$ component, respectively. The data are normalized to the broad component intensity. The magnetic flux density and the mean lifetime of $p\text{-Ps}$, τ , are indicated in the figure. The mean lifetime of $p\text{-Ps}$, $\tau_{p\text{-Ps}}$, is also indicated for the case of no magnetic field.

DBS

Doppler-Broadening Spectroscopy

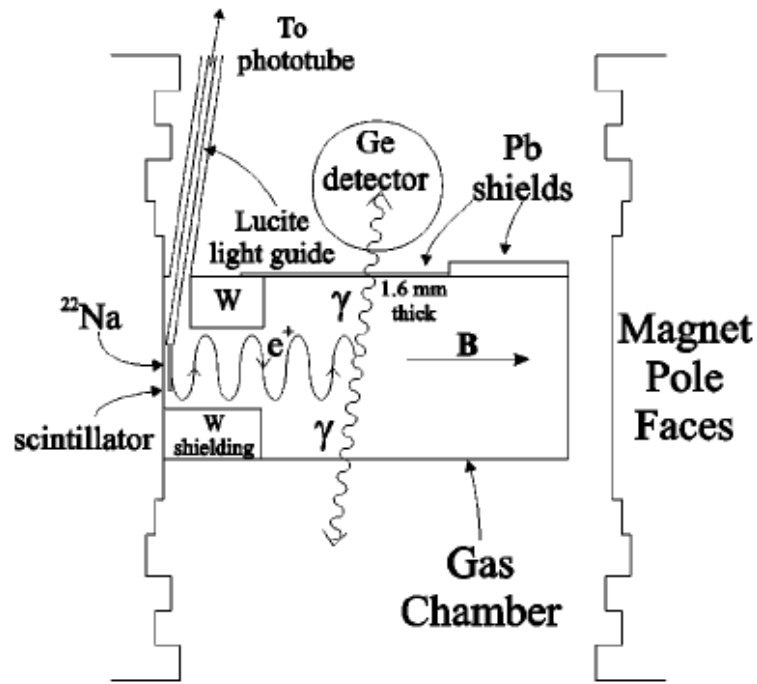


FIG. 2. Experimental apparatus. Positrons from ^{22}Na decay pass through a thin scintillator and enter a gas chamber. A magnetic field confines the trajectories near the axis. Positrons that stop in the gas can form Ps. Annihilation γ rays are detected in a Ge crystal.

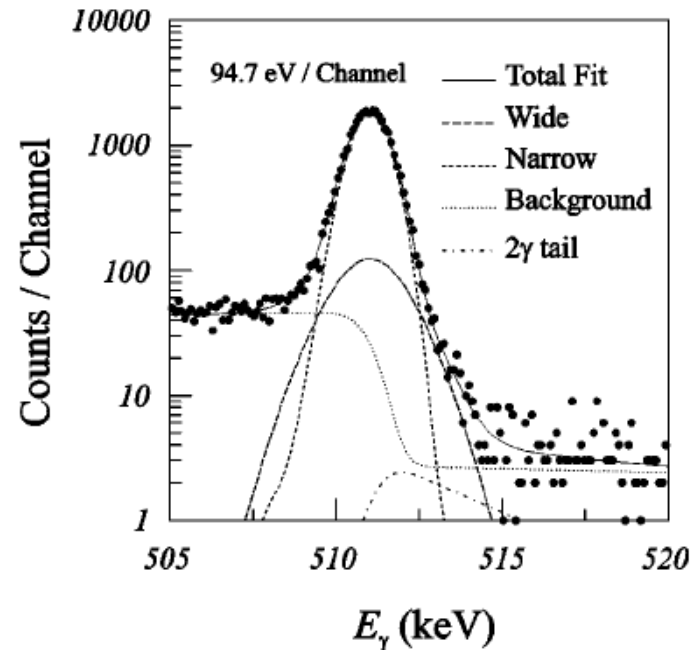
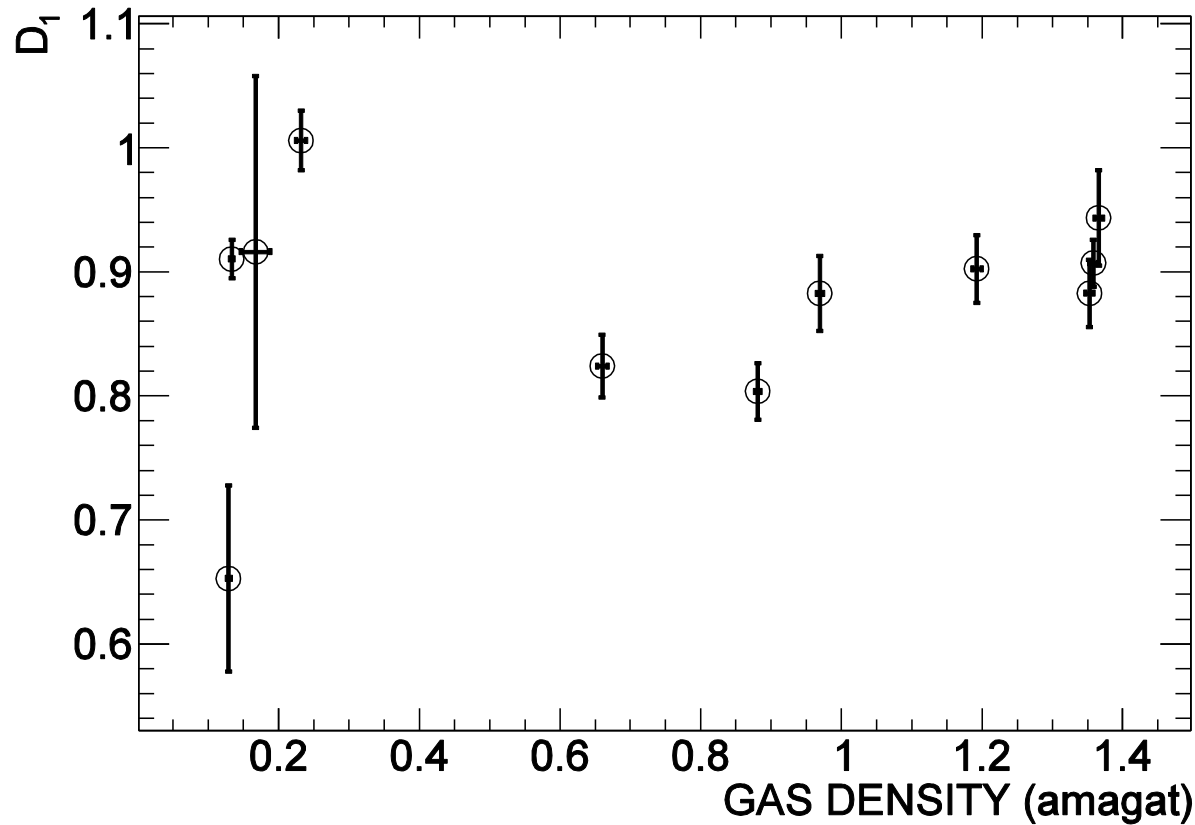


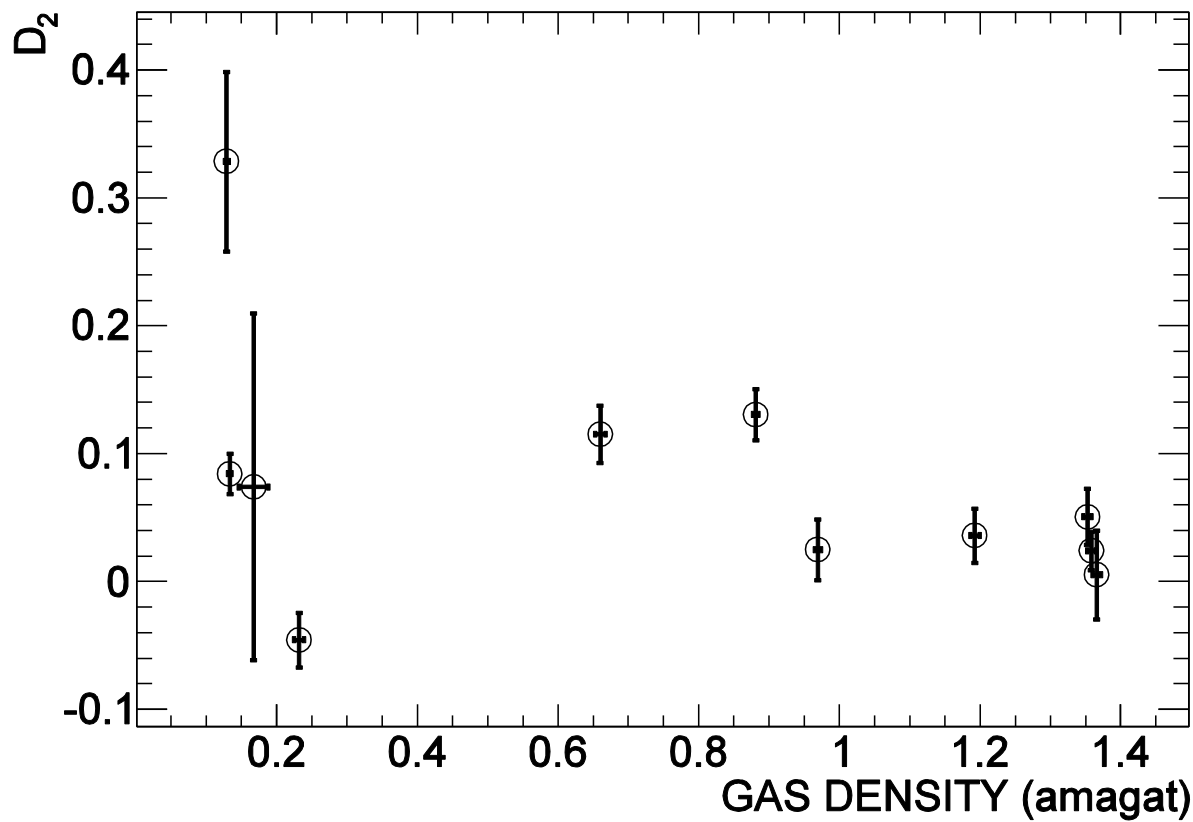
FIG. 3. Typical thermalization data. The Doppler-broadened 511-keV photopeak is resolved into two Gaussians, a step background, and a 2γ tail. The first three components are shown convoluted with the intrinsic detector resolution; the 2γ tail is also convoluted with the narrow Gaussian.

Phys. Rev. Lett. 80, 3727 (1998)
 Phys. Rev. A 67, 022504 (2003)

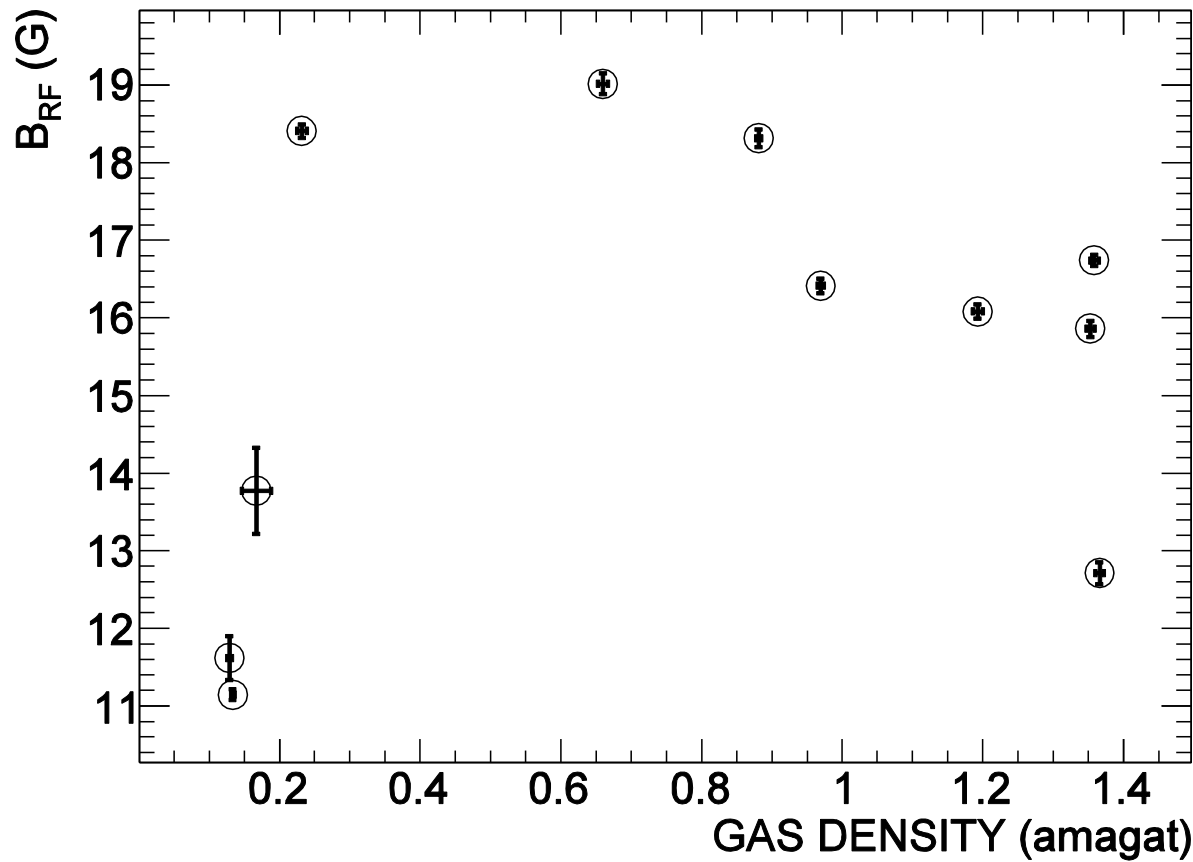
Final Fitting Parameters (D_1)



Final Fitting Parameters (D_2)



Final Fitting Parameters (B_{RF})



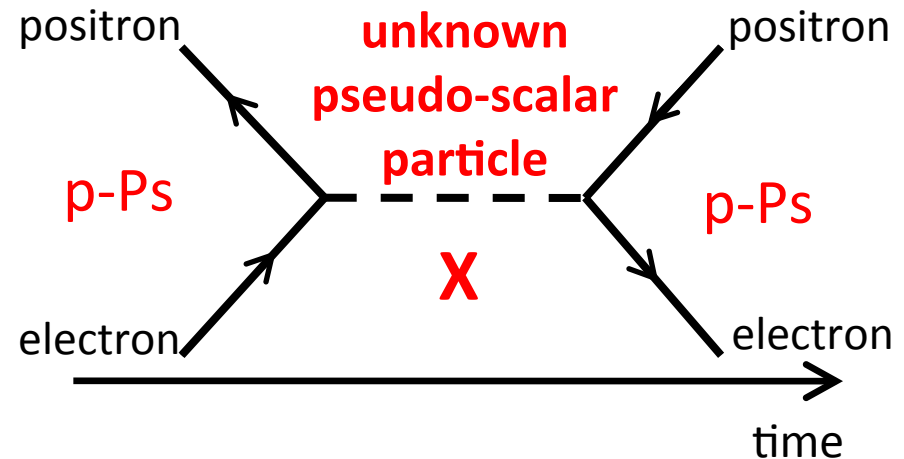
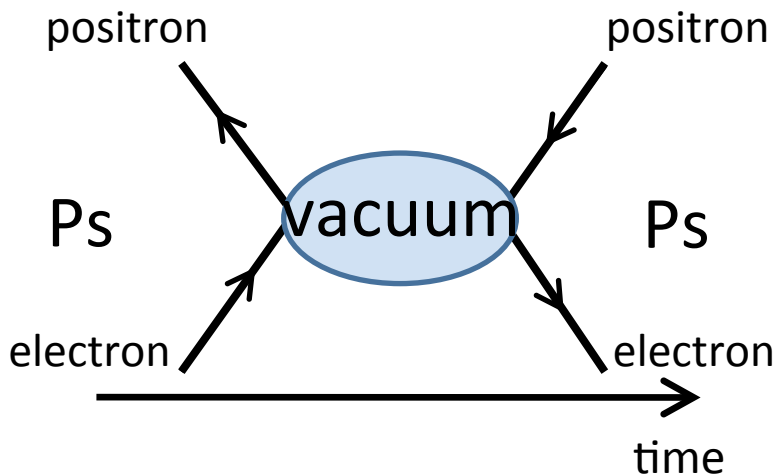
Ps-HFS theory

Term	Contribution (ppm)	HFS (GHz)	year
Leading Order ((7/12)m α^4)	1 000 000	204.386 63	1947-1951
O(α) correction	- 4 919.6	-1.005 50	1952
O(α^2) correction	57.7	0.011 80	1966-2000
O($\alpha^3 \ln \alpha^{-1}$) correction	-6.1(2.0)	-0.001 24(41)	1993-2001
Sum	995 132.1(2.0)	203.391 69(41)	

$$\Delta\nu^{\text{th}} = \Delta\nu_0^{\text{th}} \left\{ 1 - \frac{\alpha}{\pi} \left(\frac{32}{21} + \frac{6}{7} \ln 2 \right) + \frac{5}{14} \alpha^2 \ln \frac{1}{\alpha} + \left(\frac{\alpha}{\pi} \right)^2 \left[\frac{1367}{378} - \frac{5197}{2016} \pi^2 + \left(\frac{6}{7} + \frac{221}{84} \pi^2 \right) \ln 2 - \frac{159}{56} \zeta(3) \right] - \frac{3}{2} \frac{\alpha^3}{\pi} \ln^2 \frac{1}{\alpha} + C \frac{\alpha^3}{\pi} \ln \frac{1}{\alpha} + D \left(\frac{\alpha}{\pi} \right)^3 \right\}, \quad (3)$$

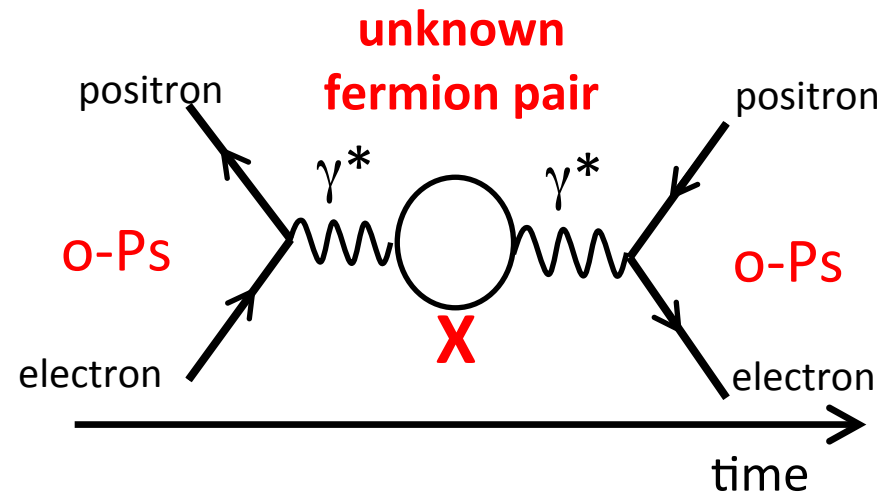
PRL 85, 5094 (2000)

Discrepancy because of rich structure of vacuum ?

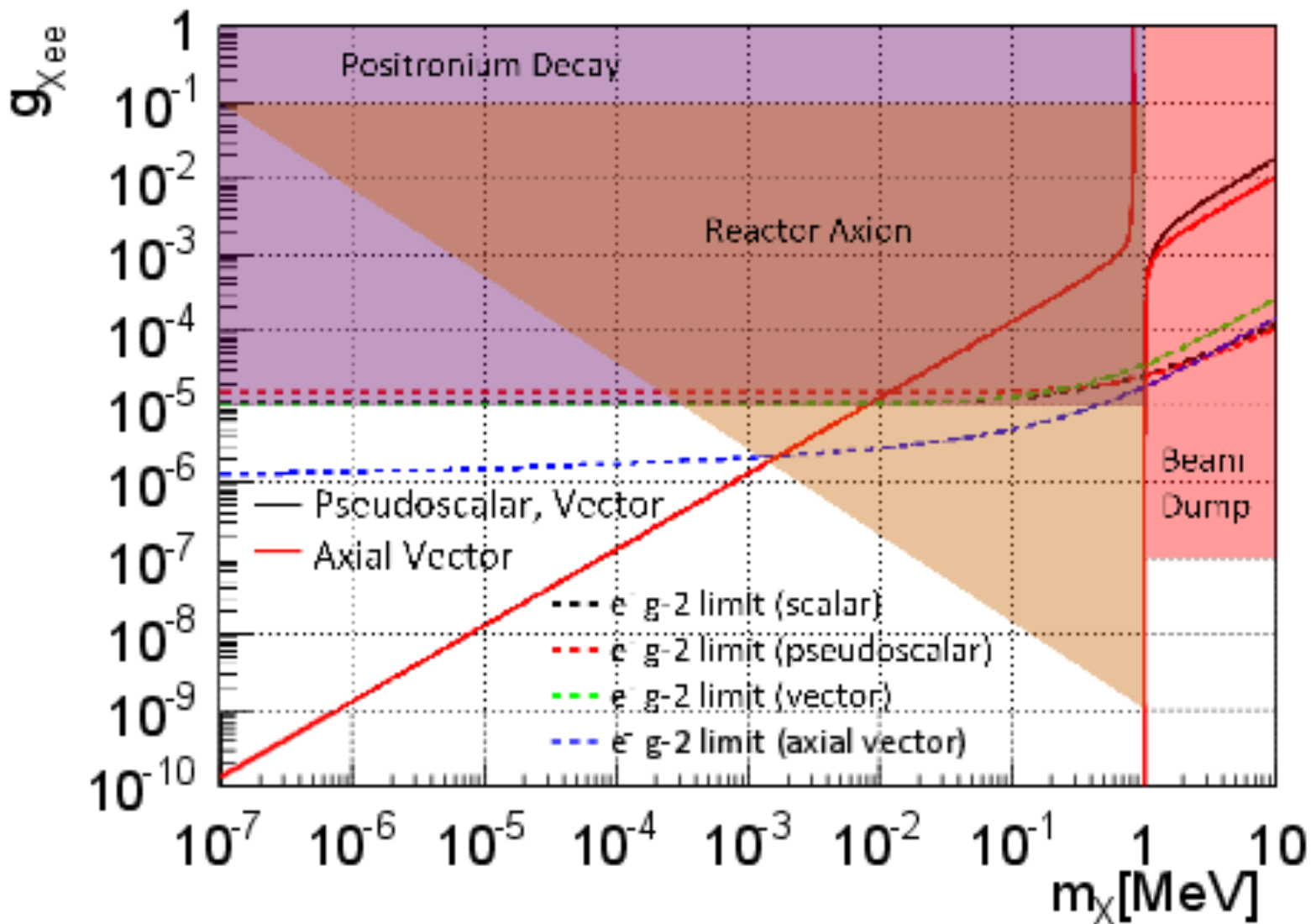


Sensitive at \sim MeV

There might be common systematic errors of previous experiments. We introduce a completely new technique to reduce such errors and independently check the discrepancy.



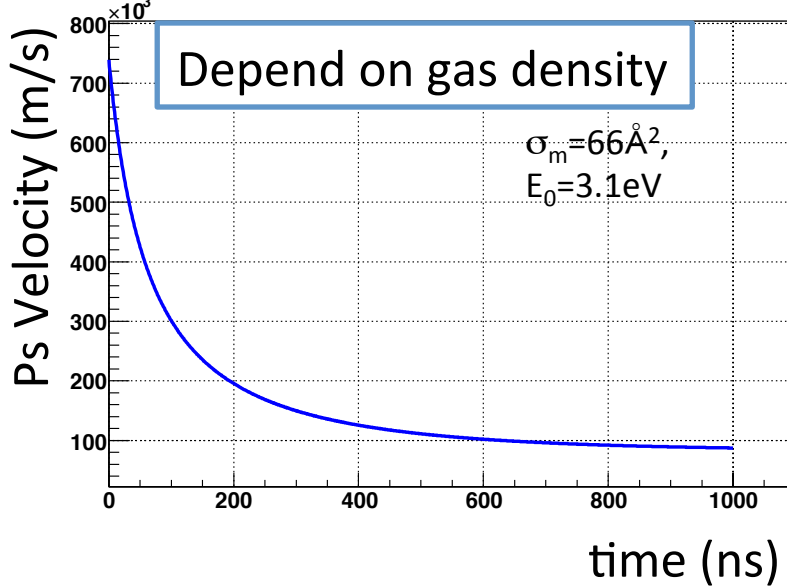
limit



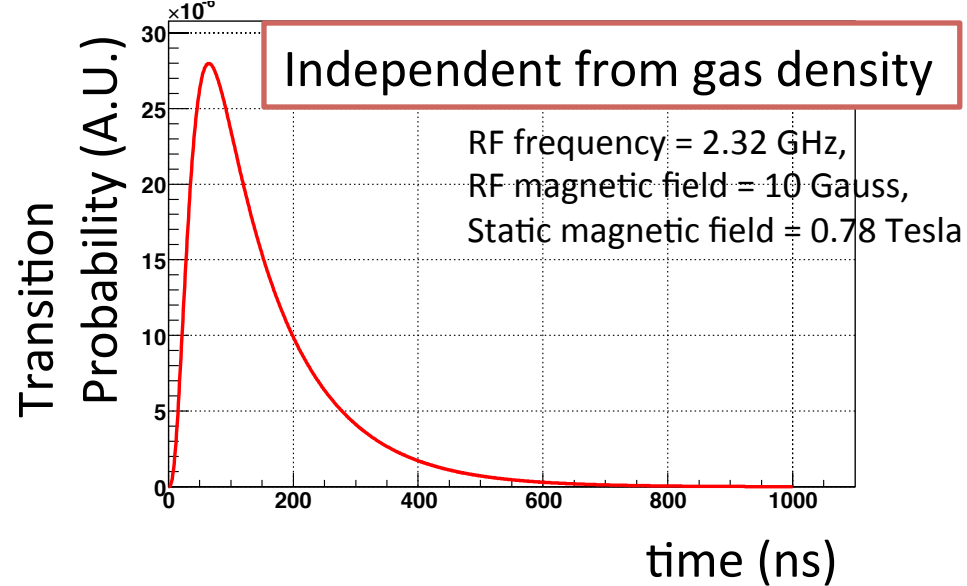
Estimate HFS correction from Thermalization parameters

- Calculate the Stark effect correction on HFS from measured σ_m .

< Thermalization @0.05atm>



< Transition Curve >



- The Stark effect is proportional to **(Ps Velocity)x(gas density)**
- And also to the $\text{o-Ps} \rightarrow 2\gamma$ **transition probability**.

HFS correction = Integration of
(Ps Velocity) x (gas density) x (transition probability)
over the timing range.

Theoretical resonance line (1)

[4,5]. The basis for the four spin eigenstates of Ps is defined as $(\psi_0, \psi_1, \psi_2, \psi_3) \equiv (|S, S_z\rangle = |0, 0\rangle, |1, 0\rangle, |1, 1\rangle, |1, -1\rangle)$. We apply a magnetic field,

$$\mathbf{B}(t) = B\hat{\mathbf{z}} + B_{\text{RF}}\hat{\mathbf{x}} \cos(\omega t), \quad (2)$$

where $\hat{\mathbf{z}}$ and $\hat{\mathbf{x}}$ are the unit vectors for the z and x directions respectively, B_{RF} is the magnetic field strength of the microwaves, ω is the frequency of the microwaves, and t is the time since Ps is formed. The phase of the microwave is randomly distributed for each Ps in this experiment, but this effect on determination of Δ_{HFS} is less than 0.1 ppm so that arbitrary phase can be taken in the calculation.

Theoretical resonance line (2)

The Hamiltonian H including the Ps decay becomes

$$H = h\Delta_{\text{HFS}}(t) \times \begin{pmatrix} -\frac{1}{2} - \frac{i}{2}\gamma_s & -q & r & -r \\ -q & \frac{1}{2} - \frac{i}{2}\gamma_t & 0 & 0 \\ r & 0 & \frac{1}{2} - \frac{i}{2}\gamma_t & 0 \\ -r & 0 & 0 & \frac{1}{2} - \frac{i}{2}\gamma_t \end{pmatrix}, \quad (3)$$

where $r = g'\mu_B B_{\text{RF}} \cos(\omega t)/(\sqrt{2}h\Delta_{\text{HFS}}(t))$, $\gamma_s = \Gamma'_{\text{p-Ps}}(t)/(2\pi\Delta_{\text{HFS}}(t))$, $\gamma_t = \Gamma'_{\text{o-Ps}}(t)/(2\pi\Delta_{\text{HFS}}(t))$, $\Gamma'_{\text{p-Ps}}(t) = \Gamma_{\text{p-Ps}} + \Gamma_{\text{pick}}(t)$, $\Gamma'_{\text{o-Ps}}(t) = \Gamma_{\text{o-Ps}} + \Gamma_{\text{pick}}(t)$, and $\Gamma_{\text{pick}}(t)$ is the pick-off ($\text{Ps} + e^- \rightarrow 2\gamma + e^-$) annihilation rate. The time-dependence of Δ_{HFS} and Γ_{pick} are caused by Ps thermalization, which is described later. The 4×4 density matrix $\rho(t)$ evolves with the time-dependent Schrödinger equation,

Theoretical resonance line(3)

$$i\hbar\dot{\rho} = H\rho - \rho H^\dagger, \quad (4)$$

where the i, j -element of $\rho(t)$ is defined as $\rho_{ij}(t) \equiv \langle \psi_i | \psi(t) \rangle \langle \psi(t) | \psi_j \rangle$ and the initial state is described as Eq. (19) of Ref. [20]. The 2γ annihilation probability ($S_{2\gamma}$), and the 3γ annihilation probability ($S_{3\gamma}$) are calculated between $t = t_0$ and $t = t_1$ as

$$S_{2\gamma} = \int_{t_0}^{t_1} \left(\Gamma'_{\text{p-Ps}}(t) \rho_{00}(t) + \Gamma_{\text{pick}}(t) \sum_{i=1}^3 \rho_{ii}(t) \right) dt, \quad (5)$$

$$S_{3\gamma} = \int_{t_0}^{t_1} \Gamma_{\text{o-Ps}} \sum_{i=1}^3 \rho_{ii}(t) dt. \quad (6)$$

Theoretical resonance line (4)

Furthermore, $S_{3\gamma}$ is divided into two components to calculate the experimental resonance line shape because of the different angular distribution of decay γ rays from Ps between $|1, \pm 1\rangle$ and $|1, 0\rangle$ states [21]. The annihilation probability of $|1, \pm 1\rangle$ state, $S_{|1,\pm 1\rangle} \equiv S_{|1,1\rangle} + S_{|1,-1\rangle}$, and the annihilation probability of $|1, 0\rangle$ state, $S_{|1,0\rangle}$, are obtained by

$$S_{|1,\pm 1\rangle} = \int_{t_0}^{t_1} \Gamma_{\text{o-Ps}} (\rho_{22}(t) + \rho_{33}(t)) dt, \quad (7)$$

$$S_{|1,0\rangle} = \int_{t_0}^{t_1} \Gamma_{\text{o-Ps}} \rho_{11}(t) dt. \quad (8)$$

Theoretical resonance line (5)

Resonance lines are fitted by the following function $F(t, n, B)$:

$$F(t, n, B) = D_1(n) \frac{R_{\text{RF-ON}}(t, n, B) - R_{\text{RF-OFF}}(t, n, B)}{R_{\text{RF-OFF}}(t, n, B)} + D_2(n), \quad (10)$$

$$R(t, n, B) \equiv \epsilon(n) S_{2\gamma}(t, n, B) + S_{|1, \pm 1\rangle}(t, n, B) + \epsilon'(n) S_{|1, 0\rangle}(t, n, B), \quad (11)$$

where n is the number density of gas molecules, $D_1(n)$ is a normalization factor, $D_2(n)$ is an offset, $\epsilon(n)$ and $\epsilon'(n)$ are the ratios of detection efficiencies of 2γ and $|1, 0\rangle$ decay, respectively, normalized by that of the $|1, \pm 1\rangle$ decay. $S_{2\gamma}$, $S_{|1, \pm 1\rangle}$, and $S_{|1, 0\rangle}$ are calculated numerically from Eqs. (5), (7), and (8), respectively. In the fitting process, $D_1(n)$ and $D_2(n)$ are treated as free parameters for each gas density because of the following three reasons. The

Theoretical resonance line (6)

The time dependence of $\Delta_{\text{HFS}}(t)$ and $\Gamma_{\text{pick}}(t)$ are estimated using the following thermalization effect and they are taken into account in the evolution of $S_{2\gamma}$, $S_{|1,\pm 1\rangle}$, and $S_{|1,0\rangle}$ as

$$\Delta_{\text{HFS}}(n, t) = \Delta_{\text{HFS}}^0 - C n v(t)^{3/5}, \quad (12)$$

$$\Gamma_{\text{pick}}(n, t) = \Gamma_{\text{pick}}(n, \infty) \times \left(\frac{v(t)}{v(\infty)} \right)^{0.6}, \quad (13)$$

where Δ_{HFS}^0 is Ps-HFS in vacuum and C is a constant. Δ_{HFS}^0 and C are common free parameters of fitting for all data points. $\Gamma_{\text{pick}}(n, \infty)$ is determined by fitting the RF-OFF timing spectra for each gas density with the following equation $N(t)$ including Ps thermalization effect [9,10]:

Timing spectra

- Based on P. G. Coleman et al., Appl. Phys. **5**, 223 (1974).
- There is another paper by another person but Coleman's paper is more general.

$$P(t)dt = (\text{probability of a stop pulse between } t \text{ and } t+dt) \\ \times (\text{probability of no stop pulse between } 0 \rightarrow t \text{ for these events}) \quad (1)$$

Important equations

$$D(t)dt = S(t)dt \left[1 - \int_0^t P(t)dt \right] + N_1(t+dt)P(t)dt$$

(2)

All the start which do not make any signal within $t \times$ Probability to get stop signal
where

$$P(t)dt = [1 - \int_0^t P(t)dt]n_2(t+dt)dt \quad (3)$$

suppression All stop that do not make any signal after t.

$$N_1(t+dt) = N_1 - \int_0^{t+dt} S(t) dt \quad (4)$$

is the total number of start pulses available for conversion by random stop pulses beyond $t + dt$, and

$$n_2(t+dt) = N_2(t+dt)/T = \frac{1}{T} \left[N_2 - \int_{t+dt}^{\infty} S(t) dt \right] \quad (5)$$

Calculation

$$S(t)dt = D(t)dt / [1 - \int_0^t P(t')dt' - [N \downarrow 1 - \int_0^t dt' S(t')dt'] \times [N \downarrow 2 - \int_t^{\infty} dt' S(t')dt']] \times dt/T \quad (A)$$

$$P(t) / [1 - \int_0^t P(t')dt'] = N \downarrow 2 - \int_t^{\infty} dt' S(t')dt' \equiv R(t) \quad (B)$$

Solve (B) and obtain P(t)

$$P(t) = e^{\int_0^t R(t')dt'} \times R(t) \rightarrow 1 / [1 - \int_0^t P(t')dt'] = e^{\int_0^t R(t')dt'} \quad (B')$$

First give S(t) as an initial input. Then calculate (B'), substitute in (A), and get a new S(t). Iterate this until it converges.

Check by Monte Carlo simulation

- Equations seem to be fine, so in order to get visual idea, check them by MC simulation.

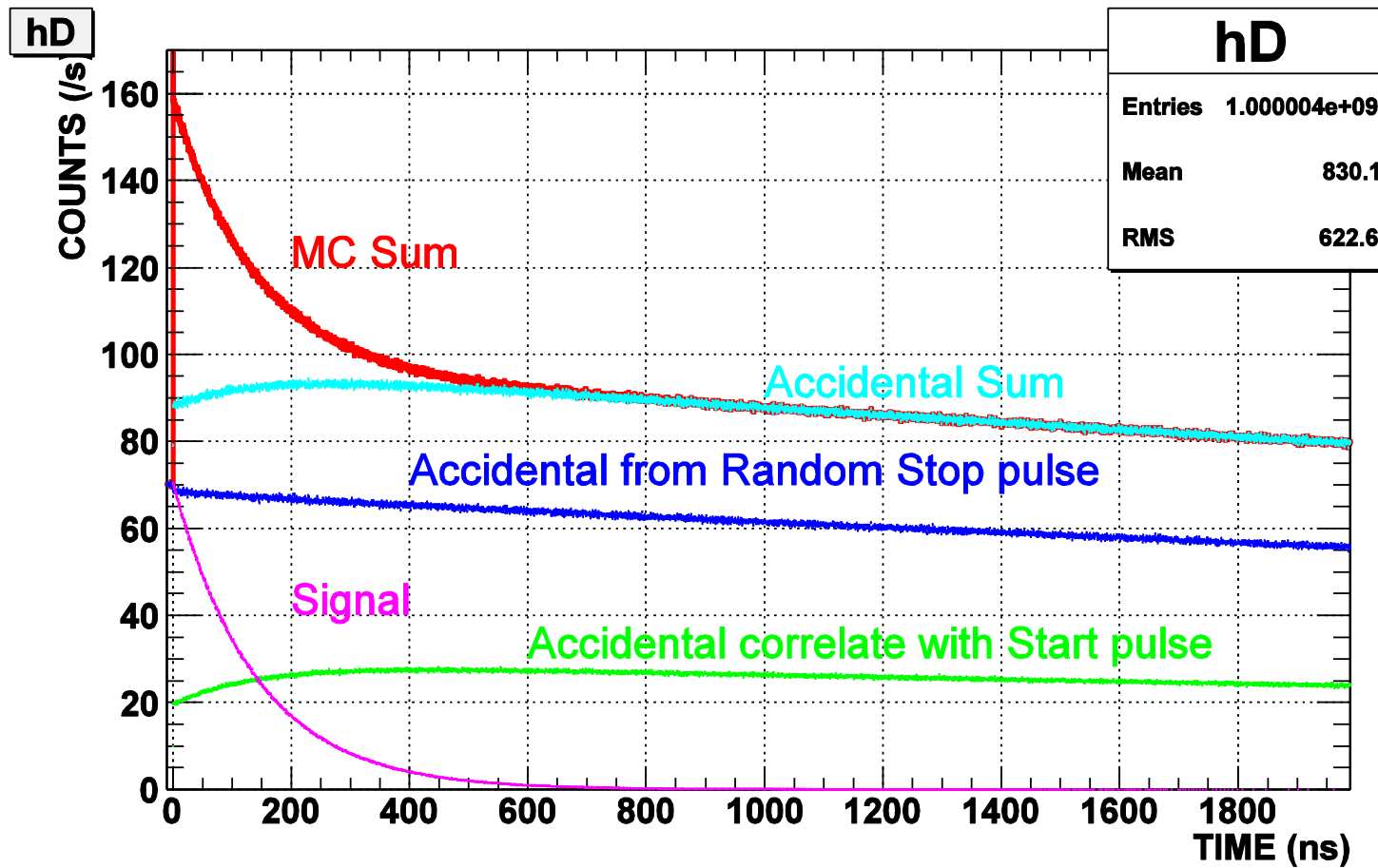
(Condition)

- Start pulse rate (N1) : 1 MHz
 - Stop pulse rate (N2) : 100 kHz
 - Signal rate (Sig) : 30 kHz

(Huge signal to see the effect more apparently)

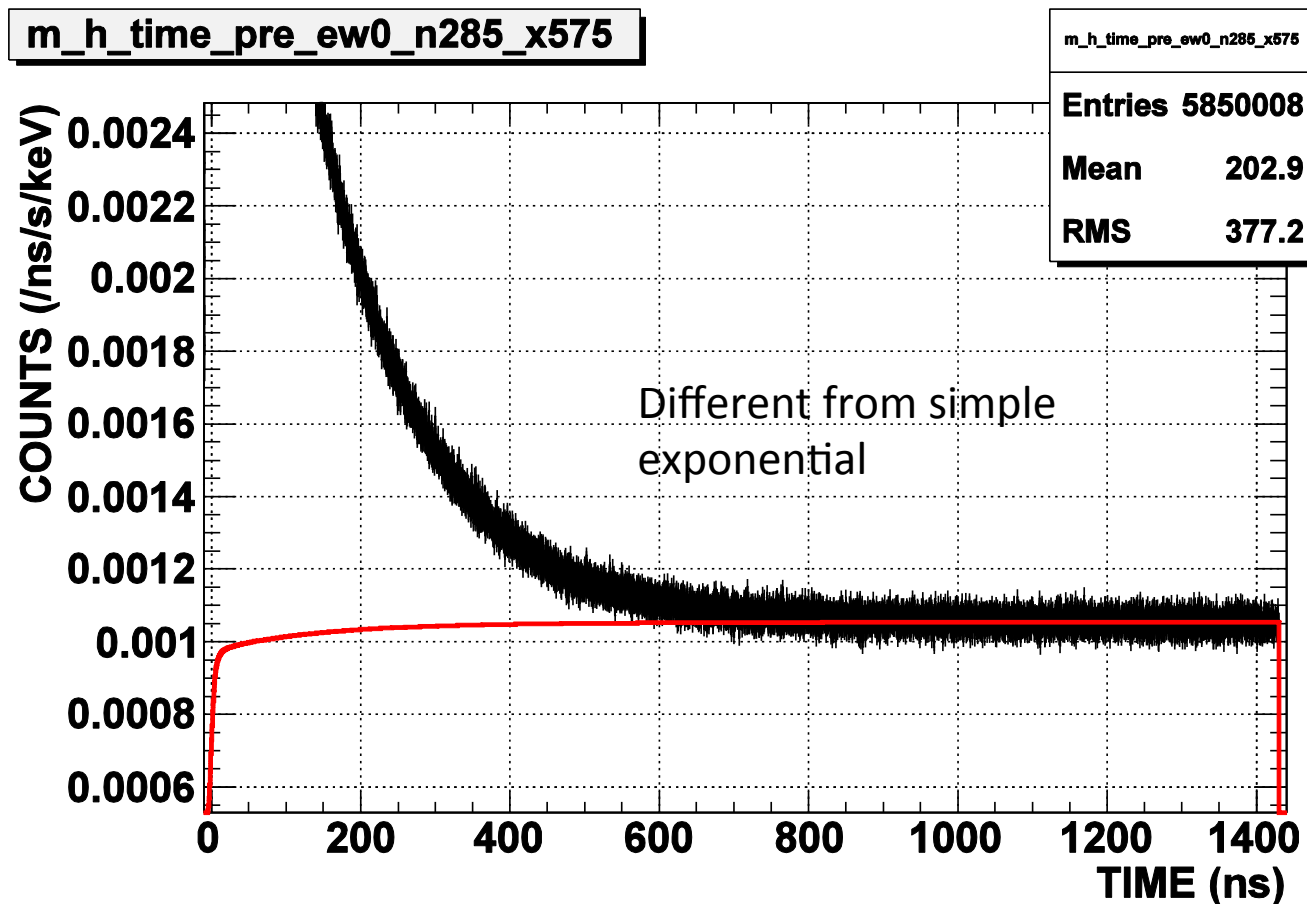
- Signal shape : Prompt delta-function + exponential (142ns) decay

Accidental (Monte Carlo)



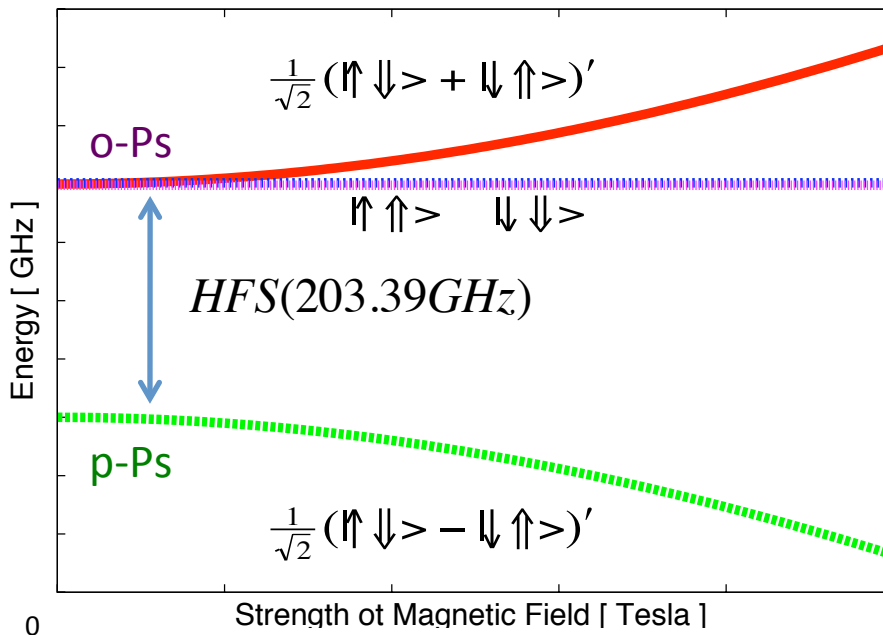
Perfect
agreement
with
Coleman's
equations.

Accidental subtraction



量子振動を利用してても、 かなりの精度で測定できます

<磁場によるPs量子準位のエネルギー分裂>



$$\chi \approx 0.275B[T]$$

$$\frac{HFS}{2} \left(\sqrt{1 + \chi^2} - 1 \right)$$

この二準位間の重ね合わせ状態を作ると、量子状態は両者のエネルギー差で振動

例: 周期26ns@100mT

$$\frac{1}{\sqrt{2}}(|\downarrow\downarrow\rangle + |\uparrow\uparrow\rangle)' \propto |S=1, m=0\rangle + \varepsilon |S=0, m=0\rangle$$

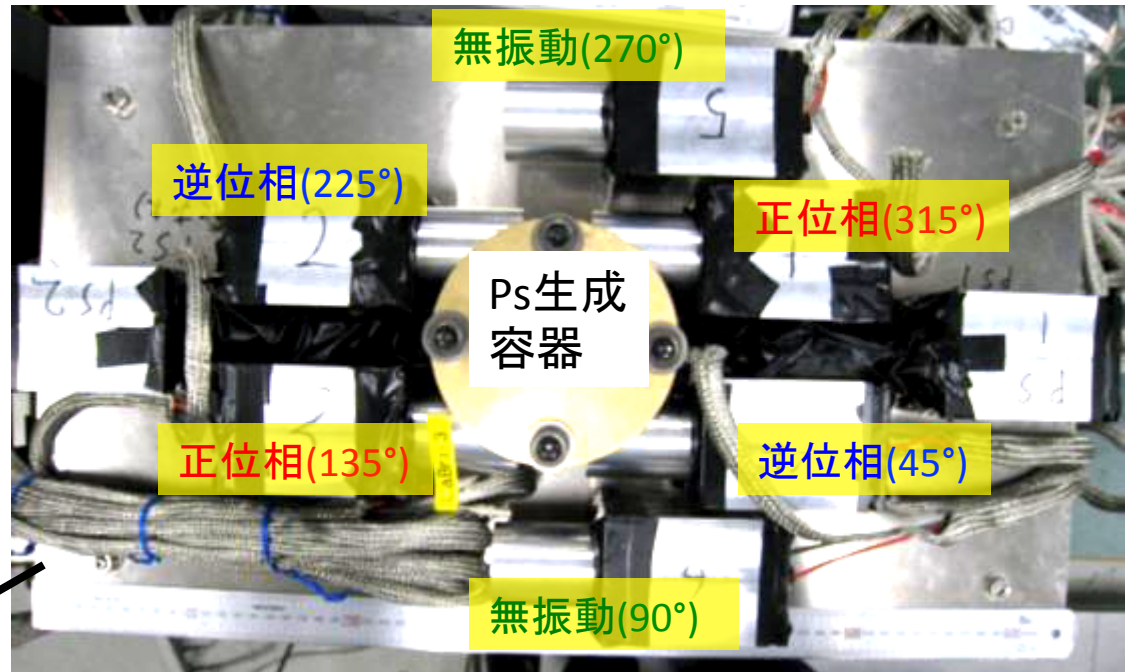
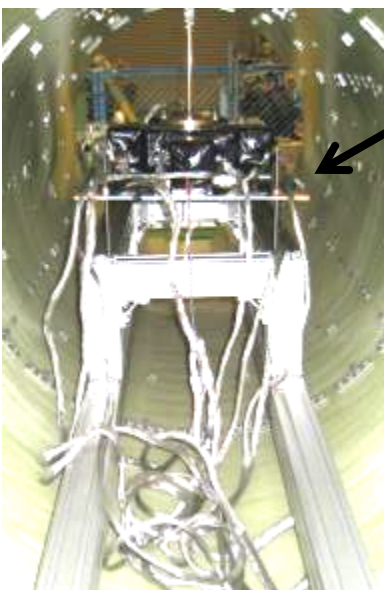
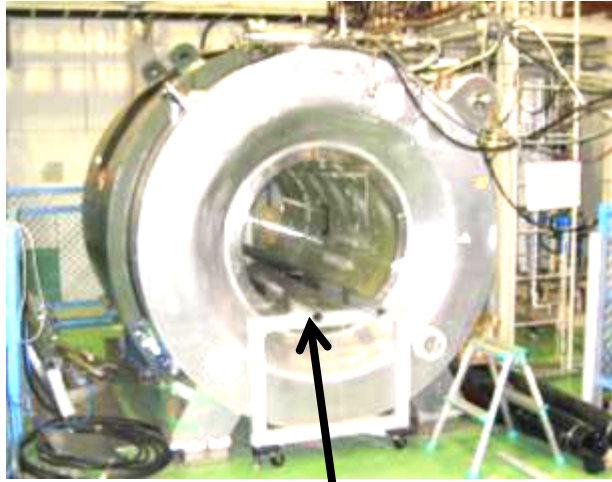
$$\frac{1}{\sqrt{2}}(|\downarrow\downarrow\rangle - |\uparrow\uparrow\rangle)' \propto |S=0, m=0\rangle + \varepsilon |S=1, m=0\rangle$$

(磁場によってp-Psと, o-Psのうちm=0の成分が少し混合)

振動の周期 → (HFS×磁場の関数)⁻¹ → PsのHFSの測定

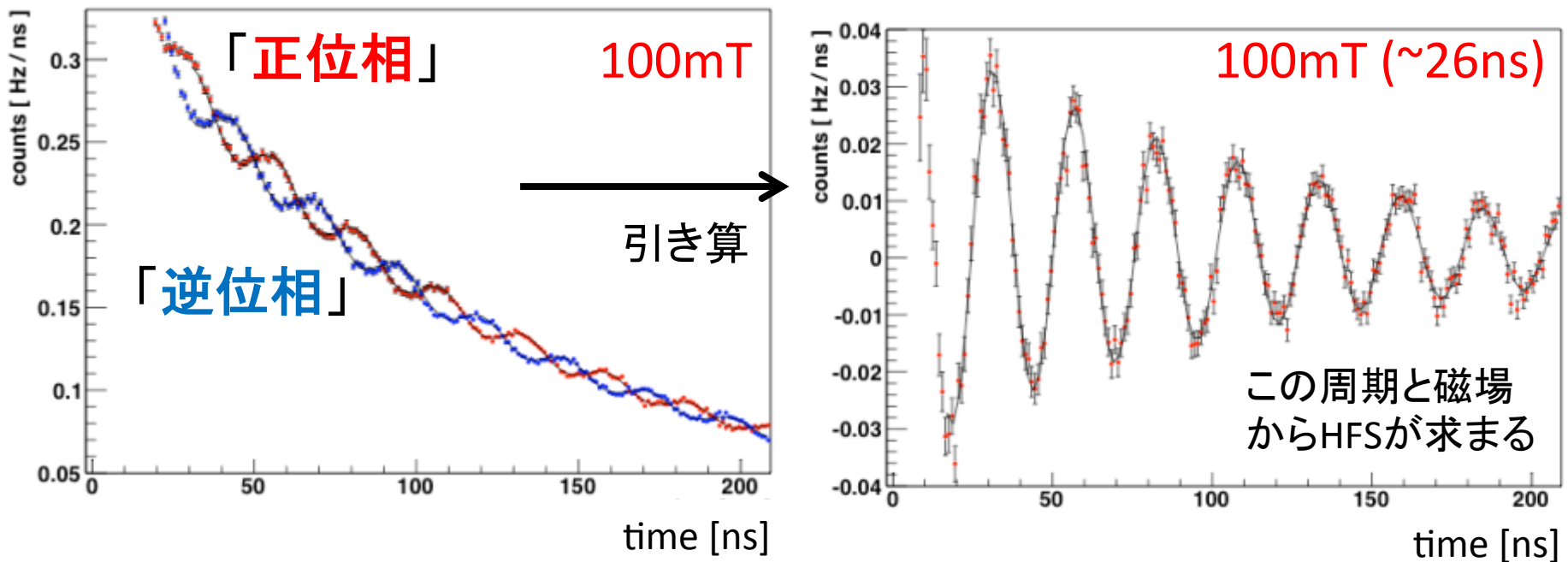
セットアップ

<先ほどの大型超伝導磁石>



崩壊ガンマ線の出る向きが振動するので、
「正位相」と「逆位相」の検出器のカウント
数を比較

量子振動による測定の結果



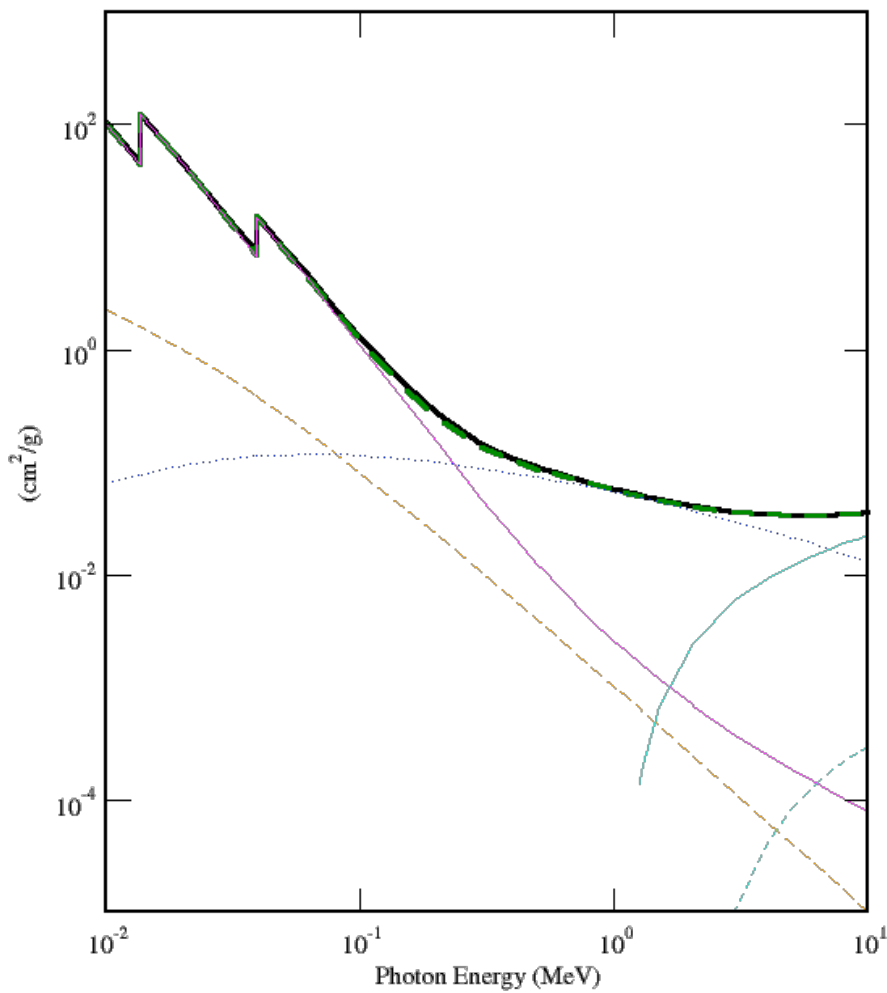
$203.324 \pm 0.039(\text{stat.}) \pm 0.015 (\text{sys.}) \text{ GHz}$

(192 ppm) (74 ppm)

Phys. Lett. B 697,
121 (2011)

理論と無矛盾な結果 (ただしまだ精度が足りないので改良が必要)

LaBr_3



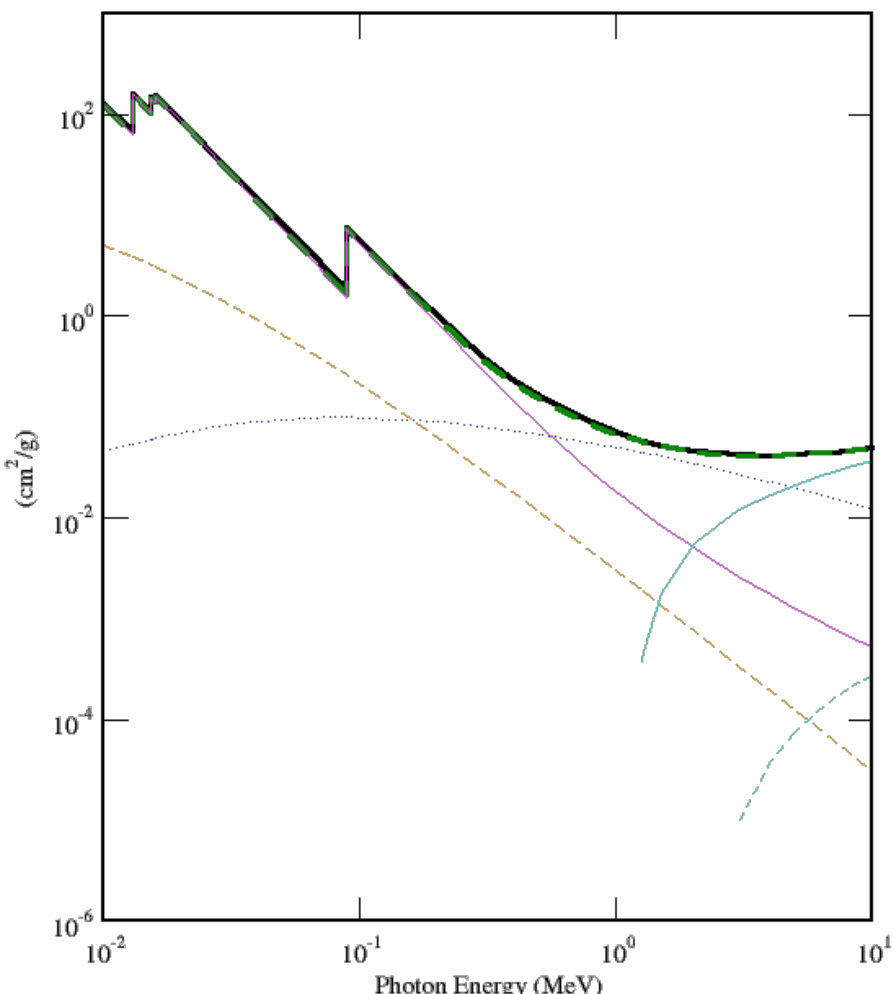
5.08 g/cm^3

$0.511 \text{ MeV } 8.851\text{e-}02 \text{ cm}^2/\text{g}$
 $\rightarrow 2.22 \text{ cm (1/e)}$

$1.275 \text{ MeV } 5.046\text{e-}02 \text{ cm}^2/\text{g}$
 $\rightarrow 3.90 \text{ cm (1/e)}$

- Total Attenuation with Coherent Scattering
- Total Attenuation without Coherent Scattering
- - - Coherent Scattering
- Incoherent Scattering
- Photoelectric Absorption
- Pair Production in Nuclear Field
- - - Pair Production in Electron Field

Pb



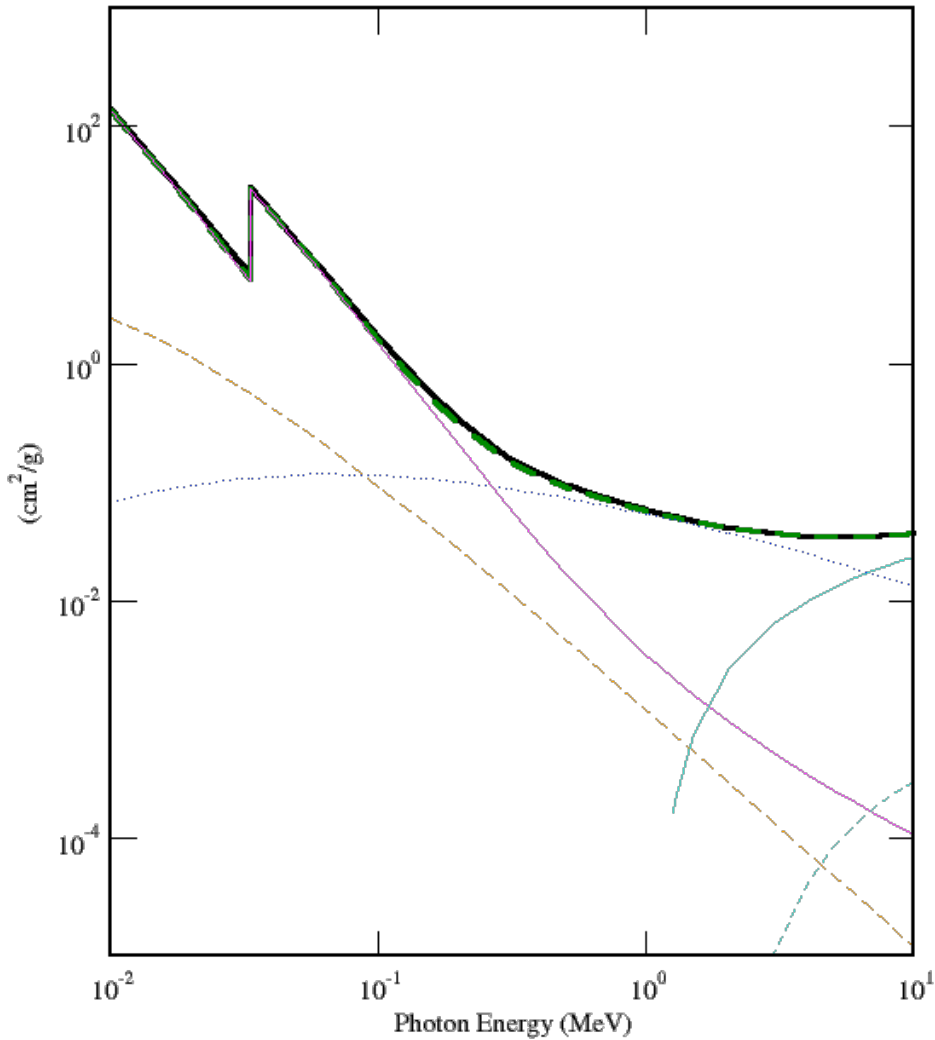
11.35 g/cm^3

$0.511 \text{ MeV } 1.562\text{e-}01 \text{ cm}^2/\text{g}$
 $\rightarrow 0.564 \text{ cm (1/e)}$

$1.275 \text{ MeV } 5.790\text{e-}02 \text{ cm}^2/\text{g}$
 $\rightarrow 1.52 \text{ cm (1/e)}$

- Total Attenuation with Coherent Scattering
- Total Attenuation without Coherent Scattering
- - Coherent Scattering
- Incoherent Scattering
- Photoelectric Absorption
- Pair Production in Nuclear Field
- - Pair Production in Electron Field

Nal



3.667 g/cm^3

$0.511 \text{ MeV } 9.326\text{e-}02 \text{ cm}^2/\text{g}$
 $\rightarrow 2.92 \text{ cm (1/e)}$

$1.275 \text{ MeV } 5.107\text{e-}02 \text{ cm}^2/\text{g}$
 $\rightarrow 5.34 \text{ cm (1/e)}$

- Total Attenuation with Coherent Scattering
- Total Attenuation without Coherent Scattering
- - - Coherent Scattering
- Incoherent Scattering
- Photoelectric Absorption
- Pair Production in Nuclear Field
- - - Pair Production in Electron Field